A passive air sampling technique for ultra-trace quantitation of perfluoroalkyl carboxylic acids

Eric Vanhauwaert

A thesis submitted to the faculty of Graduate Studies in partial fulfillment of the requirements for the degree of

Master of Science

Graduate Program in Chemistry

York University

Toronto, Ontario

June 2024

Abstract

Perfluoroalkyl carboxylic acids (PFCAs) are persistent chemicals distributed ubiquitously in the environmental despite their anthropogenic origin. Recent studies have shown that atmospheric transport is an important transport mechanism for PFCAs. Despite this, measuring mixing ratios of gaseous PFCAs in the atmosphere has been an analytical challenge, limiting the availability of atmospheric measurements. A new nylon-based passive air sampling (PAS) technique addresses many of these challenges by offering a cost-effective, low-labour solution. These samplers were calibrated for trifluoroacetic acid (TFA) in an atmospheric chamber and field measurements were compared to measurements from an ambient ion monitoring ion chromatography mass spectrometer, where good agreement was found. They were also deployed in various locations in Canada for gas-phase PFCA measurements which revealed many different trends, including the wastewater treatment plant as a point source of gas-phase TFA. These measurements have enhanced our understanding of PFCAs with calibrated, cost-effective samplers capable of ultra-trace measurements.

Acknowledgments

First and foremost, I would like to thank my supervisors, Trevor VandenBoer and Cora Young, for all their mentoring and support during this journey. I am very appreciative for all the time and commitment you both have taken in meeting with me, guiding and helping me problem solve as well editing and providing feedback on a multitude of matters, including this thesis. Your support and passion for research was really inspiring to me and I am very thankful for helping me achieve my goals during this degree.

Special thanks to Leigh for all his help and guidance for helping me make the chamber experiments a reality.

Special thanks to Jessica for providing me with the AIM-IC-MS data as well as all your help with the many challenges I faced with using the IC-MS instrument.

Thank you to my committee members, Trevor Vandenboer, Cora Young and Demian Ifa, for all their help, feedback and support during this degree.

Thank you to all members of the VDB and CJY research groups! I am incredibly grateful to the many of you who helped me in various ways in order to make this project a success. Big shout-out to Lisa, Stephen, Mayré, Fahim, Alessia, Leyla, Shira and Yash.

Table of Contents

List of Figures

List of Tables

List of Symbols and Abbreviations

”	inch
τ	atmospheric lifetime
>	greater than
<	less than
$_{(aq)}$	aqueous state
$_{(g)}$	gaseous state
$_{(l)}$	liquid state
$_{(s)}$	solid state
$[X]_m$	concentration of analyte in the mobile phase
$[X]_s$	concentration of analyte in the stationary phase
%	percent
$\bullet CH_3$	methyl radical
•Cl	chlorine atom
$\bullet O(^1D)$	singlet state oxygen atom
°C	degrees Celsius
±	plus or minus
$\propto$	directly proportional
≤	less than or equal to
≥	greater than or equal to
A	area
AE	aeration tank
AIM-IC-MS	ambient ion monitoring ion chromatography mass spectrometer
amu	atomic mass unit
APFO	ammonium perfluorooctanoate
C	concentration
C-F	carbon-fluorine bond

$C(O)F_2$	carbonic difluoride
C2-C4	two to four carbon compound(s)
C2-C6	two carbon to six carbon compound(s)
≥C3	compound(s) with 3 carbons or more
≥C4	compound(s) with 4 carbons or more
CD	conductivity detector
cm	centimeter
$CF_3(CF_2)_nC(O)OH$	perfluorocarboxylic acids
$CF_3(CF_2)_nC(O)OO•$	perfluorinated peroxyacyl radical
$CF_3(CF_2)_nC(O)X$	perfluorinated acyl halide
$CF_3(CF_2)_nCH_2F$	perfluorinated fluoroalkane
$CF_3(CF_2)_nCHCl_2$	perfluorinated dichloroalkane
$CF_3(CF_2)_nCHClBr$	perfluorinated chlorobromoalkane
$CF_3(CF_2)_nCHClOCHF_2$	perfluorinated chlorofluoroalkyl ether
$CF_3(CF_2)_nCHFCF_3$	perfluorinated alkene or a perfluorinated olefin
$CF_3(CF_2)_nCHFCl$	perfluorinated chlorofluoroalkane
$CF_3(CF_2)_nH$	perfluoroalkane
CFCs	chlorofluorocarbons
$CH_3C(O)Cl$	acetyl chloride
$CH_3C(O)OH$	acetic acid
CH_3COO^-	acetate anion
CH_4	methane
Cl^-	chloride anion
D	deposition rate
DCM	dichloromethane
DDM	diphenyl diazomethane
Df	diffusion

DIW	deionized water
DP	dual pump
dp	particle diameter
DVB	divinylbenzene
E	emission rate
e	Euler's number
ECNI	electron capture negative ionization
FEP	fluorinated ethylene propylene
F_{in}	advection gain of gasses
F_{out}	advection loss of gasses
GC-MS	gas chromotography - mass spectrometry
Gen-X	hexafluoropropylene oxide dimer acid
GTA	greater Toronto area
h	hour
H-bond	hydrogen bonding
H_2	molecular hydrogen
H_2O	water
HAAs	haloacetic acids
HCl	hydrochloric acid
HF	hydrofluoric acid
HFO-1234yf	2,3,3,3-tetrafluoropropene
H_M	height of the membrane
HNO_3	nitric acid
HO_2	hydroperoxyl radical
HPLC	high-pressure liquid chromatography
HX	hydrohalic acid
Hz	Hertz

IC-MS	ion chromotography - mass spectrometry
IS	internal standard
J	diffusion flux
k’	retention factor
K_{AW}	air-water partition coefficient
k_D	rate of diffusion
k_H	solubilization from the gas-phase
km	kilometer
K_{OA}	octanol-air partition coefficient
K_{OW}	octanol-water partition coefficient
kPa	kiloPascal
k_R	reactive uptake
L	litre
LC-MS	liquid chromatography - mass spectrometry
L_M	membrane thickness
LOD	limit of detection
LOQ	limit of quantitation
L_p	length of the analyte diffusion pathway
m	meter
M	molar (mol/L)
m^2	square meter
m^3	cubic meter
M_a	amount of analyte transported by diffusion into the sorbent
mA	milliAmpere
M_A	molar mass of air
M_B	molar mass of TFA
M_C	molar mass of HNO_3

MDL	method detection limit
min	minute
mL	milliliter
mM	millimolar
mol	mole
MS	mass spectrometer
MΩ	megaOhm
n	number of replicates or repeating units
N	total number of replicates
n/a	not applicable
Na_2CO_3	sodium carbonate
NaOH	sodium hydroxide
NaPFO	sodium perfluorooctanoate
NAPS	Government of Canada National Air Pollution Surveillance
ng	nanogram
NH_3	ammonia
NH_4NO_3	ammonium nitrate
NO_3^-	nitrate anion
NO_x	nitrogen oxides
NPT	national pipe thread
O_2	molecular oxygen
O_3	ozone
OH^-	hydroxide anion
OH, •OH	hydroxyl radical
P	partial pressure
P/N	product number
PAS	passive air sampler(s)

Pc	primary clarifier
PFA	perfluoroalkoxy alkane
PFAS	per- and polyfluoroalkyl substance(s)
PFBA	perfluorobutanoic acid
PFCA	perfluorocarboxylic acid
PFDA	perfluorodecanoic acid
PFDoDA	perfluorododecanoic acid
PFHpA	perfluoroheptanoic acid
PFHxA	perfluorohexanoic acid
PFNA	perfluorononanoic acid
PFOA	perfluorooctanoic acid
PFPeA	perfluoropentanoic acid
PFPrA	perfluoropropanoic acid
PFSA	perfluorosulfonic acid
PFTeDA	perfluorotetradecanoic acid
PFTrDA	perfluorotridecanoic acid
PFUnDA	perfluoroundecanoic acid
pg	picograms
pH	negative logarithm of the concentration of hydronium ions
pK_a	negative logarithm of the acid dissociation constant
PM	particulate matter
PP	polypropylene
ppq_v	part per quadrillion by volume
ppt_v	parts per trillion by volume
PTFE	polytetrafluoroethylene
PUF	polyurethane foam
PVDF	polyvinylidene fluoride

QA/QC	quality assurance / quality control
Rf	reference
RH	relative humidity
3σ	99.73% confidence interval
R_{min}	minimum resolution
S	permeability coefficient of the analyte in the membrane
s_n	sample standard deviation
s	second
S/N	serial number
Sc	secondary clarifier
SIM	selected ion monitoring
SKU	stock keeping unit
SLPM	standard litres per minute
SO_2	sulphur dioxide
SPE	solid phase extraction
T	temperature
t	time
$t_{calculated}$	statistical value for sample data in t-tests
TFA	trifluoroacetic acid
™	trademark
t_{table}	statistical reference value in t-tests
UV-rays, hv	ultra-violet light
v/v	volume by volume
vdW	van der Waals forces
v_i	diffusion volumes
V_m	volume of the mobile phase
VOCs	volatile organic compounds

V_S	volume of the stationary phase
W_M	width of the membrane
WWTP	wastewater treatment plant
X	pollutant
$\bar{x}$	mean
XAD	polymeric adsorbent resin
ZAG	zero-air generator
µg	micrograms
µL	microliter
Σ	summation
α	alpha; significance level
µmol	micromole

Other project undertaken during MSc

I had the pleasure to participate in THE CIX campaign during the summer of 2023 which is a subset of the NOAA-led AEROMMA aircraft campaign. This campaign included the deployment of 18 passive air samplers, for measurements of gas-phase atmospheric acids during a monthly period, as well as running an ambient ion monitoring ion chromatography mass spectrometry (AIM-IC-MS) instrument for hourly measurements for both gas-phase and particle-phase atmospheric acids. Overall, the AIM-IC-MS obtained extensive data for atmospheric acids, including TFA, and is the first of its kind to have obtained hourly particle measurements of PFPrA and PFBA over a monthly period.

Chapter One: Perfluoroalkyl carboxylic acids in the atmosphere

E. Vanhauwaert[1], C.J. Young[1], and T.C. VandenBoer[1]

[1]Department of Chemistry, York University, Toronto, ON, Canada.

Author Contributions:

EV prepared while CJY and TCV edited the chapter.

CJY and TCV conceptualized the work and acquired the funding. CJY and TCV provided the resources to support this work.

1.1 Perfluoroalkyl carboxylic acids in the atmosphere

1.1.1 Atmospheric transport and fate of pollutants

Our planet's atmosphere is composed of gasses and particles that dynamically mix, constantly transforming and distributing pollutants across the globe. It is made up of multiple different layers, including the troposphere and the stratosphere that are impacted by atmospheric pollution. The troposphere is the closest layer to Earth, found from the surface to approximately 10 km above sea level, constituting the air we breathe (NOAA, 2022). The stratosphere is found just above the troposphere, extending from 10 km to 50 km above sea levels, which includes the ozone layer that protects us from harmful UV-rays (NOAA, 2022).

The atmosphere is unique to other Earth spheres (e.g. hydrosphere, lithosphere) as long-range transport of pollutants occurs on a much faster timescale, enhancing the potential for global distribution and contamination (Young & Mabury, 2010). It also allows for the creation and transformation of various compounds through different reactions, including but not limited to: photolysis (R1.1), reactions with OH radicals (R1.2), hydrolysis (R1.3) and acid-base reactions (R1.4) (Seinfeld & Pandis, 2016):

$$\mathbf{O_3 + hv \rightarrow O_2 + \bullet O(^1D)} \quad \textbf{(R1.1)}$$

$$\mathbf{CH_4 + \bullet OH \rightarrow H_2O + \bullet CH_3} \quad \textbf{(R1.2)}$$

$$\mathbf{CH_3C(O)Cl + H_2O \rightarrow CH_3C(O)OH + HCl} \quad \textbf{(R1.3)}$$

$$\mathbf{NH_3 + HNO_3 \rightarrow NH_4NO_3} \quad \textbf{(R1.4)}$$

Pollutant levels in the atmosphere, measured by mass loading (e.g. ng/m^3) or mixing ratio (e.g. ppt_v), are also influenced by their rate of emission into the atmosphere and rate of deposition into other Earth spheres, whether by dry deposition, where pollutants are directly deposited onto surface, or by wet deposition, where the pollutants are scavenged out of the atmosphere into precipitation. A mass balance approach is typically used to describe pollutant levels in the atmosphere, which can be depicted chemically by a simple atmospheric zero dimensional kinetic box model representing a selected atmospheric domain (e.g. urban area, troposphere, global atmosphere, etc.), where E is the emission rate of a given pollutant (X) into the atmosphere, D is the deposition rate of X out of the atmosphere, P is the rate of chemical production of X from other atmospheric compounds in the atmosphere, L is the rate of chemical loss of X from reactions with different compounds in the atmosphere, F_{in} is the advection gain

of gasses and particles from other parts of the atmosphere, and F_{out} is the advection loss of gasses and particles to different parts of the atmosphere (Figure 1.1) (Jacob, 1999).

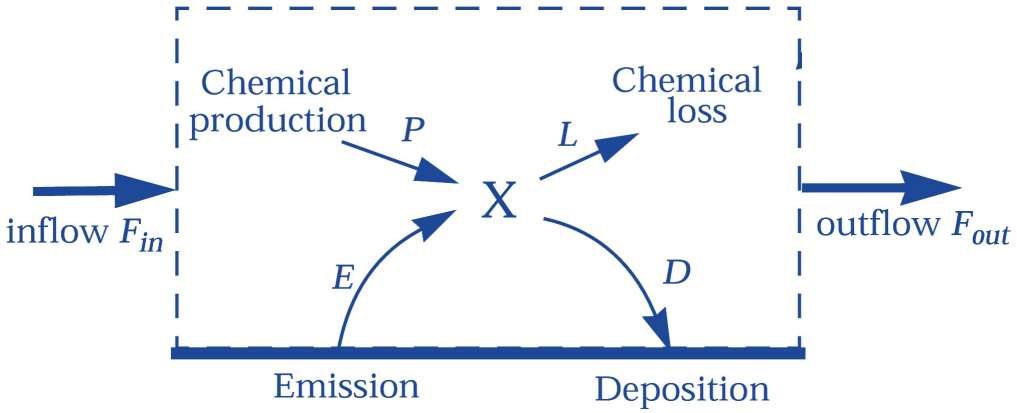

Figure 1.1: Simple atmospheric one-box model, modified from Jacob (1999).

The terms F_{in}, P and E constitute sources of X while L, D and F_{out} are termed sinks. The atmospheric lifetime is defined as the time required for the concentration of a substance in the atmosphere to decrease to 1/e (approximately 37%) of its initial value. The atmospheric lifetime (τ) of a pollutant (X) within the one-box model can be calculated as the inverse of the sum of sinks relative to the total mass available for them to act on, as shown by Equation 1.1 (Jacob, 1999).

$$\boldsymbol{\tau\,(s) = \frac{X\,(kg)}{D+L+F_{out}\,(\frac{kg}{s})}} \qquad \textbf{(E1.1)}$$

For the global atmospheric τ of X, F_{out} in Equation 1.1 is equal to zero since there is not any other one-box atmospheric models that interact with it.

Equally important to understanding the reaction pathways of pollutants is an understanding of their physical properties in the atmosphere, more notably their partitioning preference. Pollutants in the atmosphere can be found either in the gas phase or in the particle phase, where the latter is composed a complex mixture of inorganic salts, water-soluble organic matter, water-insoluble organic matter, and many other compounds (Seinfeld & Pandis, 2016). Depending on their composition and current conditions, phase separation can occur between the aqueous phase and water-insoluble organic matter (You et al., 2012). The pH in particles is also variable, where it can range from -1 to 7 (Arp & Goss, 2009; Pye et al., 2020). Partition of pollutants (X) in the atmosphere can be described in Figure 1.2, where K_{AW}, K_{OA} and K_{OW} are the air-water, octanol-air and octanol-water partitioning coefficients respectively.

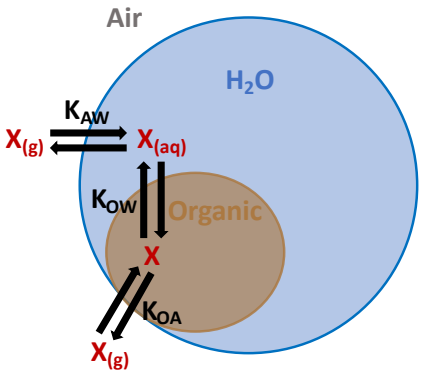

Figure 1.2: Simple schematic of pollutant partitioning in airborne particles, adapted from Tao et al. (2023).

The composition of particles can be highly variable which can impact the pollutant phase partitioning preferences. Whether they prefer to be in the gas or particle phase, based on partitioning under environmental conditions, can have a major impact on its rate of reactivity or deposition and therefore its atmospheric lifetime and global distribution (Hemond & Fechner, 2022). For example, pollutants with low reactivities that primarily exist in the gas phase, such as chlorofluorocarbons (CFCs), tend to persist longer in the atmosphere and are transported over larger distances by winds (Hemond & Fechner, 2022). Thus, an understanding of reactive pathways and atmospheric partitioning properties, as well those same properties of their precursors, is important to understanding the scale of the global impact any pollutant can have.

1.1.2 Perfluoroalkyl carboxylic acids (PFCAs)

Perfluoroalkyl carboxylic acids (PFCAs) constitute a class of compounds characterized by a fluorinated carbon tail and a carboxylic acid head group, as depicted in Figure 1.3 (Siegemund et al., 2000).

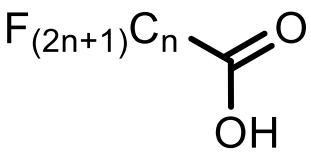

Figure 1.3: Generalised chemical structure of PFCAs, with varying chain length.

These compounds possess a dual nature: their fluorinated carbon tail exhibits minimal van der Waals (vdW) intermolecular interactions, resulting in increased hydrophobicity and volatility, meanwhile the polar carboxylic acid head is capable of hydrogen bonding (H-bond) and vdW intermolecular interactions, leading to adsorption to surfaces and head group solubility in water

(Lau et al., 2004). This combination of properties renders these molecules amphiphilic and the denotation as surfactants.

In water, PFCAs tend to be ionized across a broad range of environmentally relevant pH conditions due to their low pK_a values. Trifluoroacetic acid (TFA), for instance, has a pK_a of 0.52, which is much lower than typical carboxylic acids found in the environment (Lide, 2004). This acidity can be attributed to the presence of fully fluorinated carbons. These act as strong electron-withdrawing groups, pulling electron density away from the negatively charged carboxylate group in the conjugate base. This stabilizes the conjugate base and destabilizes the parent acid, ultimately making PFCAs more willing to release a proton and leading to its lower pK_a value. The PFCAs are a sub-class of the broader category of per- and polyfluoroalkyl substances (PFAS), which are known for their remarkable chemical stability owing to the strong carbon-fluorine bonds (Martin et al., 2003; Prevedouros et al., 2005). These substances are anthropogenic compounds, produced solely by human activity, that exhibit many distinctive properties, such as hydrophobicity, lipophobicity, thermal stability, and resistance to various chemical agents, allowing for their widespread use in a multitude of commercial applications (Manojkumar et al., 2023). Due to their unique properties, they have been incorporated in the production of: paper, firefighting foams, packaging materials, lubricants, paints, carpets, adhesives, pesticides, cosmetics, semiconductors, fume suppressants, surfactants, refrigerants, and many more (Manojkumar et al., 2023). Interest in measuring PFCAs arose when they were discovered to be widespread in organisms; no natural sources, such as from geological or biological processes, have been identified to date for their formation (Giesy & Kannan, 2001; Manojkumar et al., 2023; Joudan et al., 2021; Wang et al., 2014a). Ongoing measurements have revealed the ubiquity of PFCAs in ocean water, precipitation, snow, and air samples, a result of their physical properties and their persistence in the environment from their chemical stability (Young & Mabury, 2010; Wong et al., 2018; Ellis et al., 2004; Nelson & Kaminsky, 2021; Prevedouros et al., 2005). Initially, it was believed that the high solubility in water and short atmospheric lifetimes of PFCAs would make oceans the primary transport mechanism for their global distribution (Wong et al., 2018). However, recent studies are challenging this notion, demonstrating evidence that atmospheric transport is an important contributor to the worldwide distribution of PFCAs (MacInnis et al., 2017; Pickard et al., 2018; Sha et al., 2024; Yeung et al., 2017; Young et al., 2007).

1.1.3 Atmospheric transformation of precursors to perfluoroalkyl carboxylic acids

PFCAs found in the environment can be formed in the atmosphere as a final degradation product from some PFAS, as reviewed by Young and Mabury (2010), which is briefly summarized throughout this section. The formation of PFCAs can occur via perfluoroacyl halides or perfluoroacyl peroxy radical reactions in the atmosphere. Perfluoroacyl halides, $CF_3(CF_2)_nC(O)X$, can be transformed into PFCAs either by photolysis (R1.5) or hydrolysis (R1.6).

$$\mathbf{CF_3(CF_2)_nC(O)X + h\nu \rightarrow CF_3(CF_2)_nC(O)OH + C(O)F_2 + HF + HX} \quad \textbf{(R1.5)}$$

$$\mathbf{CF_3(CF_2)_nC(O)X + H_2O \rightarrow CF_3(CF_2)_nC(O)OH + HX} \quad \textbf{(R1.6)}$$

The hydrolysis pathway is estimated to be faster than photolysis, with hydrolysis lifetime estimates ranging from 5-14 days. While slower, photolysis of perfluoroacyl chlorides has also been found to play an important role in the formation of PFCAs with the precursor atmospheric lifetimes estimated to be 33-86 days. In comparison, the photolysis of perfluoroacyl fluorides has been found to be much slower, with predicted atmospheric lifetimes ranging from 300-7500 years. PFCAs may also be formed from perfluorinated peroxy radicals reacting with hydroperoxyl radicals (R1.7).

$$\mathbf{CF_3(CF_2)_nC(O)OO\bullet + HO_2 \rightarrow CF_3(CF_2)_nC(O)OH + O_3} \quad \textbf{(R1.7)}$$

It is important to note that other reaction pathways for perfluorinated peroxy radicals with hydroperoxyl radicals are possible and dominate for shorter chained perfluorinated peroxy radicals, where shorter chained perfluorinated peroxy are more likely to be transformed into perfluoroacyl oxy radicals rather than PFCAs.

Perfluoroacyl halides and perfluorinated peroxy radicals can be formed by several different PFAS precursors through various reactions in the atmosphere. Figure 1.4 demonstrates a simplified diagram of the transformations of PFAS precursors to form perfluoroacyl halides and perfluorinated peroxy that can eventually transform further in the

atmosphere to generate the PFCA terminal reaction products.

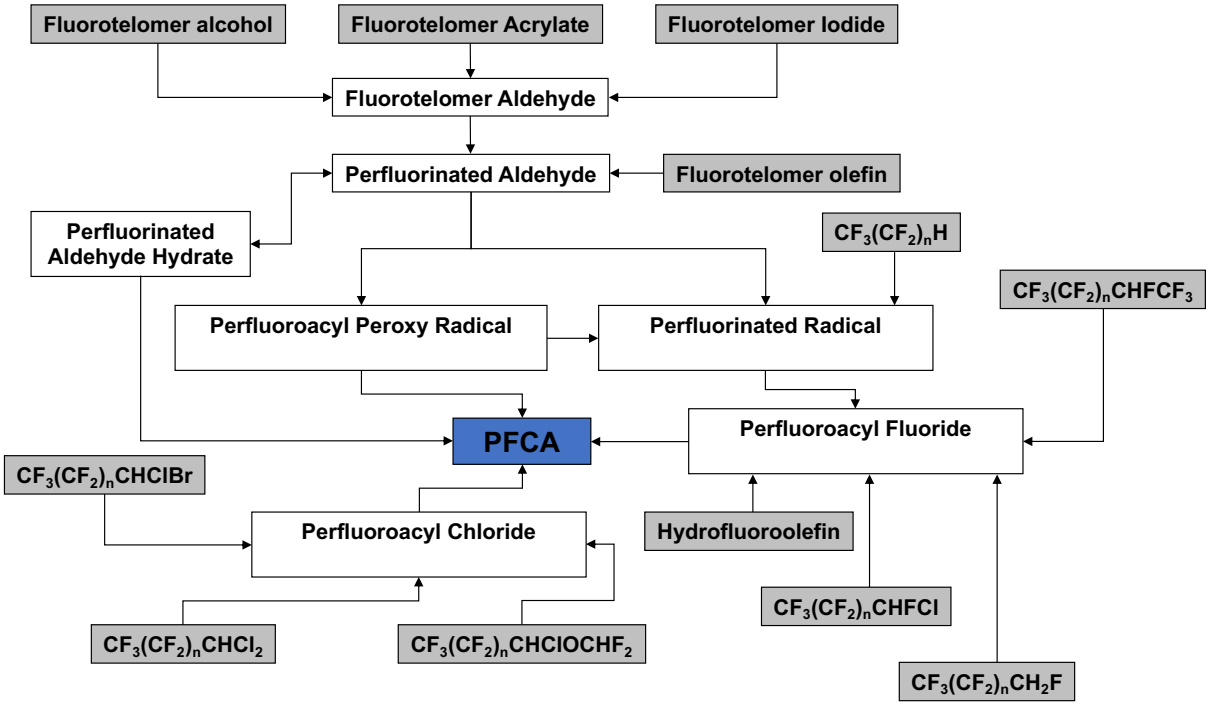

Figure 1.4: Simplified diagram of the transformation pathways of PFAS precursors to form PFCAs, modified from Young and Mabury (2010).

This diagram of atmospheric release and transformation pathways highlights the importance of volatile PFAS in generating PFCAs where many of these precursor PFAS compounds, shaded in grey, are commercially produced (Figure 1.4). More importantly, the degradation from PFAS precursors to PFCAs can take place over the course of several days to weeks in the atmosphere, resulting in the long-range transport potential of PFCAs to, and their deposition into, remote locations.

1.1.4 Commercial production and emissions of PFCAs and their precursors

The utilization of PFAS compounds spans a broad spectrum due to their unique properties (Manojkumar et al., 2023). Direct sources, being the direct emission of existing PFCAs, and indirect sources, being the formation of PFCAs from the degradation of precursor PFAS compounds, contribute to the presence of PFCAs in the environment. Each can stem from active ingredients or manufacturing process impurities of PFAS-based commercial products (Wang et al., 2014a). Notably, substances like ammonium/sodium perfluorooctanoate (APFO/NaPFO) serve as processing aids for producing popular and high-volume polymer materials like polytetrafluoroethylene (PTFE), fluorinated ethylene propylene (FEP), perfluoroalkoxy alkane (PFA), and polyvinylidene fluoride (PVDF) (Wang et al., 2014b).

Residual active ingredients or impurities from these products may leach directly into the environment during their use and degradation of the product over time or be directly emitted in waste streams. In contrast, PFCAs can also be indirectly emitted from PFAS commercial products as they degrade into these terminal products over time. For instance, the refrigerant 2,3,3,3-tetrafluoropropene (HFO-1234yf) can transform into trifluoroacetic acid (TFA), the shortest-chain PFCA, at a 90-100% yield when first reacting with the hydroxyl radical (•OH) or chlorine atom (•Cl) in the atmosphere (Burkholder et al., 2015; Luecken et al., 2009; Ye et al., 2021), similar to Reaction 1.2. A comprehensive understanding of the sources and pathways through which PFCAs enter the environment is crucial for effectively mitigating their subsequent impact on ecosystems and public health.

Long-chain perfluorinated carboxylic acids (PFCAs) have been associated with adverse health effects attributed to their bioaccumulative nature and toxicity (Conder et al., 2008; Menger et al., 2020). Consequently, major global producers of PFCAs and their precursors, particularly in North America and Europe, took measures to reduce use and production of compounds like perfluorooctanoic acid (PFOA) to address the most expected of these concerns (Wang et al., 2014a). In an effort to sustain demand for commercial products with the properties of per- and polyfluoroalkyl substances (PFAS), there has been a transition to the use of shorter-chained PFCAs and their precursors, which are suggested to exhibit reduced bioaccumulation potential, thereby mitigating their impact on mammals and apex predators in the environment (Yeung et al., 2017). Interestingly, this transition is not universal, as countries like India, China, and Russia are estimated to have increased production of long-chain PFCAs, such as PFOA, since the mid-2000s (Wang et al., 2014a). Similarly, the persistence of shorter-chained PFCAs in the environment is just like that of their longer-chained counterparts, and their biological consequences are less studied. While their precise environmental impact is not fully understood, the accumulation of any persistent substance raises significant concerns (Cousins et al., 2020). The performance of short-chain PFAS precursors is considered inferior to their long-chain counterparts, where a higher amount of short-chain PFAS is needed to manufacture the same amount of consumer products, consequently leading to greater emissions of shorter-chained PFCAs (Brendel et al., 2018). As a result, global emissions of longer-chained PFCAs and their precursors persist, while emissions of shorter-chain PFCAs will continue to rise for the foreseeable future.

1.1.5 PFCA atmospheric measurement techniques

While the potential for atmospheric formation has been recognized, there remains an increasing need to measure PFCAs in the atmosphere, as this environmental compartment has high mobility, and the deposition of these acid end products will lead to accumulation and potential negative implications to the environment worldwide. Understanding the gas-particle partitioning of PFCAs (Figure 1.2) in the atmosphere is important as it sheds light on their environmental fate via long-range transport against deposition processes such as wet and dry deposition (Ahrens et al., 2011). Most previous atmospheric PFCA measurements have involved using high volume air samplers. This technique is intended to collect both gaseous and particulate PFCAs to better understand how these compounds distribute between gas and particle phases in the atmosphere (Ahrens et al., 2011). High volume air samplers work by pulling air through a filter and sorbent where particles are collected first on a filter followed by the collection of gasses on a sorbent (Figure 1.5).

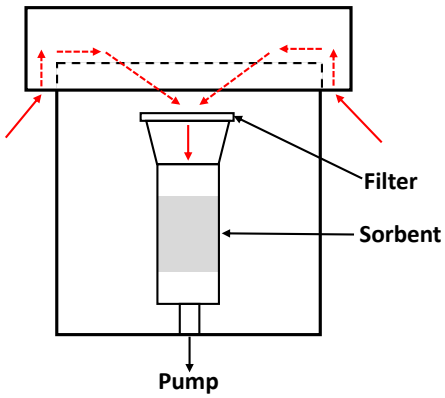

Figure 1.5: High-volume sampler schematic, adapted from Ahrens et al., 2011. The red arrows indicate the air flow.

However, these samplers have been found to exhibit "blow-on" and "blow off" sampling artifacts where there is either an overestimation or an underestimation of the measured particle composition, also affecting accurate measurement of gasses (Ahrens et al., 2011, Arp & Goss, 2008, Peters et al., 2000; Tsai & Perng, 1998). Blow-on artifacts are due to gasses partitioning or reacting to the particles already collected on the filters or adsorbing to the filters themselves before reaching the sorbent meanwhile blow-off are caused by pollutants volatilizing out of particulate matter after collection on the filters (Figure 1.5) (Young & VandenBoer, 2023). In addition to these artifacts, the typical sorbents used in these samplers for the collection of gas-phase PFAS (including PFCAs), being polyurethane foam (PUF) and/or polystyrene-divinylbenzene (XAD), have been found to obtain non-quantitative recoveries, with recoveries

ranging from 25 to 60 % (Dreyer et al., 2009). The use of diffusion denuder samplers helped address the blow-on and blow-off artifact biases by sampling gasses prior to sampling particles (Figure 1.6) (Ahrens et al., 2011, EPA, 1992; Peters et al., 2000; Tsai & Perng, 1998).

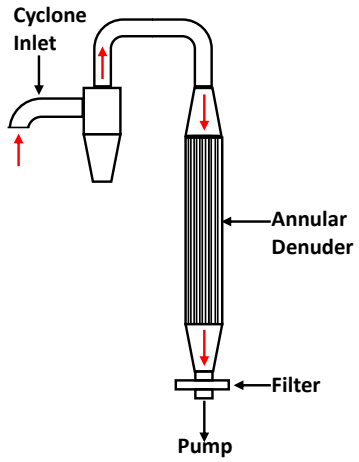

Figure 1.6: Annular diffusion denuder sampler schematic, adapted from Ahrens et al., 2011. The red arrows indicate the air flow.

The gasses are collected quantitatively to a reactive coating from a flow passing over its surface, where they have much greater diffusion coefficients compared to the inertia in the particles such that they pass through the annular rings and exit the denuder (Berg et al., 2010). This addresses the "blow-on" sampling artifacts from previous samplers by sampling gasses prior to particles. After passing through denuders, particles are then collected by impaction on a filter. These filters typically consist of PTFE filters followed by secondary filters composed of nylon and/or coatings (e.g. coated with citric acid) to reactively capture blow-off of acidic/basic gasses (Tsai & Perng, 1998), thus addressing the blow-off sampling artifacts from previous samplers. Although diffusion denuder samplers helped address many issues from previous sampling techniques, they maintained several operating challenges. Specifically, they are high cost, labour-intensive, and require a power source to induce a flow using pumps. These challenges have limited the scale of atmospheric PFCA measurements by any of these approaches and the availability of sampling locations.

1.1.6 Passive samplers

Scientists and air quality analysts have been using passive air samplers (PAS) for several decades to overcome the challenges from active air samplers, such as ease of use and simplicity. They have been used in several settings to monitor airborne pollutants, primarily outdoors. The affordability of PAS has facilitated their deployment in extensive sampling

networks, enabling the identification of specific sites as significant sources of atmospheric pollutants (Wania & Shunthirasingham, 2020; Zhan et al., 2023). Their cost-effectiveness has also permitted prolonged deployments, revealing important trends in pollutant levels (Klánová et al., 2006). Furthermore, their independence from external power sources has made PAS suitable for deployment in remote regions, allowing for the assessment of pollutant levels in challenging sampling environments (Place et al., 2018; Wania & Shunthirasingham, 2020). While passive air sampling is commonly conducted outdoors, they have also been applied indoors. The non-intrusive nature and affordability of PAS have facilitated their use in monitoring indoor pollutant levels in various households (Atkins et al., 1993; Chao, 2001; Dodson et al., 2018; Gibbs et al., 2017). It is clear that PAS have emerged as invaluable tools for monitoring airborne pollutants, proving to be, in many instances, a preferable alternative to active air samplers.

Passive air samplers typically consist of sampler housings and contain sorbents that facilitate diffusion-driven collection of analytes by their preferential collection into the sorbent material (Górecki & Namieśnik, 2002). This collection causes a concentration gradient, which drives analytes from a more concentrated region to one depleted near the sorbent surface by Fick's First Law (E1.2). Preferential collection to drive this process is achieved through partitioning or reactive uptake on sorbents.

$$\mathbf{J = Df \times \frac{\Delta C}{L_p}} \qquad \textbf{(E1.2)}$$

In Equation 1.2, J represents the diffusion flux (mol/(m^2×s)), Df is the diffusion coefficient of a target gas (m^2/s), C is the change in concentration of the analyte (mol/m^3), and L_p is the length of the analyte diffusion pathway (m) (Kawashima et al., 2021). One specific type of PAS, known as badge-type, incorporates semi-permeable membranes (Górecki & Namieśnik, 2002). These membranes can be microporous, allowing gases to permeate while preventing the intrusion, and therefore measurement bias, from the deposition of particles (Figure 1.7).

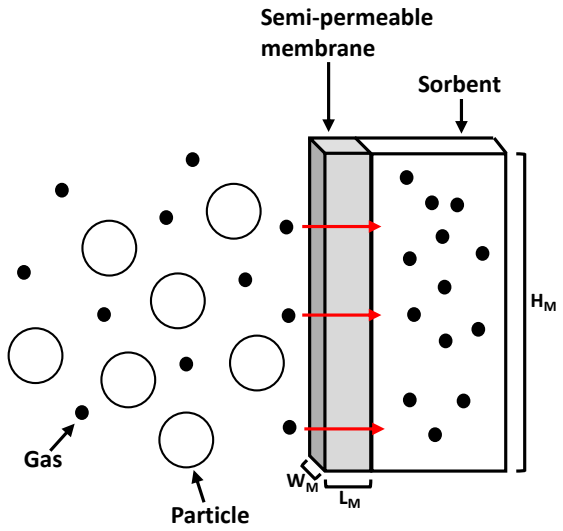

Figure 1.7: Badge-type PAS, inspired from Górecki & Namieśnik, 2002. Red arrows indicate the induced flow of gasses through the semi-permeable membrane.

Assuming 100% collection efficiency, the partial pressure of analytes, P (kPa, converted from mol/m^3), from badge-type PAS can be calculated from Equation 1.3, where M_a represents the amount of analyte transported by diffusion into the sorbent (mol), S is the permeability coefficient of the analyte in the membrane (m^2/min), L_M is the membrane thickness (m), t is the exposure time of the sampler (min), and A is the cross-sectional area of the diffusion path (m^2), the latter being W_M times H_M in Figure 1.7 (Górecki & Namieśnik, 2002).

$$P = \frac{M_a \times L_M}{S \times A \times t} = \frac{M_a \times L_M}{S \times (W_M \times H_M) \times t} \quad \textbf{(E1.3)}$$

The design of sorbents within PAS adapts to the pollutants being targeted. Some of these samplers utilize non-selective sorbents to capture a vast array of atmospheric compounds with varying properties. This includes the use samplers with polyurethane foam disks (PUF) embedded with XAD resins that captures a broad range of PFAS compounds, including PFCAs (Shoeib et al., 2008). Alternatively, samplers can leverage selective sorbents to minimize the uptake of matrix components (i.e. all other sample components that are not targets) and enhance saturation limits. A prime example of this selective approach is the use of nylon filters as a sorbent in PAS. These filters specifically target and uptake reactive atmospheric acids, and have been used to measure atmospheric $HNO_{3\,(g)}$ (Place et al., 2018) as well as $TFA_{(g)}$ in a preliminary study (Carmichael et al., 2022). Ultimately, the selection of sorbent type hinges on the specific pollutants of interest.

Some environmental variables can alter the sampling rate for PAS. Differences in meteorological conditions have been shown to have an impact on the uptake of gasses by PAS (Guo et al., 2014; Herkert et al., 2018; Li et al., 2023). Diffusion and adsorption of gasses are known to be temperature dependant, which can be described by Chapman-Enskog theory (E1.4) and the Arrhenius rate constant (E1.5) respectively (Place et al., 2018).

$$Df \propto T^{3/2} \quad \textbf{(E1.4)}$$

$$R_{ads} \propto e^{-1/T} \quad \textbf{(E1.5)}$$

Due to this dependence, passive air samplers may yield bias depending on the change in the rate of diffusion relative to PAS calibration temperatures for sampling rates. This theory means that additional potential error can be readily estimated for many molecules (e.g. ±10% from 10 to 35 °C for $HNO_{3\ (g)}$; Place et al. (2018)). Due to this temperature dependence, some calibration studies have opted to include a temperature dependence variable, determined from theoretical calculations and experimental results (Herkert et al., 2018; Ogawa USA, 2014). Passive air samplers may also be influenced by wind speeds, where strong winds can accelerate the advection of analytes in regions of the sampler where analyte collection is intended to proceed only by diffusion. This can lead to bias associated with the divergence in speed at which analytes reach the sorbents. As a result, protective weather shields have been designed to minimize the effects of strong winds and to maintain a diffusion-based regime for sampling (Herkert et al., 2018; Place et al., 2018; Wania & Shunthirasingham, 2020). These estimations and adaptations of these samplers offer a valuable means of analyte collection through diffusion, providing atmospheric monitoring at a low cost and with an efficient use of resources. Following collection, the reactive or partitioning sample media are subject to extraction and offline chemical analysis.

1.1.7 Offline analytical techniques for PFCAs

Gas and particle measurements of PFCAs to date using both active (e.g. Ahrens et al., 2011) and passive samplers (e.g. our work; Ye et al., 2023) have been performed using offline measurements applied to extracts of the sampling media. A high quality quantitative analytical technique for the analysis of such extracts is required as PFCAs are in ultra-trace levels in the atmosphere, where mixing ratios have been found between 0.07 to 687 ppt_v (equivalent to mass loadings of 1-3500 pg/m^3) (Vierke et al., 2011; Wu et al., 2014). Chromatography, frequently

employed in conjunction with a mass spectrometer as a detector, is commonly selected as the preferred technique for analyzing PFCA samples. Separation of compounds occurs between a mobile phase and a column containing the stationary phase, where compounds exhibit partitioning between both phases. Compounds with a higher partitioning coefficient, indicating a preference to partition in the stationary phase, will travel slower through the column meanwhile compounds with lower partitioning coefficient will move faster and elute earlier due to weaker interactions with the stationary phase. This gives the potential for a mixture of target compounds to be separated from each other and interfering matrix components, leading to improved detection. The partitioning extent can be described by the retention factor (k') in Equation 1.6, where $[X]_s$ is the concentration of analyte in the stationary phase, $[X]_m$ is the concentration in the mobile phase, V_S is the volume of the stationary phase, and V_m is the volume of the mobile phase (Harvey, 2016).

$$\boldsymbol{k' = \frac{[X]_S \times V_S}{[X]_m \times V_m}} \qquad \textbf{(E1.6)}$$

The k' value is dependant on several variable factors, including the stationary phase properties, the mobile phase composition, and the temperature. These variables can be adjusted to achieve optimal separation. The specific type of chromatography employed as well as the extent of separation optimisation impacts the quality of the separation of analytes and ultimately determines which technique is best suited for quantitative analysis of compounds.

Gas chromatography mass spectrometry (GC-MS) has been employed in previous studies for the quantitation of PFCAs (Dufková et al., 2012; Liu et al., 2012; Scott et al., 2006; Ye et al., 2023). GC-MS can be prefered over other types of chromotography due to it being cheaper and more widely available while still achieving high specificity, sensitivity and yielding rapid separations (Dufková et al., 2012; Hu et al., 2020; Shafique et al., 2017; Ye et al., 2023). These analytical techniques successfully covered a broad range of PFCAs, encompassing ultrashort chain PFCAs with two to four carbon chain lengths (Scott et al., 2006; Ye et al., 2023). Ye et al. (2023) in particular developed a novel method that can analyze PFCAs with carbon chain lengths ranging from two to fourteen, making this method one the most comprehensive approaches reported to date for simultaneously analyzing PFCAs of differing chain lengths. The use of derivatization agents for gas chromatography is required, where most common derivatization agents used have been akyl derivatives (Dufková et al., 2012; Liu et al., 2012; Scott et al., 2006; Shafique et al., 2017). However, some studies have used more selective derivatization agents such as phenyl-based derivatives allowing for phenyl−phenyl

interactions with the column stationary phase (Fuji et al., 2012; Ji et al., 2020; Ye et al., 2023). Although a robust analytical method, the preparation of samples is labor-intensive, requiring derivatization and solvent changes to generate volatile derivatives quantitatively (Dufková et al., 2012; Hu et al., 2020; Shafique et al., 2017; Scott et al, 2006; Ye et al., 2023). The additional sample handling steps, for example, can lead to an elevation in contamination levels in the blanks from volatile ultra-short chain PFCAs, specifically TFA and perfluoropropionic acid (PFPrA), adversely elevating method detection limits (Ye et al., 2023).

As an alternative to GC-MS, liquid chromatography mass spectrometry (LC-MS) has been utilized for PFCA analysis. While LC-MS methods can allow for the direct injection of some aqueous samples (Borrull et al., 2020), sample cleanup prior to injection using methods such as solid phase-extration (SPE) is usually required in order to separate PFCAs from interfering matrix compounds in order to achieve good detection limits, leading to similar sample preparation drawbacks like current GC-MS methods (EPA, 2020; González-Barreiro et al., 2006; Gremmel et al., 2016; Wolf & Reagen, 2011). Despite this, LC-MS methods have been able to achieve low detection limits for PFCAs, especially when configured with a triple quadrupole detection strategy, while simultaneously being able to detect other PFAS compounds (EPA, 2020; González-Barreiro et al., 2006;). However, most LC-MS methods for PFCA analysis operate in reverse-phase mode, utilizing a non-polar stationary phase which is non-selective to PFCAs (Liang et al., 2023). Using this type of stationary phase leads to the inadequate retention ($k' < 1$) of ultra-short chain PFCAs, such as TFA and PFPrA, due to their polar/ionic character, which preferentially partitions them into the aqueous fraction of the mobile phase, found to be typically elevated in reverse phase separations leading them to be eluted in the dead volume of the system (i.e. does not interact significantly enough with the stationary phase and is carried through the column by the solvent). Consequently, most studies employing LC-MS instruments for PFCAs analysis have been limited to reliably measuring PFCAs with chain lengths of four carbons or higher (≥C4) (Borrull et al., 2020; Gremmel et al., 2016; Surma et al., 2015; Vierke et al., 2011). Some studies have addressed this limitation. For example, Janda et al. (2018) acidified the mobile phase with formic acid, allowing for the longer retention of TFA and PFPrA. The study speculated that the introduction of formic acid protonated some of residual silanoate groups in the C18 stationary phase, thereby introducing more possible H-bond sites to the unfunctionalized surface of the microporous silica packing particles, which improved the retention of TFA and PFPrA through a non-ideal interaction within the column. A drawback in this approach is that the mechanism for retention is unrelated

to the C18 stationary phase and the reproducibility in this approach is likely low, as exposed silanoate fractions are likely poorly controlled. In contrast, Taniyasu et al. (2008) employed a mixed mode ion-exchange column, resulting in stronger retention of TFA and PFPrA. Both cases demonstrate that either H-bond or ionic interactions in the stationary phase are crucial for the retention and separation of ultra-short chain PFCAs from each other and matrix components in liquid chromotography in order to obtain reliable quantitative analytical outcomes.

Ion chromatography, a form of liquid chromatography, has been utilized in the past for the separation and analysis of TFA (Barron & Paull, 2006). Ion chromatography employs a charged ionic-exchange stationary phase and an aqeuous mobile phase with dissolved competing ions to separate and elute analyte ions. Typically, weaker ions that do not interact strongly with the stationary phase (e.g. hydroxide) are employed as competing ions in the aqueous phase. Despite being weak, they can still displace strong ions (e.g. phosphate) when at high concentrations in the aqueous phase. This allows for flexibility in separating a wider range of ions, including both weak and strong ions. Unlike most liquid chromatography systems, ion chromatographs are coupled with a suppressor before the detector to eliminate the competing ions in the mobile phase. This significantly lowers background conductivity, leading to improved detection limits, and safeguards the detector from potential damage caused by the reactive acidic or basic competing ions in the eluent. Ion chromatography systems are commonly paired with a conductivity detector (IC-CD) and have more recently been integrated with mass spectrometers (IC-MS). Two studies have successfully analyzed haloacetic acids (HAAs) using a direct injection IC-MS method (Wu et al., 2017; Zhang et al., 2020), which share similar properties to PFCAs. Given that PFCAs have very low pK_a values, rendering them ionic under most pH conditions, the use of ion chromatography for the separation and quantitation of PFCAs is promising. When coupled with a mass spectrometer, it can offer efficient separation and quantitation of ultra-short chain PFCAs and environmentally abundant anions (e.g. nitrate, sulphate), allowing for direct injection by eliminating the need for sample cleanup. However, due to its high selectivity for charged compounds like TFA, another analysis method would be required to analyse non-charged PFAS compounds, which is not a limitation for standard LC-MS methods (Gremmel et al., 2016). The overall chemical and physical properties of the compounds of interest ultimately determines which of these established or potential analysis methods will be the most suitable.

1.1.8 Objectives

The first objective of this work is to validate a nylon-based PAS technique for gas-phase TFA using chamber calibrations and to compare the results to predicted sampling rates by two molecular diffusion estimates from theory and then to extend those results for the collection of other PFCAs. The second objective of this work is to deploy passive air samplers at 6 sites across Canada, located in the Greater Toronto Area (GTA) in Ontario, Tadoussac in Quebec, and Saturna Island in British Columbia, to quantify gas-phase PFCAs at multiple locations simultaneously. Measurements were performed at these locations for varying durations, ranging from one week to four months, and up to one year. In the GTA, a targeted set of observations was made at a wastewater treatment plant to confirm its role as an important point source of gaseous PFCAs. The above objectives will be achieved using GC-MS, IC-CD and IC-MS for the quantitative analysis of PFCAs, followed by the determined or approximated sampling rates to derive PFCA atmospheric levels with confidence using PAS.

1.2 References

Ahrens, L., Shoeib, M., Harner, T., Lane, D. A., Guo, R., & Reiner, E. J. (2011). Comparison of annular diffusion denuder and high volume air samplers for measuring per- and polyfluoroalkyl substances in the atmosphere. *Analytical Chemistry*, *83*(24), 9622–9628. https://doi.org/10.1021/ac202414w

Arp, H. P. H., & Goss, K. (2009). Gas/Particle Partitioning Behavior of Perfluorocarboxylic Acids with Terrestrial Aerosols. *Environmental Science & Technology*, *43*(22), 8542–8547. https://doi.org/10.1021/es901864s

Atkins, D., & Lee, D. S. (1993). Indoor concentrations of ammonia and the potential contribution of humans to atmospheric budgets. *Atmospheric Environment. Part a. General Topics*, *27*(1), 1–7. https://doi.org/10.1016/0960-1686(93)90064-6

Barron, L., & Paull, B. (2006). Simultaneous determination of trace oxyhalides and haloacetic acids using suppressed ion chromatography-electrospray mass spectrometry. *Talanta*, *69*(3), 621–630. https://doi.org/10.1016/j.talanta.2005.10.032

Berg, J. M., James, D., Berg, C. F., Toda, K., & Dasgupta, P. K. (2010). Gas collection efficiency of annular denuders: A spreadsheet-based calculator. *Analytica Chimica Acta*, *664*(1), 56–61. https://doi.org/10.1016/j.aca.2010.02.006

Borrull, J., Colom, A., Fábregas, J., Pocurull, E., & Borrull, F. (2020). A liquid chromatography tandem mass spectrometry method for determining 18 per- and polyfluoroalkyl substances in source and treated drinking water. *Journal of Chromatography A*, *1629*, 461485. https://doi.org/10.1016/j.chroma.2020.461485

Brendel, S., Fetter, É., Staude, C., Vierke, L., & Biegel-Engler, A. (2018). Short-chain perfluoroalkyl acids: environmental concerns and a regulatory strategy under REACH. Environmental Sciences Europe, 30(1), 1-11. https://doi.org/10.1186/s12302-018-0134-4

Burkholder, J. B., Cox, R. A., & Ravishankara, A. R. (2015). Atmospheric degradation of ozone depleting substances, their substitutes, and related species. *Chemical Reviews*, *115*(10), 3704–3759. https://doi.org/10.1021/cr5006759

Carmichael, L. (2022). *Determining the Sampling Rates for a New Nylon Passive Sampler to Estimate the Atmospheric Concentrations of Nitric Acid and Perfluoroalkyl Acids Pollutants* (Master's thesis). York University. Retrieved from https://hdl.handle.net/10315/26310

Chao, C. Y. H. (2001). Comparison between indoor and outdoor air contaminant levels in residential buildings from passive sampler study. *Building and Environment*, *36*(9), 999–1007. https://doi.org/10.1016/s0360-1323(00)00057-3

Conder, J. M., Hoke, R. A., De Wolf, W., Russell, M. H., & Buck, R. C. (2008). Are PFCAs Bioaccumulative? A Critical Review and Comparison with Regulatory Criteria and Persistent Lipophilic Compounds. *Environmental Science & Technology*, *42*(4), 995–1003. https://doi.org/10.1021/es070895g

Cousins, I. T., DeWitt, J. C., Glüge, J., Goldenman, G., Herzke, D., Lohmann, R., Ng, C. A., Scheringer, M., & Wang, Z. (2020). The high persistence of PFAS is sufficient for their management as a chemical class. *Environmental Science. Processes & Impacts*, *22*(12), 2307–2312. https://doi.org/10.1039/d0em00355g

Dodson, R. E., Bessonneau, V., Udesky, J. O., Nishioka, M., McCauley, M. W., & Rudel, R. A. (2018). Passive indoor air sampling for consumer product chemicals: a field evaluation study. *Journal of Exposure Science and Environmental Epidemiology*, *29*(1), 95–108. https://doi.org/10.1038/s41370-018-0070-9

Dreyer, A., Matthias, V., Temme, C., & Ebinghaus, R. (2009). Annual time series of air concentrations of polyfluorinated compounds. *Environmental Science & Technology*, *43*(11), 4029–4036. https://doi.org/10.1021/es900257w

Dufková, V., Čabala, R., & Ševčík, V. (2012). Determination of C5–C12 perfluoroalkyl carboxylic acids in river water samples in the Czech Republic by GC–MS after SPE preconcentration. *Chemosphere*, *87*(5), 463–469. https://doi.org/10.1016/j.chemosphere.2011.12.029

Fujii, Y., Harada, K. H., & Koizumi, A. (2012). Analysis of Perfluoroalkyl Carboxylic Acids in Composite Dietary Samples by Gas Chromatography/Mass Spectrometry with Electron Capture Negative Ionization. *Environmental Science & Technology*, *46*(20), 11235–11242. https://doi.org/10.1021/es302536g

Gibbs, J. L., Yost, M. G., Negrete, M., & Fenske, R. A. (2017). Passive sampling for indoor and outdoor exposures to chlorpyrifos, Azinphos-Methyl, and oxygen analogs in a rural agricultural community. *Environmental Health Perspectives*, *125*(3), 333–341. https://doi.org/10.1289/ehp425

Giesy, J. P., & Kannan, K. (2001). Global distribution of perfluorooctane sulfonate in wildlife. *Environmental Science & Technology*, *35*(7), 1339–1342. https://doi.org/10.1021/es001834k

González-Barreiro, C., Martínez-Carballo, E., Sitka, A., Scharf, S., & Gans, O. (2006). Method optimization for determination of selected perfluorinated alkylated substances in water samples. *Analytical and Bioanalytical Chemistry*, *386*(7–8), 2123–2132. https://doi.org/10.1007/s00216-006-0902-7

Görecki, T., & Namieśnik, J. (2002). Passive sampling. *Trends in Analytical Chemistry*, *21*(4), 276–291. https://doi.org/10.1016/s0165-9936(02)00407-7

Gremmel, C., Frömel, T., & Knepper, T. P. (2016). HPLC–MS/MS methods for the determination of 52 perfluoroalkyl and polyfluoroalkyl substances in aqueous samples. *Analytical and Bioanalytical Chemistry*, *409*(6), 1643–1655. https://doi.org/10.1007/s00216-016-0110-z

Guo, H., Lin, H., Zhang, W., Deng, C., Wang, H., Zhang, Q., Shen, Y., & Wang, X. (2014). Influence of meteorological factors on the atmospheric mercury measurement by a novel passive sampler. *Atmospheric Environment*, *97*, 310–315. https://doi.org/10.1016/j.atmosenv.2014.08.028

Harvey, D. (2016). *Analytical Chemistry 2.1*. LibreTexts Chemistry. Retrieved November 29, 2023, from https://chem.libretexts.org/Bookshelves/Analytical_Chemistry/Analytical_Chemistry_2.1_(Harvey)/12%3A_Chromatographic_and_Electrophoretic_Methods/12.02%3A_General_Theory_of_Column_Chromatography

Hemond, H. F., & Fechner, E. J. (2022). *Chemical fate and transport in the environment*. Academic Press.

Herkert, N. J., Scott, N. A., Smith, A., Schuster, J. K., Harner, T., Martínez, A., & Hornbuckle, K. C. (2018). Calibration and evaluation of PUF-PAS sampling rates across the Global Atmospheric Passive Sampling (GAPS) network. *Environmental Science: Processes & Impacts*, *20*(1), 210–219. https://doi.org/10.1039/c7em00360a

Hogue, C. (2019, May 11). *Governments endorse global PFOA ban, with some exemptions*. Chemical & Engineering News. https://cendev.acs.org/articles/97/i19/Governments-endorse-global-PFOA-ban.html

Hu, Z., Li, Q., Xu, L., Zhang, W., & Zhang, Y. (2020). Determination of perfluoroalkyl carboxylic acids in environmental water samples by dispersive liquid–liquid microextraction with GC-MS analysis. *Journal of Liquid Chromatography & Related Technologies*, *43*(7–8), 282–290. https://doi.org/10.1080/10826076.2020.1728311

Jacob, D. J. (1999). *Introduction to Atmospheric Chemistry*. Princeton University Press.

Janda, J., Nödler, K., Brauch, H., Zwiener, C., & Lange, F. T. (2018). Robust trace analysis of polar (C2-C8) perfluorinated carboxylic acids by liquid chromatography-tandem mass spectrometry: method development and application to surface water, groundwater and drinking water. *Environmental Science and Pollution Research*, *26*(8), 7326–7336. https://doi.org/10.1007/s11356-018-1731-x

Ji, Y., Cui, Z., Wang, Z., Cao, Y., Li, X., & Li, A. (2020). Simultaneous determination of seven perfluoroalkyl carboxylic acids in water samples by 2,3,4,5,6-pentafluorobenzyl bromide derivatization and gas chromatography-mass spectrometry. *Environmental Pollution*, *266*, 115043. https://doi.org/10.1016/j.envpol.2020.115043

Joudan, S., De Silva, A. O., & Young, C. J. (2021). Insufficient evidence for the existence of natural trifluoroacetic acid. *Environmental Science: Processes & Impacts*, *23*(11), 1641–1649. https://doi.org/10.1039/d1em00306b

Kawashima, H., Ogata, R., & Gunji, T. (2021). Laboratory-based validation of a passive sampler for determination of the nitrogen stable isotope ratio of ammonia gas. *Atmospheric Environment*, *245*, 118009. https://doi.org/10.1016/j.atmosenv.2020.118009

Klánová, J., Kohoutek, J., Hamplová, L., Urbanová, P., & Holoubek, I. (2006). Passive air sampler as a tool for long-term air pollution monitoring: Part 1. Performance assessment for seasonal and spatial variations. *Environmental Pollution*, *144*(2), 393–405. https://doi.org/10.1016/j.envpol.2005.12.048

Lau, C., Butenhoff, J. L., & Rogers, J. M. (2004). The developmental toxicity of perfluoroalkyl acids and their derivatives. *Toxicology and Applied Pharmacology*, *198*(2), 231–241. https://doi.org/10.1016/j.taap.2003.11.031

Li, Y., Zhan, F., Shunthirasingham, C., Lei, Y. D., Hung, H., & Wania, F. (2023). Unbiased Passive Sampling of All Polychlorinated Biphenyls Congeners from Air. *Environmental Science and Technology Letters*, *10*(7), 565–572. https://doi.org/10.1021/acs.estlett.3c00271

Liang, S., Steimling, J. A., & Chang, M. (2023). Analysis of ultrashort-chain and short-chain (C1 to C4) per- and polyfluorinated substances in potable and non-potable waters. *Journal of Chromatography Open*, *4*, 100098. https://doi.org/10.1016/j.jcoa.2023.100098

Lide, D. R. (Ed.). (2004). CRC handbook of chemistry and physics (Vol. 85). CRC press.

Liu, W., Ko, Y., Hwang, B., Li, Z., Yang, T. C., & Lee, M. (2012). Determination of perfluorocarboxylic acids in water by ion-pair dispersive liquid–liquid microextraction and gas chromatography–tandem mass spectrometry with injection port derivatization. *Analytica Chimica Acta*, *726*, 28–34. https://doi.org/10.1016/j.aca.2012.03.019

Luecken, D., Waterland, R. L., Papasavva, S., Taddonio, K. N., Hutzell, W. T., Rugh, J., & Andersen, S. O. (2009). Ozone and TFA Impacts in North America from Degradation of 2,3,3,3-Tetrafluoropropene (HFO-1234yf), A Potential Greenhouse Gas Replacement. *Environmental Science & Technology*, *44*(1), 343–348. https://doi.org/10.1021/es902481f

MacInnis, J. J., French, K., Muir, D. C. G., Spencer, C., Criscitiello, A. S., De Silva, A. O., & Young, C. J. (2017). Emerging investigator series: a 14-year depositional ice record of perfluoroalkyl substances in the High Arctic. *Environmental Science: Processes & Impacts*, *19*(1), 22–30. https://doi.org/10.1039/c6em00593d

Manojkumar, Y., Pilli, S., Rao, P. V., & Tyagi, R. D. (2023). Sources, occurrence and toxic effects of emerging per- and polyfluoroalkyl substances (PFAS). *Neurotoxicology and Teratology*, *97*, 107174. https://doi.org/10.1016/j.ntt.2023.107174

Martin, J. W., Mabury, S. A., Solomon, K. R., & Muir, D. C. G. (2003). Bioconcentration and tissue distribution of perfluorinated acids in rainbow trout (*Oncorhynchus mykiss*). *Environmental Toxicology and Chemistry*, *22*(1), 196–204. https://doi.org/10.1002/etc.5620220126

Menger, F., Pohl, J., Ahrens, L., Carlsson, G., & Örn, S. (2020). Behavioural effects and bioconcentration of per- and polyfluoroalkyl substances (PFASs) in zebrafish (Danio rerio) embryos. *Chemosphere*, *245*, 125573. https://doi.org/10.1016/j.chemosphere.2019.125573

National Oceanic and Atmospheric Administration (NOAA). (2022). What is ozone and where is it in the atmosphere?. Retrieved February 28, 2024, from https://www.weather.gov/media/shv/education_resource_library/atmosphere/Atmosphere_TeachersGuide.pdf

Nelson, B., & Kaminsky, D. B. (2021). A growing drive to get rid of cancer-linked “forever chemicals.” *Cancer Cytopathology*, *129*(1), 7–8. https://doi.org/10.1002/cncy.22403

Ogawa USA. (2014, April). Calculations for the concentration in ambient air. Retrieved February 26, 2024, from http://ogawausa.com/wp-content/uploads/2014/04/ConcentrationInAmbientAir_.pdf

Peters, A. J., Lane, D. A., Gundel, L. A., Northcott, G. L., & Jones, K. C. (2000). A comparison of high volume and diffusion denuder samplers for measuring semivolatile organic compounds in the atmosphere. *Environmental Science & Technology*, *34*(23), 5001–5006. https://doi.org/10.1021/es000056t

Pickard, H. M., Criscitiello, A. S., Spencer, C., Sharp, M., Muir, D. C. G., De Silva, A. O., & Young, C. J. (2018). Continuous non-marine inputs of per- and polyfluoroalkyl substances to the High Arctic: a multi-decadal temporal record. *Atmospheric Chemistry and Physics*, *18*(7), 5045–5058. https://doi.org/10.5194/acp-18-5045-2018

Place, B. K., Young, C. J., Ziegler, S. E., Edwards, K. A., Salehpoor, L., & VandenBoer, T. C. (2018). Passive sampling capabilities for ultra-trace quantitation of atmospheric nitric acid (HNO3) in remote environments. *Atmospheric Environment*, *191*, 360–369. https://doi.org/10.1016/j.atmosenv.2018.08.030

Possanzini, M., Di Palo, V., Gigliucci, P., Scianò, M. C. T., & Cecinato, A. (2004). Determination of phase-distributed PAH in Rome ambient air by denuder/GC-MS method. *Atmospheric Environment*, *38*(12), 1727–1734. https://doi.org/10.1016/j.atmosenv.2003.12.024

Prevedouros, K., Cousins, I. T., Buck, R. C., & Korzeniowski, S. H. (2005). Sources, Fate and transport of perfluorocarboxylates. *Environmental Science & Technology*, *40*(1), 32–44. https://doi.org/10.1021/es0512475

Pye, H. O. T., Nenes, A., Alexander, B., Ault, A. P., Barth, M. C., Clegg, S. L., Collett, J. L., Fahey, K. M., Hennigan, C. J., Herrmann, H., Kanakidou, M., Kelly, J. T., Ku, I., McNeill, V. F., Riemer, N., Schaefer, T., Shi, G., Tilgner, A., Walker, J. T., . . . Zuend, A. (2020). The acidity of atmospheric particles and clouds. *Atmospheric Chemistry and Physics*, *20*(8), 4809–4888. https://doi.org/10.5194/acp-20-4809-2020

Seinfeld, J. H., & Pandis, S. N. (2016). *Atmospheric Chemistry and Physics: From Air Pollution to Climate Change*. John Wiley & Sons.

Sha, B., Johansson, J., Salter, M., Blichner, S. M., & Cousins, I. T. (2024). Constraining global transport of perfluoroalkyl acids on sea spray aerosol using field measurements. *Science Advances*, *10*(14). https://doi.org/10.1126/sciadv.adl1026

Shafique, U., Schulze, S., Slawik, C., Kunz, S., Paschke, A., & Schüürmann, G. (2017). Gas chromatographic determination of perfluorocarboxylic acids in aqueous samples – A tutorial review. *Analytica Chimica Acta*, *949*, 8–22. https://doi.org/10.1016/j.aca.2016.10.026

Shoeib, M., Harner, T., Lee, S. C., Lane, D. A., & Zhu, J. (2008). Sorbent-Impregnated polyurethane foam disk for passive air sampling of volatile fluorinated chemicals. *Analytical Chemistry*, *80*(3), 675–682. https://doi.org/10.1021/ac701830s

Siegemund, G., Schwertfeger, W., Feiring, A. E., Smart, B. E., Behr, F. E., Vogel, H. A., & McKusick, B. C. (2000). Fluorine Compounds, organic. *Ullmann's Encyclopedia of Industrial Chemistry*. https://doi.org/10.1002/14356007.a11_349

Surma, M., Wiczkowski, W., Zieliński, H., & Cieślik, E. (2015). Determination of selected perfluorinated acids (PFCAs) and perfluorinated sulfonates (PFASs) in food contact materials using LC-MS/MS. *Packaging Technology and Science*, *28*(9), 789–799. https://doi.org/10.1002/pts.2140

Taniyasu, S., Kannan, K., Yeung, L. W. Y., Kwok, K., Lam, P. K., & Yamashita, N. (2008). Analysis of trifluoroacetic acid and other short-chain perfluorinated acids (C2–C4) in precipitation by liquid chromatography–tandem mass spectrometry: Comparison to patterns of long-chain perfluorinated acids (C5–C18). *Analytica Chimica Acta*, *619*(2), 221–230. https://doi.org/10.1016/j.aca.2008.04.064

Tao, Y., VandenBoer, T. C., Ye, R., & Young, C. J. (2023). Exploring controls on perfluorocarboxylic acid (PFCA) gas–particle partitioning using a model with observational constraints. *Environmental Science: Processes & Impacts*, *25*(2), 264–276. https://doi.org/10.1039/d2em00261b

Tsai, C., & Perng, S. N. (1998). Artifacts of ionic species for hi-vol PM10 and PM10 dichotomous samplers. *Atmospheric Environment*, *32*(9), 1605–1613. https://doi.org/10.1016/s1352-2310(97)00387-7

U.S. Environmental Protection Agency [EPA]. (2020). Method 537.1: Determination of Selected Per- and Polyflourinated Alkyl Substances in Drinking Water by Solid Phase Extraction and Liquid Chromatography/Tandem Mass Spectrometry (LC/MS/MS). Retrieved from https://cfpub.epa.gov/si/si_public_record_report.cfm?dirEntryId=348508&Lab=CESER&simpleSearch=0&showCriteria=2&searchAll=537.1&TIMSType=&dateBeginPublishedPresented=03%2F24%2F2018

Vierke, L., Ahrens, L., Shoeib, M., Reiner, E. J., Guo, R., Palm, W., Ebinghaus, R., & Harner, T. (2011). Air concentrations and particle–gas partitioning of polyfluoroalkyl compounds at a wastewater treatment plant. *Environmental Chemistry*, *8*(4), 363. https://doi.org/10.1071/en10133

Wang, Z., Cousins, I. T., Scheringer, M., Buck, R. C., & Hungerbühler, K. (2014). Global emission inventories for C4–C14 perfluoroalkyl carboxylic acid (PFCA) homologues from 1951 to 2030, Part I: production and emissions from quantifiable sources. *Environment International*, *70*, 62–75. https://doi.org/10.1016/j.envint.2014.04.013

Wania, F., & Shunthirasingham, C. (2020). Passive air sampling for semi-volatile organic chemicals. *Environmental Science: Processes & Impacts*, *22*(10), 1925–2002. https://doi.org/10.1039/d0em00194e

Wolf, S. T., & Reagen, W. K. (2011). Method for the determination of perfluorinated compounds (PFCs) in water by solid-phase extraction and liquid chromatography/tandem mass spectrometry (LC/MS/MS). *Analytical Methods*, *3*(7), 1485. https://doi.org/10.1039/c1ay05190c

Wong, F., Shoeib, M., Katsoyiannis, A., Eckhardt, S., Stohl, A., Bohlin-Nizzetto, P., Li, H., Fellin, P., Su, Y., & Hung, H. (2018). Assessing temporal trends and source regions of per- and polyfluoroalkyl substances (PFASs) in air under the Arctic Monitoring and Assessment Programme (AMAP). *Atmospheric Environment*, *172*, 65–73. https://doi.org/10.1016/j.atmosenv.2017.10.028

Wu, J., Martin, J. W., Zhai, Z., Lu, K., Li, L., Fang, X., Jin, H., Hu, J., & Zhang, J. (2014). Airborne Trifluoroacetic Acid and Its Fraction from the Degradation of HFC-134a in Beijing, China. *Environmental Science & Technology*, *48*(7), 3675–3681. https://doi.org/10.1021/es4050264

Wu, S., Anumol, T., Gandhi, J., & Snyder, S. A. (2017). Analysis of haloacetic acids, bromate, and dalapon in natural waters by ion chromatography–tandem mass spectrometry. *Journal of Chromatography A*, *1487*, 100–107. https://doi.org/10.1016/j.chroma.2017.01.006

Ye, G., Fang, Y., Zhang, G., Ni, H., Youxiang, Z., Han, X., & Chen, G. (2021). Experimental Investigation of Vapor–Liquid Equilibrium for 2,3,3,3-Tetrafluoropropene (HFO-1234yf) + *trans*-1,3,3,3-Tetrafluoropropene (HFO-1234ze(E)) at Temperatures from 284 to 334 K. *Journal of Chemical & Engineering Data*, *66*(4), 1741–1753. https://doi.org/10.1021/acs.jced.0c01033

Yeung, L. W. Y., Dassuncao, C., Mabury, S. A., Sunderland, E. M., Zhang, X., & Lohmann, R. (2017). Vertical profiles, sources, and transport of PFASs in the Arctic Ocean. *Environmental Science & Technology*, *51*(12), 6735–6744. https://doi.org/10.1021/acs.est.7b00788

You, Y., Renbaum-Wolff, L., Carreras-Sospedra, M., Hanna, S., Hiranuma, N., Kamal, S., Smith, M. L., Zhang, X., Weber, R. J., Shilling, J. E., Dabdub, D., Martin, S. T., & Bertram, A. K. (2012). Images reveal that atmospheric particles can undergo liquid–liquid phase separations. *Proceedings of the National Academy of Sciences of the United States of America*, *109*(33), 13188–13193. https://doi.org/10.1073/pnas.1206414109

Young, C. J., & Mabury, S. A. (2010). Atmospheric perfluorinated Acid Precursors: Chemistry, occurrence, and impacts. In *Reviews of Environmental Contamination and Toxicology* (pp. 1–109). https://doi.org/10.1007/978-1-4419-6880-7_1

Young, C. J., Furdui, V. I., Franklin, J. M., Koerner, R. M., Muir, D. C., & Mabury, S. A. (2007). Perfluorinated acids in Arctic snow: new evidence for atmospheric formation. *Environmental Science & Technology*, *41*(10), 3455–3461. https://doi.org/10.1021/es0626234

Young, C., & VandenBoer, T. (2023, October 9). *Separations and selectivity for measurements of atmospheric PFAS*. Separation Science. Retrieved from https://www.sepscience.com/separations-and-selectivity-for-measurements-of-atmospheric-pfas/

Zhan, F., Shunthirasingham, C., Li, Y., Oh, J., Lei, Y. D., Chaaben, A. B., Castilloux, A. D., Lu, Z., Lee, K., Gobas, F. A., Alexandrou, N., Hung, H., & Wania, F. (2023). Sources and environmental fate of halomethoxybenzenes. *Science Advances*, *9*(41). https://doi.org/10.1126/sciadv.adi8082

Zhang, X., Saini, C., Pohl, C. A., & Liu, Y. (2020). Fast determination of nine haloacetic acids, bromate and dalapon in drinking water samples using ion chromatography–electrospray tandem mass spectrometry. *Journal of Chromatography A*, *1621*, 461052. https://doi.org/10.1016/j.chroma.2020.461052

Chapter Two: Method development and validation of gas-phase PFCAs nylon-based passive air samplers using an atmospheric chamber for calibration.

E. Vanhauwaert[1], L. R. Crilley[1], C.J. Young[1], and T.C. VandenBoer[1]

[1]Department of Chemistry, York University, Toronto, ON, Canada.

Author Contributions:

EV prepared with CJY and TCV editing the chapter/manuscript.

CJY and TCV conceptualized the work and acquired the funding. CJY and TCV provided the resources to support this work.

EV and LC conceptualized the design of the chamber components and conducted all the chamber experiments.

EV performed all other experiments, sample collection and analysis under the guidance of CJY and TCV.

This chapter is formatted in preparation for publication.

2.1 Introduction

2.1.1 Current PFCAs sampling limitations

Perfluorocarboxylic acids have been found to be ubiquitous in the environment, even though they are not naturally occurring (Joudan et al., 2021a; Wong et al., 2018). Their chemical stability has prevented them from degrading in the environment and some PFCAs have been found to be harmful to mammals even at low concentrations (Elis et al., 2004; Prevedouros et al., 2006). Transport of PFCAs through the atmosphere is a major pathway for global contamination (Tao et al., 2023; Wong et al., 2018). The importance of studying the movement and fate of perfluorocarboxylic acids (PFCAs) in the atmosphere has led to the need for atmospheric measurements of these compounds (Wong et al., 2018). Most previous atmospheric PFCA measurements involved using high volume air samplers. This technique collects both gaseous and particulate PFCAs to better understand how these compounds distribute between gas and particle phases in the atmosphere (Ahrens et al., 2011a). However, these samplers were found to have significant flaws, including the generation of artifacts (Ahrens et al., 2011a). Although diffusion denuder samplers helped address these issues, they came with their own set of operating challenges such as being high-cost, labour-intensive, intrusive and requires a power source. These challenges have hindered large-scale measurements of PFCAs and limited the availability of sampling locations.

In contrast, passive air samplers (PAS) have been employed by scientists and air quality analysts for many years to overcome various challenges associated with active sampler methods (Górecki & Namieśnik, 2002). They offer several advantages, such as affordability, low labour, non-intrusiveness, compact size, independence from a power source, and ease of use (Place et al., 2018). These features make them suitable for challenging deployments, including in remote areas, and in large numbers to capture different -spatial scale changes in environmental concentrations. PAS operate by having the analytes of interest sorb onto a collecting medium (Górecki & Namieśnik, 2002), which occurs either due the analytes preferentially partitioning onto the collecting medium or through a reactive uptake process (Górecki & Namieśnik, 2002; Roadman et al., 2003).

A few studies have explored the use of PAS with Polyurethane Foam Disks (PUF), different types of XAD resin, or a combination of both for sampling PFCAs (Karásková et al., 2018; Shoeib et al., 2008). However, the sorption of PFCAs onto PUF was generally found to be low, with PUF disks reaching partitioning equilibrium for most compounds after just one

day (Shoeib et al., 2008). Although the addition of XAD embedded resin improved this by approximately two orders of magnitude, several challenges remained (Shoeib et al., 2008). A linear sampling uptake was observed for only several weeks, limiting their usefulness for long-term sampling (Shoeib et al., 2008). Additionally, these PAS required extensive sample preparation involving hours of Soxhlet, a continuous extraction method for compounds from solids using solvents, and further time for concentrating the extract using rotary evaporation under nitrogen gas (Ahrens et al., 2011b). While reported spike and recovery values, representing the percentage of spiked compounds in a real sample recovered by the extraction method, for PFCAs in these samplers ranged from 71 % to 113 %, these values had been corrected using mass-labeled internal standards and did not represent a true recovery (Karásková et al., 2018). Furthermore, the offline method analysis for these samplers did not sample some of the ultra-short-chain PFCAs, such as trifluoroacetic acid (TFA) and perfluoropropionic acid (PFPrA), which are known to be present in atmospherically-derived samples at much higher levels then PFCAs with 4 carbons or more (≥C4) (Ahrens et al., 2011b; Scott et al., 2006; Tao et al., 2023). Thus, there is a need for a different type of passive air sampler and analysis method to address these challenges, especially considering the unique reactive acid properties of PFCAs which have not been targeted by PAS methods to date.

2.1.2 Measurement of gas-phase atmospheric acids using nylon-based passive air samplers

Nylon-based passive air samplers have been established as effective collectors of atmospheric acids. The suitability of nylon, a polyamide material, as a collecting medium for atmospheric acids dates back to the 1980s when it was found to efficiently collect gases like hydrochloric acid and nitric acid ($HNO_{3\,(g)}$) (Perrino et al., 1988; Sturges & Harrison, 1989). Since then, nylon has been used as a collection medium in PAS for the collection of $HNO_{3\,(g)}$ in the atmosphere (Bytnerowicz et al., 2005; Bytnerowicz et al., 2001; Place et al., 2018). Unlike PUF-XAD-based PAS, the extraction process for nylon-based PAS is minimal and the nylon sorbents have been demonstrated to be reusable (Ahrens et al., 2011b; Place et al., 2018). These samplers were first calibrated for $HNO_{3\,(g)}$ using a continuous stirred tank (Padgett et al., 2004) and deployed in the southern California with $HNO_{3\,(g)}$ levels ranging from 1.7-4.1 $\mu g/m^3$ (0.6-1.7 ppb_v) (Bytnerowicz et al., 2005). They were later launched in remote regions of Newfoundland and Labrador, where $HNO_{3\,(g)}$ was detected as low as 9 ppt_v during a 35-day period or longer, demonstrating their ultra-trace capabilities (Place et al., 2018). Considering PFCAs are strong atmospheric acids and are found at ultra-trace levels, these nylon-based PAS

present a promising option for sampling gas-phase PFCAs. Nylon-based passive samplers, which have been well-characterized for collecting $HNO_{3\,(g)}$ in the atmosphere (Place et al., 2018), have been applied to $PFCAs_{(g)}$ in a preliminary study (Carmichael, 2022). $TFA_{(g)}$ was detected in the nylon-based PAS extracts in Toronto and Halifax, while other $PFCAs_{(g)}$ were found to be below the detection limits. These findings are promising, as the nylon-based PAS successfully quantified TFA, the dominant $PFCA_{(g)}$ in the atmosphere. However, the study did not assess the extraction efficiency of TFA, and the accuracy of the predictive dose-response for PFCAs in these samplers remains uncertain. Thus, calibration of these samplers for PFCAs is required.

Calibration of gas-phase samplers can be performed by controlled chamber experiments or by orthogonal measurements in the field, where orthogonal measurements are defined as independent measurements of the same compound(s) using fundamentally different sampling and/or techniques. The prior calibration technique is preferred as values obtained from orthogonal field measurements can be subject site-specific variability caused by factors such as winds speeds and air temperatures, which may hinder the applicability of the data under different circumstances (Tromp et al., 2019). Controlled chamber calibrations provide more time flexibility, where several measurements at different mixing ratios can be performed in a much shorter period. This allows for the possibility of a more robust calibration across the dynamic range of expected environmental concentrations. Denuders have been used as an orthogonal sampling technique to calibrate nylon-based PAS for gas-phase HNO_3, both in the field and using an atmospheric chamber (Bytnerowicz et al., 2005, Carmichael, 2022, Place et al., 2018). This sampling technique has also been used to quantify gas-phase PFCAs, even though it has not yet been fully validated for sampling gas-phase PFCA (Ahrens et al., 2011a; Wu et al., 2014). Despite this, the use of denuders for calibrating PFCAs is considered the best option available to date which overcomes sampling biases from previous sampling techniques (Ahrens et al., 2011a; Tao et al., 2023).

2.1.3 Objectives

The goal of this work is to validate the use of nylon PAS for $PFCAs_{(g)}$ by calibrating the PAS and validating an extraction method, which are then paired with established quantitative techniques. The calibration was conducted for TFA using our in-house atmospheric chamber with gas mixtures controlled through a combination of $PFCA_{(g)}$ permeation devices and a zero-air generator. The dose-response of other PFCAs was predicted using Graham and Fuller's law based off the TFA calibration. Positive and negative controls on the PAS sampler

method steps were performed to ensure efficient extraction of PFCAs and to remove contamination bias. This resulting method provides a validated $TFA_{(g)}$ sampling method that overcomes many of the current challenges for this measurement such as selectivity, dynamic range including ultra-trace detection limits, sampling site selection, and maintenance requirements, while also minimizing costs.

2.2 Methods

2.2.1 Materials and chemicals

Sodium carbonate (Na_2CO_3) (>99.5%), Glycerol (>99%), Dichloromethane (DCM; ACS reagent Grade) and NaOH stock solution (49-51% in DIW) were obtained from Sigma Aldrich. Methanol of both HPLC and Optima® LC-MS grades were obtained from Fisher Chemical. The purchase of TFA (HPLC grade) was made from EMD Millipore (MA, US); PFPrA, PFBA and PFPeA (>97%) were purchased from Sigma Aldrich (MO, US); PFHxA (>97%) from Synquest, (FL, US). Stock solutions of native PFCAs for GC-MS were prepared in ethyl acetate (EtAc; HPLC Grade; Anachemia VWR, PA, US) at 500 µg/mL, which were diluted to working stock concentrations. Mass-labeled $^{13}C_2$-TFA (>97%) was purchased from Toronto Research Chemicals; $^{13}C_3$-PFBA, $^{13}C_2$-PFOA, and $^{13}C_2$-PFDA were purchased as a mixture in MeOH (2 µg/mL; MPFAC-C-IS) from Wellington Laboratories. These compounds were combined into one methanol (MeOH) solution and used as internal standards (IS) for GC-MS analysis. The sodium salts of TFA (>98%) and PFPrA (>99%) were obtained from Sigma Aldrich. Stock solutions for IC-CD analysis of these salts were prepared in Milli-Q water at 1000 µg/ml, which were diluted to working stock concentrations. Ultrapure Milli-Q water (18.2 MΩ·cm at 25 °C) was obtained from an in-house system (Direct 8; EMD Millipore). Diphenyl diazomethane (DDM; >90%) was synthesized in-house using established methods (Javed & Brewer, 2007) or purchased from Toronto Research Chemicals (ON, Canada), but at a lower purity (Ye et al., 2023).

2.2.2 Atmospheric Chamber and Zero-Air Generator components

To effectively calibrate our nylon-based PAS for TFA, its sampling rate needs to be established using orthogonal measurements such as denuders, the best sampling technique to date for gas-phase PFCAs. Ideally, these experiments should be performed under controlled conditions to minimize the bias that may come from changes in temperature, humidity levels and different wind speeds. This can be achieved by using a chamber that contains consistent and relevant TFA mixing ratios and humidity levels. Concentrations of TFA within the chamber

will be atmospherically relevant, but also higher than typical outdoor levels to allow calibration experiments to be performed within a few days rather than a few weeks or months which will facilitate numerous experiments across a wide dynamic range to be performed. Known gas mixtures of TFA were produced and introduced into the atmospheric chamber where the extent of dilution is controlled by a zero-air generator and the levels are monitored by an annular denuder (Figure 2.1).

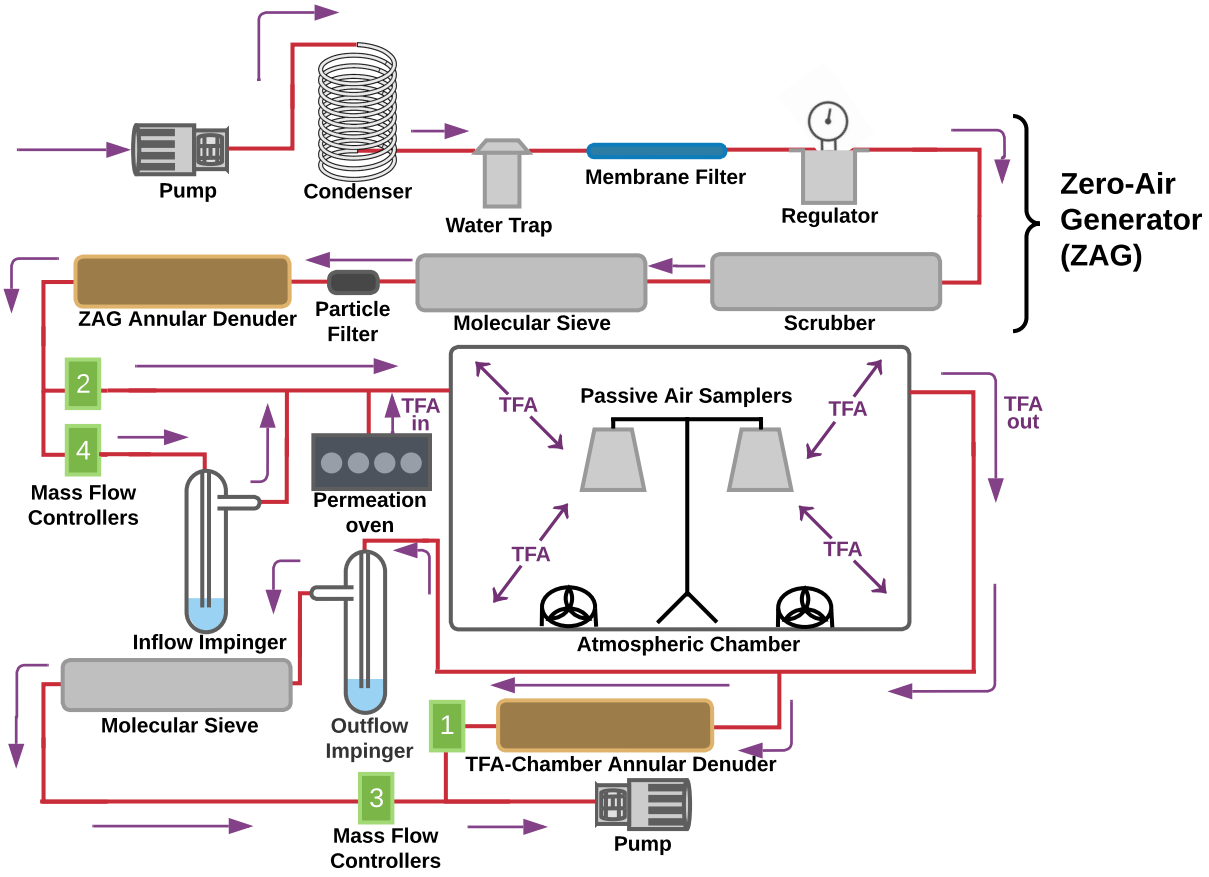

Figure 2.1: Components of the atmospheric chamber to create known amounts of gas phase TFA to calibrate the passive air samplers. Purple arrows indicated the direction of air flow.

This follows previous work that employed the use of a different chamber configuration to calibrate nylon PAS for $HNO_{3\,(g)}$ (Bytnerowicz et al., 2005; Padgett et al., 2004). Our chamber setup was developed in-house, with certain components of the zero-air generator adapted from Crilley et al. (2023) (Figure 2.1). The condenser, water trap, membrane filter, regulator, scrubber, molecular sieve, particle filters and ZAG annular denuder are part of a zero-air generator (ZAG). All the gas handling lines in the chamber system are composed of ¼" perfluoroalkoxy alkane (PFA) tubing (51805K72, McMaster Carr, Aurora, OH, U.S.A) an inert material that minimizes surface adsorption of polarizable molecules. The pumps push and pull air through the system following the direction of the purple arrows (Figure 2.1), starting with

room air being pulled towards the condenser. The regulator (SMCAR20KN02HZB / Regulator, Modular, ¼" NPT, Proax Technologies Ltd) controls the pressure delivered by the system, so that the mass-flow controllers (MFC, MKS Instruments, Inc.; M100B00814CS1BV, M100B24CS1BV, M100B00813CS1BV and S/N 1162B01322184; 10 SLPM, 20 SLPM, 1 SLPM and 10 SLPM) can accurately deliver the rate of gas flow through the system. The condenser and the water trap (SMCAF20N02CCZA / Filter, Modular, ¼" NPT, 5 μm, Float Auto Drain, Metal Bowl Guard, Proax Technologies Ltd) reduce the water vapour content of the gas flow. The membrane dryer (SMC membrane dryer, SMCIDG1N02, Proax Technologies Ltd) removes much of the remaining of water vapour in the air flow, which then enters the scrubber composed of equal amounts of Purafil SP®, Purakol® & Puracarb® (Purafil, incorporated, Doraville, GA, USA). This mixture removes NO_x, sulphur dioxide (SO_2), ozone (O_3), ammonia (NH_3) and volatile organic compounds (VOCs). The molecular sieve (moisture filter, S/N C237248, Thermo Scientific) scrubs out any remaining water vapour and VOCs. The particle filter (Swagelok, P/N B-4F2-15, 15 μm) ensures any suspended solid material generated by this system is removed from the final gas flow. This then flows into the ZAG annular denuder, coated with Na_2CO_3, to ensure any trace gas-phase acids present are quantitatively removed. The flow then passes through the inflow impinger which contains PFCA-free water (i.e. Milli-Q water extracted with Strata X-AW sorbents; 6 mL × 200 mg × 33 μm; Phenomenex, CA, US) to precisely control the relative humidity of the gas flow while ensuring the system is free of PFCA contamination. The permeation oven then introduces a consistent known amount of gas-phase TFA. The atmospheric chamber (Welch Fluorocarbon, Inc., Custom Teflon™ Simulation Chamber, 4165, 48"×48"×48") is composed of transparent PFA, an inert material. Clips (Welch Fluorocarbon, Inc., Clip-n-Seal® Large Closure Device, P00020-21-LA) were used to seal the access sleeve of the chamber when in use and gases were flowing through it. Retort stands to hold the passive samplers were inserted through the access sleeve, as were fans (Orion fans, OA4715-12TB) which were used to keep the air in the chamber well mixed to prevent concentrations gradients from developing within the chamber. The atmospheric chamber was also outfitted with a Pimoroni Enviro+ low-cost sensor (ONA47D9XCF) to measure the humidity and temperature in the chamber. On the outflow of the chamber, the TFA-chamber annular denuder is used to collect and quantify gas-phase TFA in the chamber, as this compound was expected to undergo interactions with the chamber walls, reducing the available mixing ratio compared to what would be expected if we relied on the quantified permeation rate alone (Krechmer et al., 2020; Matsunaga & Ziemann, 2010; Zhang

et al., 2014). The outflow impinger is used as a final gas scrubber followed again by molecular sieve to prevent water vapour from condensing in the MFC controlling the outflow or in the associated pump. The developed standard operation procedure for conducting calibrations using the atmospheric chamber can be found in Section S2.1 in Appendix A.

2.2.3 Permeation devices and permeation oven

Our established in-house procedure for making custom made permeation devices, as well as the use of our custom-built permeation ovens, described by Lao et al. (2020), was used to generate gas-phase TFA for the calibration experiments. First, a 9 cm PFA tube (3.2 mm i.d. with 5 mm o.d., PN: 5733K73; McMaster-Carr, Aurora, OH) is treated with a high temperature heat gun, so that it can be welded shut with a 1 cm PTFE plug (3.2 mm diameter, PN: 84935K64; McMaster-Carr) on one end and left to cool. Approximately 400 µL of a 1:1 (v/v) TFA:Milli-Q Water mixture is added to the open end of the tube, which is then sealed in the same manner. A 3:7 TFA:Milli-Q Water (v/v) permeation tube was also made. The permeation tube is placed in a ½" PFA tube (PN: 51805K11, McMaster Carr, Aurora, OH, U.S.A) housed inside a custom-fabricated aluminum oven block which is heated to 60 °C using a PID temperature controller (Omega™; CN 7823, Saint-Eustache, QC, Canada) connected to a cartridge heater with integrated thermocouple. At the inflow end of the PFA tube is a critical orifice connected to a nitrogen gas line (Linde, high-purity nitrogen, 99.998%, PP 4.8, Toronto, ON) which controls the flow through the oven (Figure 2.2).

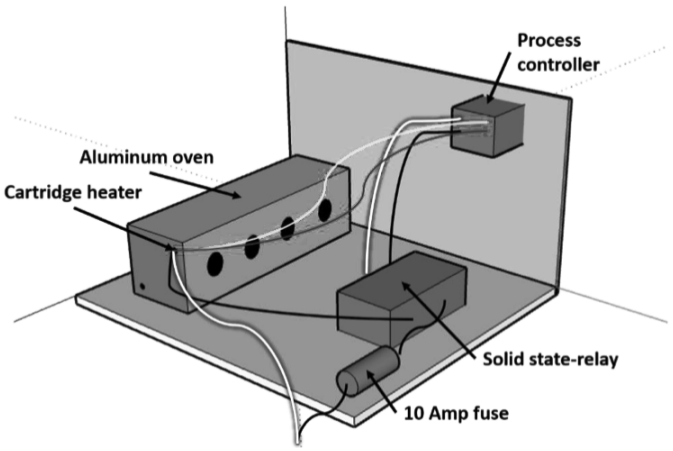

Figure 2.2: Permeation oven schematic, modified from Furlani (2021).

The outflow can be delivered to an experimental setup like the atmospheric simulation chamber, or simply scrubbed into a Nalgene bottle containing Milli-Q water when stabilizing its output upon system start-up, between experiments, or to quantify the output. For the latter, the bubbler solution can be analyzed by IC-CD to determine the permeation rate.

2.2.4 Nylon-based passive air samplers' components, sample preparation and extraction

Our group's custom-built nylon-based passive air samplers (PAS) are based on an adaptation from the design presented by Place et al. (2018). They have previously been used to measure ultra-trace levels of $HNO_{3\,(g)}$ and are applied to measure $PFCAs_{(g)}$ in this study. The filter pack sampler assembly is composed of one nylon membrane filter (47 mm, 0.45 µm, Sartorius, Fisher Scientific, P/N 2500647N), one polypropylene (PP) filter (47mm, 2.0 µm, Tisch, Tisch Scientific, SKU: SF14908), one petri dish (60 x 15 mm, Fisher Scientific), two PTFE rings (52 x 2 mm, McMaster Carr, P/N 8547K33), and one polycarbonate ring (53 x 4 mm, McMaster Carr, P/N 8486K541) (Figure 2.3) (Carmichael, 2022).

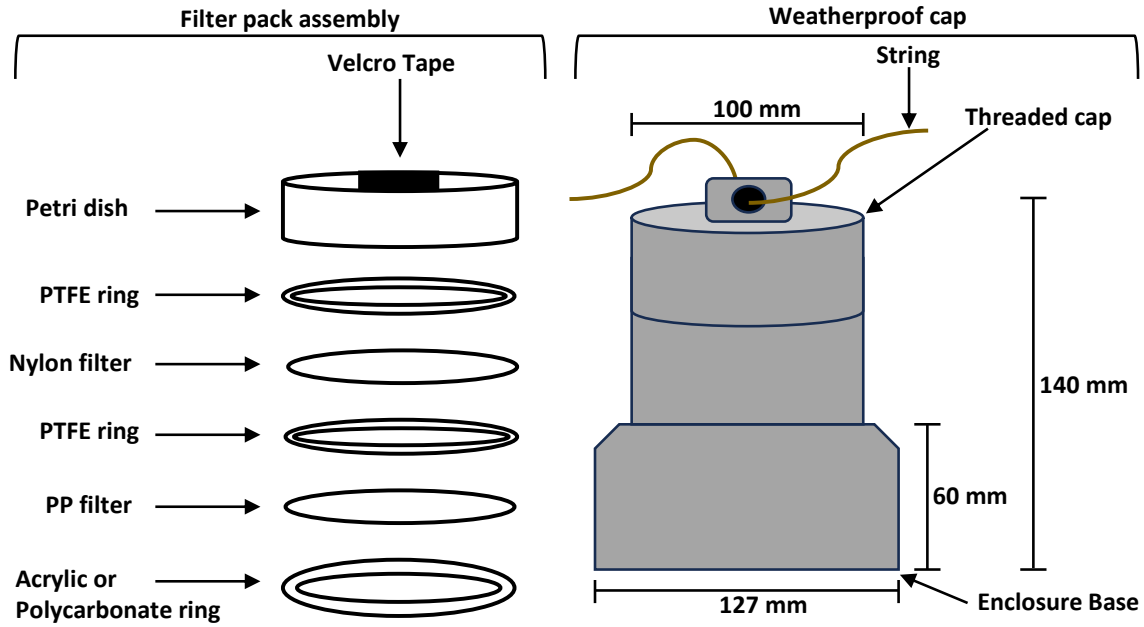

Figure 2.3: PAS sampler components, adapted from Carmichael (2022).

The PTFE and PP materials were used as inert surfaces to minimize sorption bias. Weatherproof enclosures are used to help protect the filter pack assembly from strong winds that would cause sampling to diverge from diffusion alone, from precipitation which may introduce contaminants and alter the sampling rate, and to reflect sunlight to reduce light absorption that would lead to a higher temperature in the filter pack assembly compared to the temperature of ambient air. Atmospheric acids, including PFCAs, sorb onto the nylon filters through an acid-base reaction, with a proposed mechanism illustrated in Figure 2.4.

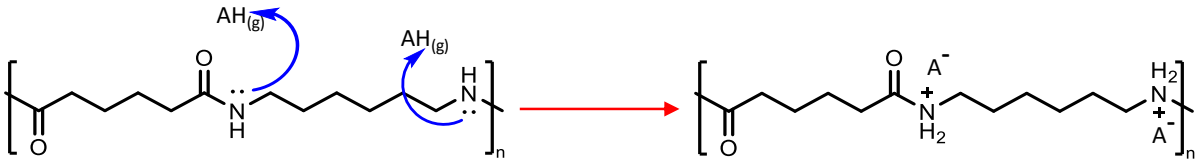

Figure 2.4: Proposed reactive uptake mechanism of atmospheric acids to nylon filters.

The PP filter, a deactivating material, physically blocks particles from reaching the nylon to create contamination. This allows gas molecules, inclusive of acids, to permeate through the material pores (K_D) (Figure 2.5) followed by selective adsorption of acids on the nylon filters.

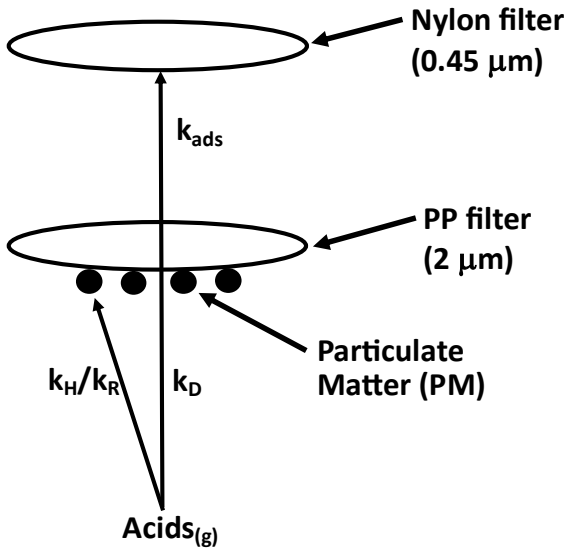

Figure 2.5: Diffusion and uptake of PFCAs in PAS, adapted from Place et al. (2018).

A concentration gradient is created between the PP filter, facilitating the continuous diffusion of acids to the nylon sampling substrate (Figure 2.4). The sampling uptake rate of acids may be reduced by the solubilization (k_H) or reactive uptake (k_R) of gas-phase acids to the PP filters when water or particulate matter (PM) have been accumulated (Figure 2.5) (Bytnerowicz et al., 2005; Place et al., 2018). Details on our custom-made passive air sampler standard operating procedures of our passive air samplers have been revised in this work and are below.

The following washing, assembling and extraction procedures of PAS are adapted from Place et al. (2018), where we have replaced their protective PTFE filters with PP filters, as the former could be a source of PFCA contamination from the release of processing aids or oxidative aging of the material. A cleaning procedure for the polypropylene filters (PP) that was effective needed to be developed. They were rinsed 6 times in a 1 L polypropylene Nalgene® container with DIW and then soaked in DIW for 12 h then rinsed an additional 6 times and soaked again. nylon membrane filters were similarly rinsed 6 times in a polypropylene container with ultrapure DIW. Nylon membrane filters are soaked for a

minimum of 12 h in 0.015 M of Na_2CO_3 to displace any bound acid impurities. Nylon membrane filters were then rinsed again 6 times with DIW and soaked in DIW for a minimum of an additional 12 h. Both types of filters are then air dried for 2 h between two Kim wipes before being installed into filter pack assemblies.

PAS are assembled with clean gloves and tweezers. The rings are added to the petri dishes with the nylon and PP filters tightly secured between the rings. The PAS are capped to form covered petri dishes, with the covers secured using lab tape to reduce entry of analytes into the devices, and then placed into sealed Ziploc bags and refrigerated to reduce diffusive sampling of any analytes within the Ziploc bag until deployment.

At sampling locations, including within the experimental chamber, the passive samplers are removed from the Ziploc bags, separated from the petri dish caps, and then secured at the top of the weather shield using adhesive Velcro, as shown in Figure S2.1, found in Appendix A. The weather shields are hung on a stable structure. Removing the passive samplers from the shields during sample collection occurs in the reverse order of Figure S2.1. Field blanks are transported to the sampling locations, exposed to the surrounding air for 10 seconds, then reconnected to the petri dish caps and placed back into the Ziploc bags.

For extraction of the PAS samples and blanks, 15 mL Falcon® Conical tubes are first rinsed six times with DIW and once with HPLC MeOH. Nylon filters are taken out of the passive samplers with DIW-cleaned tweezers and gently rolled to transfer into the Falcon® Conical tubes. For IC-CD analysis, 3 or 4 mL of 3 mM NaOH in DIW is added to the tubes containing the nylon filters and sonicated for 15 min to extract the analytes. The filters in the extraction solvent are stored in a fridge overnight to improve the extraction efficiency under cold conditions and the filters are removed from the extracts once taken out of the fridge. The likely reason for our observed improvement is suspected to be because colder temperatures lead to a larger ionic hydrated ion radius. This makes the analytes less readily retained by the stationary phase as the larger hydrated radius will reduce the overall charge density of a given ion (Harris & Lucy, 2015). The samples are now ready for IC-CD analysis. For GC-MS analysis, 4 mL of 0.1 M NaOH in Optima® methanol is added to the Falcon® Conical tube containing nylon filters and sonicated for 15 min. In either extraction, the filters are removed prior to analysis or further sample preparation. Internal standards are added prior to sample preparation for GC-MS analysis, adapted from the method of Ye et al. (2023). Nylon filter extracts in 0.1 M NH_4OH in MeOH are blown down with nitrogen gas at 30 °C. Samples were

reconstituted in 500 µL of ethyl acetate and 500 µL DCM. Ten microliters of 0.1 M diphenyl diazomethane (DDM) in DCM is added to derivatize the extracted PFCA analytes as depicted in Figure S2.2. The tubes are twice vortexed for 10 s and sonicated for 15 min to promote the reaction. The samples are now ready to be injected onto the GC-MS.

2.2.5 Multi-channel annular denuder components sample preparation and extraction

University Research Glassware, Corp. (URG) multi-channel annular glass denuders in aluminum sleeves (URG-2000-30x150-3CSS, URG-2000-30x242-3CSS; Chapel Hill, NC, USA) were used. The following procedure used our established in-house procedure for quantitative and contamination-managed PFCA collection, described by Ye et al. (2023) which is modified from the EPA Compendium Method IO-4.2 (Winberry et al., 1999). They are uncapped from the inflowing side and DIW was added. The denuders were recapped and inverted while rotating several times, being careful not to shake the fragile denuders. The denuders were uncapped and emptied. This was repeated 4 more times then followed by 5 mL of HPLC methanol. The annular denuders were dried using zero air (Linde, ultra-zero air, purity 0.0UZ, Toronto, ON) at 2.5 L/min for at least 15 min. Following this, they are uncapped on the inflowing side where the flow straightener is located and 15 mL of denuder coating (20 g/L Na_2CO_3 & 10 g/L glycerol in 1:1 (v/v) DIW:Optima MeOH) was added. The denuders were recapped and inverted while rotating several times then excess coating solution was emptied. The denuder coatings were then dried using zero air at 2.5L/min for at least 15 min. Annular denuders are then capped and stored until sampling began. Sampling with these devices is performed by connecting both ends to ¼" PFA tubing and pulling air through the device close to ~8.5 L/min to ensure quantitative collection according to their design. Denuders are recapped once the sampling period is finished. For the extraction of annular denuders, 15 mL Falcon® Conical tubes are first washed six times with DIW and once with HPLC MeOH. To extract, 5 mL of DIW are added to the flow straightener end of the denuder, then recapped and rotated while inverting several times. The extract was poured into the clean falcon tube and the process was repeated a second time. The denuder extracts were then diluted 20x to eliminate matrix effects when analyzed by IC-CD.

2.2.6 Ion chromatography with conductivity detector (IC-CD)

The ion chromatography system with conductivity detector is composed of a Dionex™ ICS-3000 system outfitted with dual pump (DP) and dual column and detector (DC) compartments. The autosampler uses a syringe connected to an autosampler sample handling

loop to inject 300 µL on a Thermo Scientific™ Dionex™ IonPac™ TAC-ULP1 anion-selective concentrator column (5×23mm, 18 µm dp, 6% DVB) or 250 µL to a sample loop flushed with an additional 250 µL of the sample to prevent carry over and/or losses of analytes. A Thermo Scientific™ Dionex™ IonPac™ AG23 guard (4×50mm, 11 µm dp) and AS23 analytical column combination (4×250 mm, 6 µm dp, 55% DVB, alkanol quaternary ammonium exchanger) was used for the separation. The flow rate and gradient used for the separation is as follows: 1 ml/min, 1mM NaOH in DIW for 10 min, increased from 1 mM to 2 mM NaOH for 1 min, kept at 2 mM NaOH for 14 min, increased from 2 mM to 20 mM of NaOH for 1 min, kept at 20 mM for 6 min, decreased from 20 mM NaOH to 1 mM NaOH for 1min. Column temperature was set to 15 °C. A 4 mm Thermo Scientific™ Dionex™ ADRS 600 Dynamically Regenerated Suppressor was operated in recycled eluent mode at a current of 55 mA to remove Na^+ from and neutralize OH^- in the column effluent before reaching the conductivity detector. A Thermo Scientific™ Dionex™ Conductivity Detector was operated at 34 °C with a data acquisition rate of 5 Hz.

2.2.7 Gas chromatography with mass spectrometer (GC-MS)

An Agilent 7890 A gas chromatograph coupled to a 5975c mass spectrometer was used with a CTC Combi PAL autosampler, along with a hydrogen (H_2) generator (model QL-500A, Shandong Saikesaisi Hydrogen Energy Co. Ltd., Shandong, China) following our in-house optimized methodology (Ye et al., 2023). Briefly, the autosampler used a 10 µL syringe to make 1 µL pulsed (25 psig) splitless injections. An HP-5MS column (5% phenyl methyl-polysiloxane, 0.18 µm × 0.18 mm × 20 m) was used for the separation of the derivatized analytes. The flow rate and programmed temperature gradient are as follows: H_2 gas at 1 mL/min, 65 °C for 0.5 min than 30 °C/min until 130 °C and held for 2 min, then 35 °C/min until 270 °C and held for 2 min before returning to initial conditions. The inlet and MS transfer line temperatures were 240 and 250 °C, respectively. The MS was operated in ECNI mode with methane as the reagent gas in selected ion monitoring (SIM), with a measured mass range up to 1050 amu, and selected ion monitoring (SIM). The source and quadrupole were operated at 150 °C.

2.3 Results and discussion

2.3.1 Ion chromatography with conductivity detector method and optimisation

An on-demand analysis method with little to no sample preparation is required to monitor the chamber experiments with little delay. Ion-chromatography with conductivity detection was chosen as the analysis method for this reason. Figure 2.6 demonstrates the separation of TFA from unidentified compounds in the chamber sample. While TFA does co-elute with PFPrA with the current 15 °C method (Figure S2.3 in Appendix A), PFPrA was not expected to be detected in chamber samples as the composition was carefully controlled.

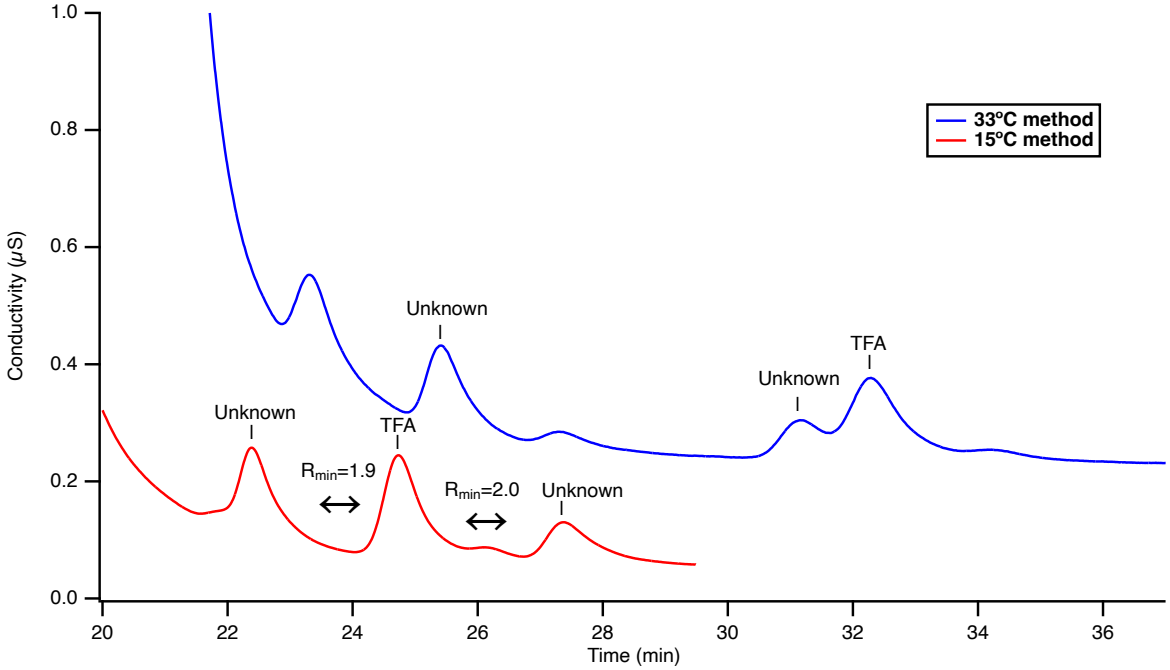

Figure 2.6: Chromatogram of TFA separation in a chamber sample. If PFPrA were present in the sample, it would be expected to elute at 36 min in the 33°C method and at 25.5 min in the 15°C method, as in Figure S2.3 found in Appendix A.

To confirm this, the same separation as the method outlined in Section 2.2.7 was performed except at a temperature of 33 °C and the 2 mM of NaOH was held for 11 min longer. This gradient and temperature have been shown to give good resolution between TFA and PFPrA (Figure S2.3 in Appendix A) but poor separation between TFA and the unidentified compounds (Figure 2.6). PFPrA was not detected at its expected retention time in the chamber sample when subject to the alternative method with PFPrA selectivity as shown in Figure 2.6.

Concentrator columns are used in ion chromatography systems to concentrate analytes when using large sample volumes, often ranging from 0.5-2 mL, prior to injection on the

analytical columns (Haddad, 1988; Thermo Fisher Scientific, 2022). In contrast to samples loops, concentrator columns can on-column focus the analytes while partially eluting weaker bound matrices such as OH^- (Thermo Fisher Scientific, 2022). This prevents peak-broadening when injecting large sample volumes. Figure 2.7 demonstrates the peak areas of TFA when injecting different amounts of TFA with large amounts OH^- ions as acting as competing ions to the binding sites.

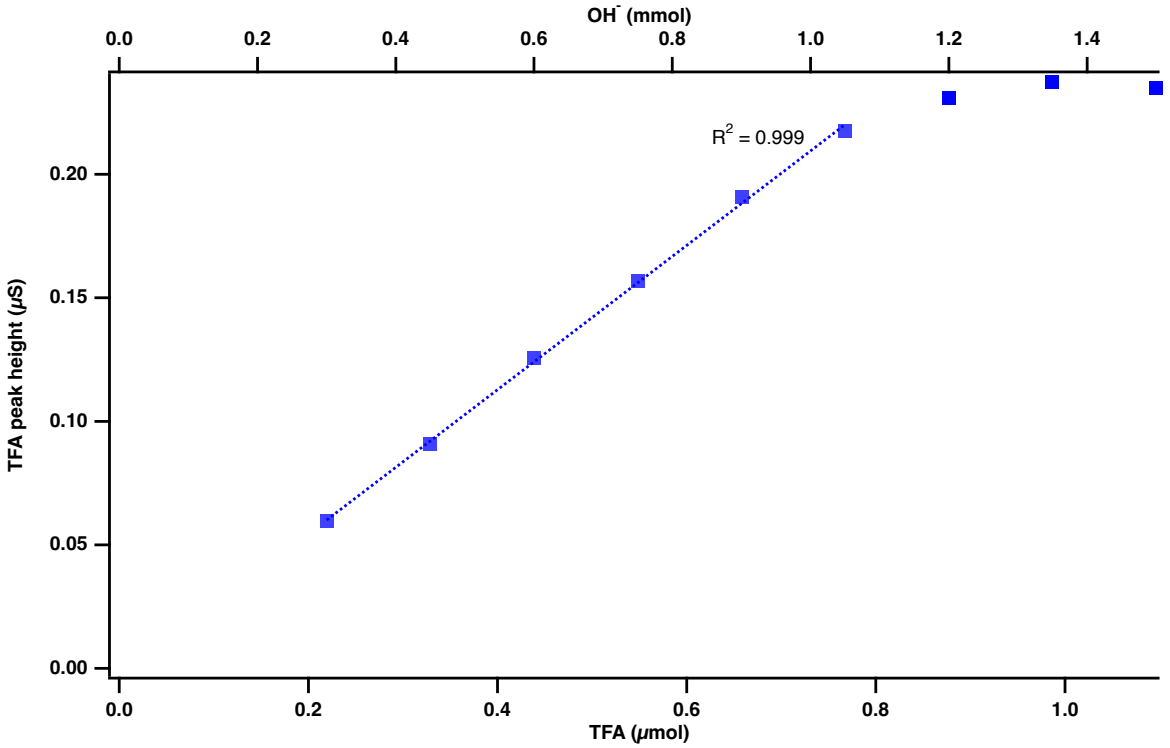

Figure 2.7: PAS matrix matched TFA standard loading on a concentrator column. The bottom x-axis represents the loading of TFA on the concentrator column and the top x-axis represents the matrix loading, being OH-, on the concentrator column.

At 1.05 mmol of OH^-, the increases in peak height of TFA are no longer linear (Figure 2.7), indicating TFA is starting to elute from the concentrator column during sample loading. As such, 900 µmol of OH^- was found to be the optimal amount of PAS extract matrix for this specific concentrator column to obtain the best preconcentration column performance, or in other words, the maximum amount of co-injected OH^- that does not lead to TFA signal losses. The column capacity is indicated to be 25 µeq (equivalent to 25 µmol of a singularly charged ion) by the manufacturer, which is greater than the amount of injected TFA in the calibrated range. The capacity is impacted in the presence of TFA below this limit because the amount of OH^- coinjected (900 µmol or higher) competes with the TFA interactions on the stationary

phase exchange sites, leading to a slow elution off the concentration column because OH^- acts as a weak competing ion.

2.3.2 Quality assurance/quality control

Positive controls were performed on both the GC-MS and IC-CD extraction methods to validate their efficiencies (Figures 2.8 and 2.9). Spike levels for the GC-MS method fell well

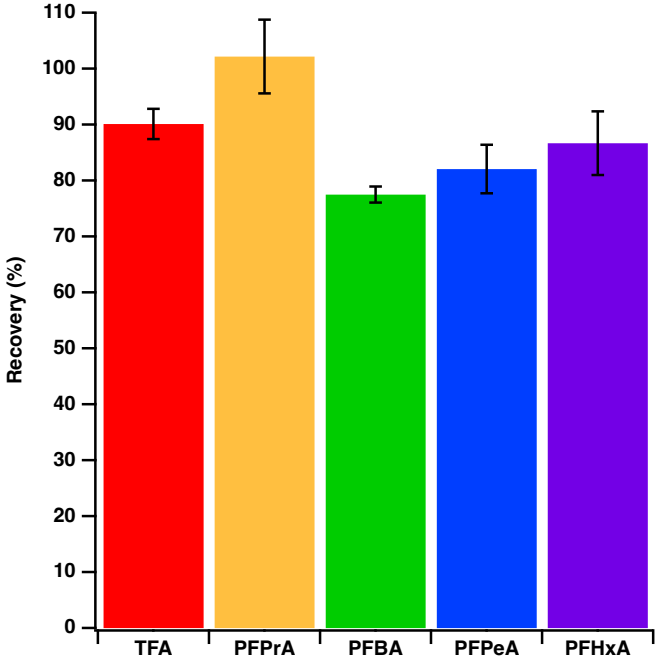

Figure 2.8: The recoveries of 100 ng of the C2-C6 PFCAs spiked in method blanks (n=3) and quantified by the GC-MS methodology. The error bars represent one standard deviation of the replicates.

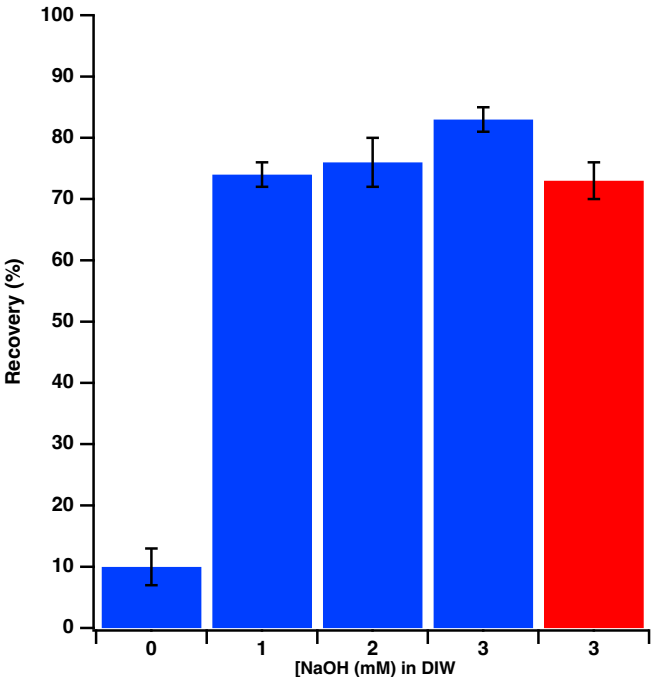

Figure 2.9: The recoveries of 400 ng of TFA spiked in method blanks spiked with matrices of NaOH in DIW (n=3) and quantified by the IC-CD analysis method. Blue bars indicate an extraction at 4 °C meanwhile red bar indicate an extraction at room temperature. The error bars represent one standard deviation of the replicates.

within levels of TFA and PFPrA measured in this study but are higher compared to observed PFBA, PFPeA and PFHxA levels (see Section 2.3.3). The recoveries were found to lie within the 70-120% range, which are considered quantitative recoveries (Chung & Lam, 2014; EPA, 2018; EPA, 2019; Saber, 2019; Taylor, 2022; Yu & Xu, 2017).

Spiked levels for the IC-CD method fell well within expected TFA levels for chamber experiments (Section 2.3.5). The spike and recovery using 3 mM of NaOH at 4 °C obtained a quantitative recovery of 83 ± 2%, which was found to be more efficient than extractions with

lower concentrations of NaOH and at the same temperature (Figure 2.9). This demonstrates the importance of using enough competing ions to obtain adequate recoveries. Furthermore, the same concentration of 3mM of NaOH at room temperature obtained an extraction efficiency of 73 ± 3%, which is 10% lower than at 4 °C (Figure 2.9). A more efficient extraction at lower temperature resulted in all quantitative analyses being subject to these extraction conditions. This is consistent with theory, our IC separation (Figure 2.6), and another study that has shown haloacetic acids, including TFA, are less retained in ion chromatography at lower temperatures (Barron et al., 2005). Similarly, free amino and amide functional groups at our nylon filter surfaces behave as ion binding sites when placed in extraction solvent, and the analytes are found to be more readily displaced at lower temperature. Positive controls were also performed with denuder extracts by spiking them with known amount of TFA. The spiked denuder extract obtained a recovery of 100.7 ± 0.4% (n=3), indicating negligeable bias associated with the diluted matrix.

Negative controls have been performed in the form of extraction solvent, method, and field blanks for PAS. For the GC-MS, extraction solvent, method, and fields blanks ($n \geq 3$ each) were found to be below the limit of detection (LOD), indicating minimal contamination from the PAS method and from the field. For analysis with the IC-CD, no detectable signal of TFA and PFPrA was observed in the extraction solvent, method, or field blanks of PAS. Overall, each analysis method leads us to believe the introduction of PFCA contaminants from the assembling, transport, storage and disassembling of PAS is minimal relative to the detection limits of these two techniques. Negative controls were also assessed for our annular denuders in the form of solvent and method blanks. Since these were quantified on the IC-CD, the same method was used and no detectable signal of TFA or PFPrA was found in the method blanks.

2.3.3 Polypropylene as a replacement to discontinued PTFE overlying filters in PAS

Our custom-built passive air samplers previously featured polytetrafluoroethylene (PTFE) membrane overlying filters (47 mm, 2.0 μm, Zeflour™, Pall Corporation, P/N P5PJ047) (Carmichael, 2022). However, these filters have been discontinued. Furthermore, while they are deemed reusable, they can (and do) become damaged or lost over time. As such, these filters are semi-consumable and replacement filters need to be identified. Alternatives were therefore sought to replace the PTFE membrane filters. Current air sampling PTFE membrane filters from Pall were found to be expensive and defeats our PAS low-cost objective (Cytiva, 2023). Polypropylene (PP) filters were investigated as potential overlying filter

replacements for PAS (Tisch Scientific, 2023) as this is an inert material and are nearly 50 times more affordable per filter. While both commercial materials have been shown to contain extractable PFCAs (mostly seen in PTFE), sequential aqueous extraction of the materials leads to quantitative extraction of these potential contaminants (Joudan et al., 2024). Therefore, considering the extensive washing procedure of this method, these materials are highly unlikely to be a source of contamination to the overall method. The PP filters were investigated to determine their suitability as a replacement to PTFE filters in PAS (Figure 2.10).

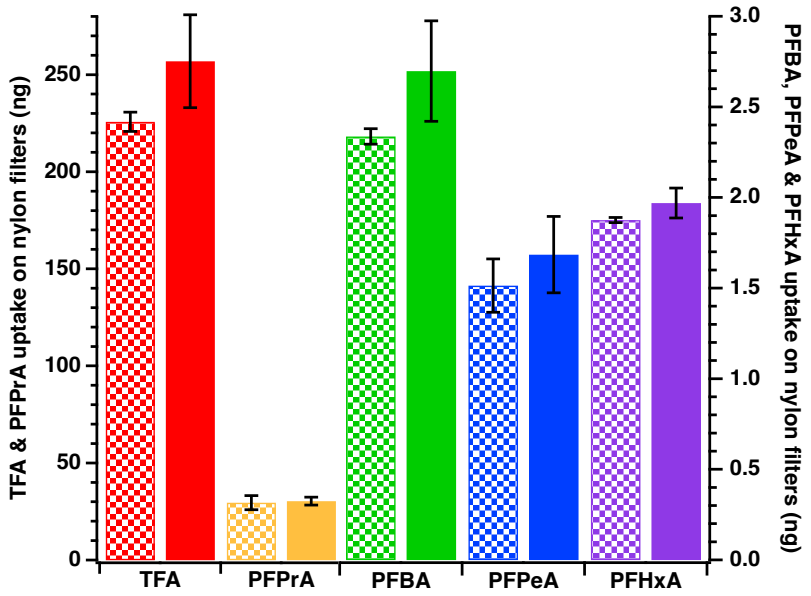

Figure 2.10: Sampling of PFCAs using PAS performed in an indoor laboratory with relatively large PFCA emissions (see Section 3.3.4 for more details). Both PTFE and PP filters were employed as overlying filters in PAS for uptake intercomparison, where the former is represented by the pattern bars and the latter by solid bars. The error bars represent one standard deviation of the replicates (n=3).

The comparability of the results was assessed by performing a Welch t-test ($\alpha = 0.05$) which indicates no significant difference in the sampling rate between the selection of overlying filter (Table S2.1; Appendix A). These results confirms that the porosities of both inert materials, which directly impacts to the rate of effusion, are similar. This result was expected as the porosity specified by both manufacturers was 2.0 µm. The error associated with the standard deviation of the triplicates for PTFE overlying filters was found to range between 0.7-12.3% while the PP overlying filters error ranged from 4.1-12.5% (Figure 2.10). The error between replicates is generally comparable between the PTFE and the PP. Other PAS reports using nylon-based PAS with PTFE overlying filters to measure $HNO_{3\ (g)}$ obtained comparable or

higher errors in replicates than are found for the PP filters here (Carmichael, 2022; Place et al., 2018). This suggests that PTFE filters do not have any performance improvement in reducing replicate error and that the more affordable PP filters are suitable for the collection of our target analytes. A final recommendation for best practice is that users should aim to use the same materials reported in both the calibrations and measurements in the literature in order to obtain the most accurate results. Where these materials and/or their properties are altered, validation that PAS performance has not been changed should be undertaken.

2.3.4 Chamber cleanup

Before any chamber experiments can be performed, it is ideal that a chamber cleanup is performed to minimize TFA levels as well as minimize the magnitude of contaminants that co-elute with the target molecules in the IC or GC methods and/or reduce the sampling capacity of PAS in a way that is not atmospherically relevant. It was especially important to do so for our chamber as it has been previously used for PFAS experiments, where PFCAs are known to have been produced (Joudan et al., 2021b). Chamber cleanup is performed by flushing it with dry zero-air. This strongly reduces the humidity in the chamber and therefore the amount of water adsorbed on the chamber walls. This promotes the partitioning of volatile contaminants from being adsorbed with this water on the surfaces into the gas-phase. The effectiveness of flushing the chamber with zero air was evaluated over the course of several days to reduce the amount of gaseous acids corresponding to the protonated anions from undergoing uptake on PAS, including PFCAs and close co-eluting compounds **(**Figure 2.11). This example represents a chamber that was dirtier than usual due to it being the first thorough flush after being left open to room air and subject to humidification with tap water instead of 18.2 MΩ·cm DIW (Figure 2.11).

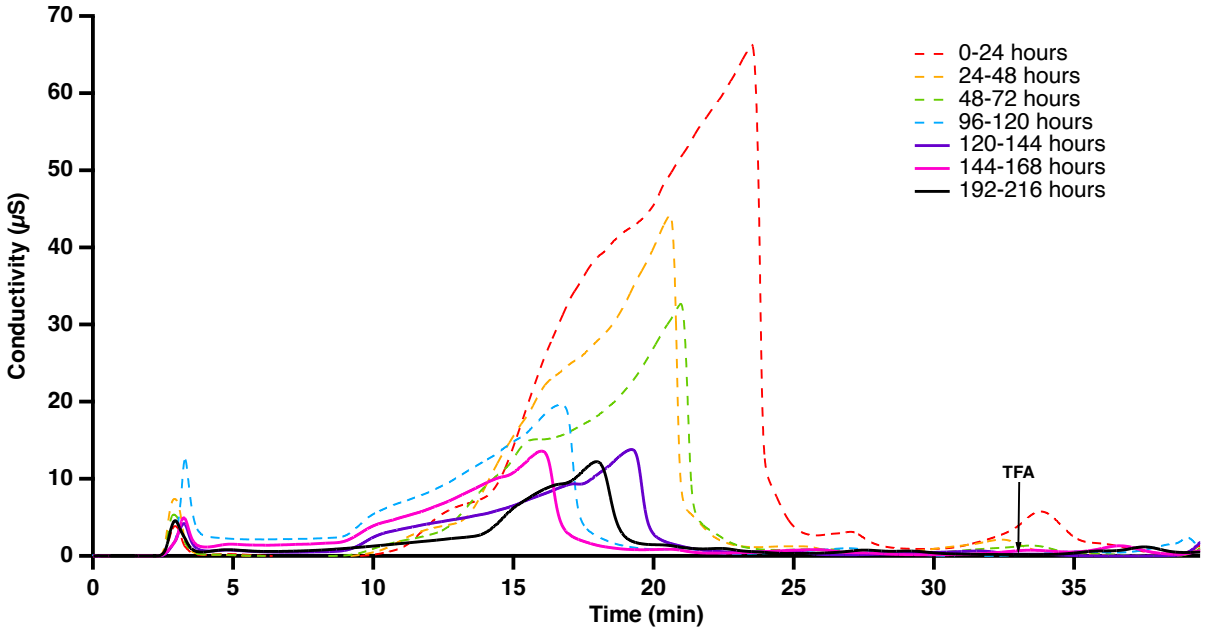

Figure 2.11: Total anion conductivity of denuder extracts used to monitor chamber flushing effectiveness. Each denuder chamber flush was run for approximately 24 hours. Note: the 33 °C method was employed, and denuder extracts were not diluted. In this method, TFA is expected to elute at 33 min (arrow indicator) when no matrix effects are exhibited. Dilution to reduce matrix effects and the use of the 15 °C method for more accurate results had not yet been developed. Dashed lines represent the least clean chamber runs meanwhile the solid lines represents cleaner chamber runs where flushing had minimal to no effect in improving peak contaminants.

Many of the compounds contributing to the total anion conductivity are likely common organic and inorganic acids, recovered as anions (e.g. Cl^-, NO_3^-, CH_3COO^-, etc.). The IC method employed cannot provide quantitative data in the presence of such major matrix effects because these effects shift retention and cause peak broadening, hindering separation and compound identification by retention time. It is recommended to minimize the total anion conductivity, or any observable background interferences in other analytical methods, as much as possible before starting chamber experiments. Here, this was determined to be accomplished when additional flushing no longer made a difference for peaks in the chromatogram. Chromatogram peak levels were found to stabilize between 120-216 hours of dry flushing (Figure 2.11). Although the chamber cleanup helped minimize close co-eluting compounds, it is not a perfect solution. Good separation of TFA from other compounds using the 15 °C method with elimination of matrix effects was still required, as shown in Section 2.3.1.

2.3.5 Chamber calibration of TFA using a simulated atmospheric chamber

With an appropriately clean chamber, our nylon-based PAS were calibrated for TFA by inserting them into a simulated atmospheric gas mixture containing gas-phase TFA and performing orthogonal measurements of gas phase TFA by its collection on Na_2CO_3-coated annular denuders. These chamber experiments were performed at a temperature of 27 ± 3 °C and at a relative humidity (RH) of 40 ± 5 %. In total, 42 PAS and 14 annular denuders were used to generate the dose-response curve via the linear regression of TFA extracted from nylon filters in our PAS (ng) compared to the concentration of TFA present in the chamber measured by the annular denuder (Figure 2.12).

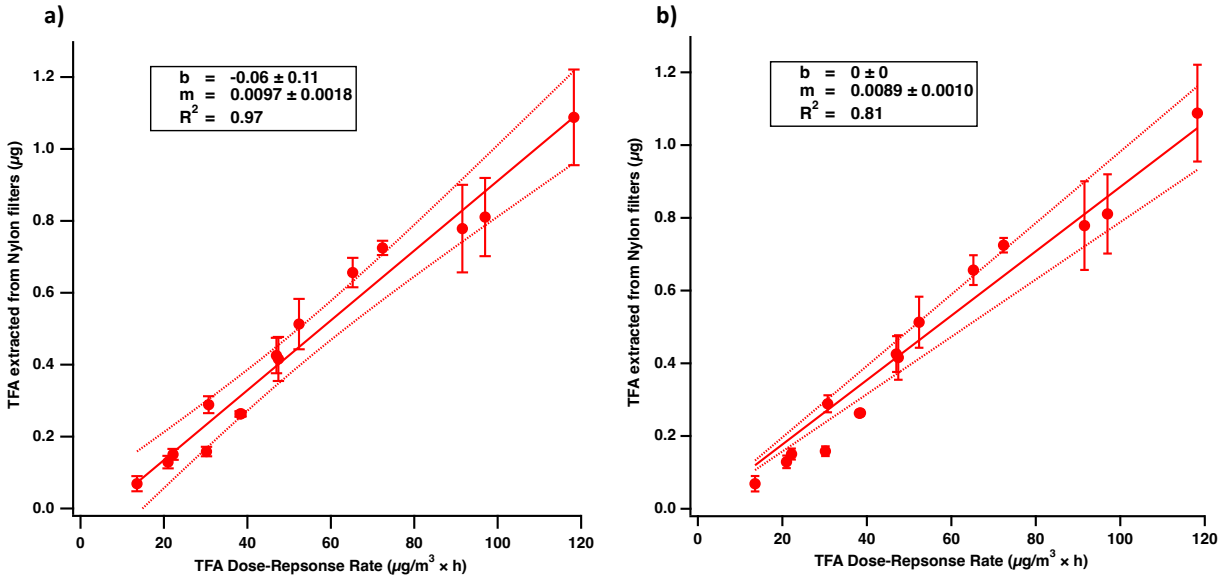

Figure 2.12: Chamber calibration of PAS for TFA using the least-squares linear regression. The variable b represents the intercept, m represents the slope and the R2 is the coefficient of determination. Dashed lines represent the confidence bands of the linear regression at a 99.73% confidence interval. Each data point represents the mean measurement of triplicate PAS (y-axis) versus annular denuder measurements times exposure time (x-axis). The error bars are the standard deviation of triplicate PAS. (A) includes the calculation of a b-intercept. The intercept in (B) was forced to zero.

The TFA monitored by annular denuders (ng/m^3) directly corrects for any wall losses, and the observed quantities are multiplied by the sampling period in the chamber (h) to obtain the dose-response relationship commonly reported in the literature (Bytnerowicz et al., 2005; Bytnerowicz et al., 2001; Kawashima et al., 2021). The amount of TFA extracted from nylon filters in our PAS was corrected for the known 83% extraction efficiency (Section 2.3.2). The relative error between PAS replicates ranged from 2%-30%, with n=12 out of N=14 being 15%

or below. This highlights the importance of taking PAS replicates to improve the precision of measurements when translated to atmospheric abundances. The reproducibility of the Sartorius filters was previously reported to be higher than the discontinued Nylasorb filters (Carmichael, 2022), making the need for replicates (n≥3) of importance for this PAS method. There are 4 data points which fall outside the 3σ confidence bands of the dose-response linear regression, due to sampler variability (Figure 2.12a). Precautions have been taken in advance to minimize these issues, such as replicates to improve the precision of the measurements between the samplers. The chamber composition is known to be homogenous as we use fans to keep the air in the chamber well mixed in order to minimize the potential of concentration gradients near the samplers or stagnant air pockets near the chamber surfaces. It is important to note that the experiments at higher concentrations showed the greatest variability, as those were the earliest experiments conducted during the initial development of the complex chamber methodology, which resulted in less consistent results compared to the later experiments where proficiency had increased. Variability arising from these variables is reported by other chamber studies for PAS, including the previous calibration of nylon PAS for HNO_3. (Bytnerowicz et al., 2005; Bytnerowicz et al., 2001; Kawashima et al., 2021; Melymuk et al., 2011). The negative intercept in Figure 2.12a may suggest negative bias with the TFA quantified by the PAS or positive bias with the TFA quantified by annular denuders. In Section 2.3.2, it was shown that quantitative recoveries were obtained for annular denuders, with method blanks showing no detectable signal. Additionally in Section 2.3.2, PAS spike and recoveries experiments achieved quantitative outcomes, the efficiency of which were corrected for in Figure 2.12a, again with no detectable signals in PAS blanks. Therefore, it would not be possible for this calibration to have a non-zero intercept since the blanks show no bias, and any bias related to the spike and recoveries has been corrected for. Furthermore, both the PAS and annular denuders extracts have been quantified above the instrument limit of quantification (LOQ), validating the accuracy of each data point. These findings would be consistent with assigning the origin as a known point on the chamber dose-response curve. Furthermore, the error associated with the intercept clearly encompass the origin point (Figure 2.12a). Consequently, our findings strongly suggest that an intercept near the origin will obtain the best measurement accuracy. This approach is consistent with many PAS-chamber calibration studies that have also shown PAS negative controls to be free of bias or that are able to apply blank correction (Bytnerowicz et al., 2005; Bytnerowicz et al., 2001; Melymuk et al., 2011).

Based on these justifications, the dose-response function passing through the origin is the most representative approach for accurate analytical determinations (Figure 2.12b). Taking the inverse of the slope, the dose-response for TFA was found to be $113 \pm 12 \frac{\mathrm{TFA_{(g)}(ng \cdot m^{-3}) \cdot t(h)}}{\mathrm{TFA_{(filter)}(ng)}}$. This is the first time that a nylon passive air sampler has been calibrated for TFA. For this reason, a direct comparison to other studies is not possible. The linear least square-regression from Figure 2.12b obtained a coefficient of determination (R^2) of 0.81 indicating a highly reliable linear response in the dose-response value for quantifying TFA within sampling periods of a few days to a week on the order of 56-204 ppt_v levels in atmospheric samples. While longer sampling times improve detection limits, shorter periods were chosen for our chamber experiments to gather more data points within the two-month timeframe. Despite better linearity in Figure 2.12a then Figure 2.12b, our rigorous QA/QC ensures Figure2.12b is the more accuracy and reliable calibration. This linearity also suggests that PAS did not near saturation. While saturation levels of Sartorius nylon filters have not been quantified in the current setup PAS, it has been characterized with no overlying semi-permeable filters for Nylasorb nylon filters to be 5700 $\mu g/m^3 \times h$ of HNO_3 or 411 μg of NO_3^- extracted, which is more than 2 orders of magnitude higher than the amount of TFA recovered in our most concentrated extract (Bytnerowicz et al., 2001). Considering the current Sarturious nylon filters are thicker with more binding sites compared to the Nylasorb nylon filters (Carmichael, 2022) and that the current setup includes a PP overlying filters that reduces the uptake rate of gas-phase acids and block particle-phase acids, it is expected that the saturation level of these new alternative filters will be greater.

2.3.6 Evaluation of Graham and Fuller's law for predicting the dose-response for TFA

The calibration of our nylon-based PAS was the very first ever performed for gas-phase TFA and a direct intercomparison of previous studies for TFA PAS is thus not possible. Previous studies have calibrated these samplers for $HNO_{3(g)}$, with minor differences in the design. Using established laws such as Graham's and Fuller's Laws, the dose-response of $TFA_{(g)}$ can be predicted from those previous studies and compared to the dose-response obtained for $TFA_{(g)}$ from the chamber experiments. The differences between the experimental and predicted dose-responses range from 12-62%. A study from Carmichael (2022) has the closest nylon-based PAS design to our study, with the only difference being the use of a PTFE overlying filter rather than a PP overlying filter. This study obtained a dose-response of $136 \pm 51 \frac{\mathrm{HNO_{3\ (g)}(ug \cdot m^{-3}) \cdot t(h)}}{\mathrm{NO_3^-{}_{(filter)}(ug)}}$ for $HNO_{3\ (g)}$ by making outdoor PAS alongside orthogonal measurements from Na_2CO_3-coated

annular denuders. Place et al. (2018) also used a similar nylon-based PAS setup to our study, with differences lying in the use of Nylasorb nylon filters and PTFE overlying filters rather than our Sarturius nylon filters and PP overlying filters. They obtained a similar dose-response of $134 \pm 9 \frac{HNO_{3\,(g)}(ug \cdot m^{-3}) \cdot t(h)}{NO_3^-{}_{(filter)}(ug)}$, also from outdoor PAS paired with orthogonal measurements from Na_2CO_3-coated annular denuders. Place et al. (2018) had also predicted the dose-response from a previous chamber study (Bytnerowicz, 2005) that used the same type of sampler with different dimensions to be $131 \pm 22 \frac{HNO_{3\,(g)}(ug \cdot m^{-3}) \cdot t(h)}{NO_3^-{}_{(filter)}(ug)}$. Overall, they all obtained similar dose-responses for the same compound, despite small differences in sampler design and sampling conditions.

Since Carmichael (2022) has the closest nylon-based PAS design to this study and the measurements were performed at the conditions closest to our chamber, we have opted to compare to this result. Nevertheless, since the previous studies obtained nearly identical dose-responses, this comparison should be representative for them as well. Graham's and Fuller's Laws were used to obtain a predicted dose-response for TFA from Carmichael (2022) previous HNO_3 dose-response calibration (Equations 2.1 and 2.2, respectively).

$$\frac{\textbf{rate of effusion B}}{\textbf{rate of effusion C}} = \sqrt{\frac{M_C}{M_B}} \qquad \textbf{(E2.1)}$$

$$\frac{\textbf{rate of effusion B in air}}{\textbf{rate of effusion C in air}} = \frac{\sqrt{\frac{1}{M_A}+\frac{1}{M_B}}}{\left(\sqrt[3]{\sum_A v_i}+\sqrt[3]{\sum_B v_i}\right)^2} \times \frac{\left(\sqrt[3]{\sum_A v_i}+\sqrt[3]{\sum_C v_i}\right)^2}{\sqrt{\frac{1}{M_A}+\frac{1}{M_C}}} \qquad \textbf{(E2.2)}$$

In Graham's and Fuller's Laws equations, M_A, M_B and M_C are the molar mass of gasses A, B and C, which are air, TFA and HNO_3 respectively, and $\Sigma\, v_i$ is the sum of the diffusion corrected volumes of those gasses (Fuller et al., 1966). Diffusion volumes were obtained from Gu et al., (2018). The dose-responses using both laws were predicted for TFA. (Table 2.1).

Table 2.1: Demonstrates the predicted nylon-based PAS TFA dose-responses ($\frac{\mathbf{TFA_{(g)}(ng \cdot m^{-3}) \cdot t(h)}}{\mathbf{TFA_{(filter)}(ng)}}$) from previous studies using Graham's and Fuller's Laws based on previous $HNO_{3\,(g)}$ calibrations. A Welch t-test at a 95% confidence interval was performed between Graham and Fuller's law TFA predicted dose-responses and our studies' TFA dose-response. This test was performed at a 95% confidence interval. The t_{table} value was obtained from Excel.

Studies	**Predicted dose-response**		**Predicted dose-response, assuming a 70% extraction efficiency correction**		**T-test**	
	Graham's Law	**Fuller's Law**	**Graham's Law**	**Fuller's Law**	$\mathbf{t_{calculated}}$	$\mathbf{t_{table}}$
Carmichael (2022)	183 ± 69	182 ± 68	128 ± 48	127 ± 48	1.02	2.01
Place et al. (2018), field derived	180 ± 12	180 ± 12	126 ± 8	126 ± 8	2.97	2.10
Place et al. (2018), calculated from Bytnerowicz (2005)	176 ± 30	176 ± 30	126 ± 21	126 ± 21	1.22	2.10

Both laws predict nearly identical dose-responses for TFA (Table 2.1), meanwhile the dose-response obtained from this chamber study was 113 ± 12 $\frac{TFA_{(g)}(ng \cdot m^{-3}) \cdot t(h)}{TFA_{(filter)}(ng)}$. A relative difference of 62 % exists between the predicted TFA dose-responses drawing from the HNO_3 sampling rate reported by Carmichael (2022) and the dose-response measured for TFA in the chamber calibrations, where the latter is the most accurate dose-response determined. A higher dose-response indicates, for a given atmospheric mixing ratio, that the rate at which molecules adsorb to the Nylon filters is lower for the molecule in question. One obvious reason for this discrepancy is that the previous studies assumed their extraction efficiency was quantitative and both were validated in the field (Carmichael, 2022; Place et al., 2018). While they found the extraction to be quantitative, the exact extraction efficiency of NO_3^- was not determined and, as a result, was not corrected in the dose-response as this was normalized for by the

experimental approach. Considering they used a weaker extraction solvent (1 mM of OH^- instead of 3 mM of OH^-) and that NO_3^- is usually more strongly retained then TFA in ion chromatography, and therefore also on the nylon sorption sites, it is reasonable to assert that an extraction efficiency lower than 100% could have resulted.

Assuming Carmichael (2022) obtained a recovery of 70% instead of 100 % (see Section 2.3.2), the predicted dose-response slopes were then compared to the TFA chamber results which also include consideration of this loss process for the target analyte (Table 2.1). A t-test between the resulting predicted dose-response and the dose-response from our study was performed and found to be not statistically significant at the 95% confidence interval (Table 2.1). However, it is important to note that we had assumed the worst possible extraction efficiency for quantitative recovery of the prior study, as this provides a conservative estimate. Because the dose-response from Carmichael (2022) has a significantly larger error compared to Place et al. (2018), the latter study is statistically different due to the better precision of the dose-response achieved with the discontinued Nylasorb sampling filters (Table 2.1). If the extraction efficiency from Carmichael (2022) was better (i.e. 82% or higher), the t-test would have returned a significant difference. Therefore, it is more likely that a statistical difference exists between the prediction and calibration even when accounting for the extraction efficiency.

Possible drivers of the remaining discrepancy could arise from a lack of consideration of some physical properties of gas-phase TFA and HNO_3, or the sampling apparatus, which the theoretical frameworks of Graham and Fuller's Laws would not account for. These include differences in meteorological conditions from both studies, including differences in temperature, humidity, as well as the abundance and chemical composition particulate matter. Place et al. (2018) had determined that changes in temperature, that are not accounted for in the dose-response, can generate bias on the order of ±10% across an ambient temperature range of 10 to 35 °C. However, given the similarity between the temperatures in our study (27 ± 3 °C) and those reported by Carmichael (2022) (23 ± 4 °C), temperature is unlikely to be responsible for this discrepancy. Bytnerowicz et al. (2005) has speculated that a difference in RH could have caused a ~30 % decrease in the uptake of $HNO_{3\,(g)}$ on their PAS for their outdoor measurement calibrations compared to their controlled chamber calibrations. Padgett et al. (2010) also observed a 50 % decrease of the uptake $HNO_{3\,(g)}$ on Nylon filters with PTFE overlying filters when performed in a wet chamber versus a dry chamber. This likely happened because more water adsorbed and/or condensed on the PTFE overlying filters in the wet

chamber, allowing them to absorb more $HNO_{3\,(g)}$, leading to a smaller uptake of $HNO_{3\,(g)}$ on the Nylon which would lead to the PAS having a higher dose-response value. While the experiments from Bytnerowicz et al. (2005) and Padgett et al. (2010) conducted chamber experiments under dry air conditions (~0% RH), the specific RH levels during their outdoor measurement experiments (Bytnerowicz et al., 2005; Padgett et al., 2004) and during wet chamber experiments (Padgett et al., 2010) are not specified. In contrast to these findings, a large range of RH has been reported by Carmichael (2022) and Place et al. (2018) of 69 ± 12 % and 57 ± 15 % respectively where the field-derived dose-responses from both studies are nearly identical. This demonstrates that differences in ambient RH do not necessarily cause large bias to the dose-response. It may be that only extreme conditions of low RH values (~0 %) cause the bias to become large. Considering that the chamber experiments conducted here were at an atmospherically relevant RH (40 ± 5 %), it is unlikely to be the cause for the discrepancy between our measured and predicted dose-response values.

Bytnerowicz et al. (2005) has also speculated that particulate matter may deposit on overlying filters in PAS to cause bias in the uptake of acids to Nylon filters and to be responsible for discrepancies seen in their results between their chamber calibrations (at ~0% RH) and their outdoor measurement calibrations of PAS. It is uncertain how much varying particulate matter levels might impact the uptake of atmospheric acids on nylon-based PAS. Place et al. (2018) used annular denuders for validation of the dose-response for PAS in Toronto, which measure gases before particles, eliminating the impact of blow on and blow off bias for gas-phase measurements. This provides a convenient situation in which to consider potential particle impacts on HNO_3 sampling bias. Place et al. (2018) also calculated the dose-response for their newer PAS design, based off on Bytnerowicz et al. (2005) chamber calibration experiments with samplers of different dimensions. Despite those chamber experiments being performed free of particles, the Place et al. (2018) outdoor calibration measurements were exposed to elevated levels of particles in an urban environment, yet the dose-responses in both studies remained nearly identical. This demonstrates that differences in particulate matter at atmospherically relevant conditions likely does not exert a large effect on the dose-response of these samplers and therefore is unlikely to be solely responsible for the difference we see between our measured and predicted dose-response values. While, Bytnerowicz et al. (2005) did see a 30% decrease in the uptake of $HNO_{3\,(g)}$ for their outdoor measurements versus their chamber experiments. Their results suggest that blow-on effects (e.g. $HNO_{3\,(g)}$ adsorbing or reactive uptake to particles containing soot, $CaCO_3$, H_2O, and/or other; R2.1) were more

prominent than blow off effects (e.g. $HNO_{3\,(g)}$ in R2.2 leaving the PP overlying filter), yet both could have been active source of bias during their measurements.

$$\mathbf{2HNO_{3\,(g)} + CaCO_{3\,(s)} \rightarrow Ca(NO_3)_{2\,(aq)} + H_2O_{(l)} + CO_{2\,(g)}} \quad \textbf{(R2.1)}$$

$$\mathbf{NH_4NO_{3\,(s)} \leftrightarrow NH_{3\,(g)} + HNO_{3\,(g)}} \quad \textbf{(R2.2)}$$

It is important to note that their measurements were performed in 2002 in the greater Los Angeles area, which was a time when the region was experiencing problematic levels of pollutants, including very high levels of particulate matter (Lurmann et al., 2014). Therefore, it may only be at very high levels of particulate matter (e.g. forest fire plumes, high pollutant levels) when this bias would have a noticeable impact on the dose-response rate of these PAS.

Another important aspect to consider which may be responsible for this discrepancy may lie in the differences between the physical properties of $HNO_{3\,(g)}$ and $TFA_{(g)}$, where surface losses to the protective filter via k_H/k_R in Figure 2.5, or even to the inner surfaces of the weatherproof cap, may be larger for HNO_3 than TFA, resulting in a larger dose-response. While both compounds are strong acids and exhibit intermolecular interactions from hydrogen bonds (H-bond), dipole-dipole interactions and van der Waals (vdW), TFA is different from HNO_3 where half of its structure contains C-F bonds which does not exhibit H-bond or polar bonding and experiences very minimal vdW interactions. Therefore, it is possible that this may lead HNO_3 to be more susceptible to adhere to water droplets or particles that have adsorbed, condensed, or impacted on the surfaces within the nylon-based PAS compared to TFA, which would result in a higher dose-response. However, the actual significance of this difference remains uncertain due to the absence of experiments directly comparing these two molecules in this context. Despite this, it is currently the most plausible explanation for the observed discrepancy.

Assuming the discrepancy is likely driven by a difference in physical properties between $HNO_{3\,(g)}$ and $TFA_{(g)}$, Graham and Fuller's Laws may still be promising in their predictive capabilities of diffusion for gas-phase acids with similar properties sampled by the nylon PAS, such as other PFCAs.

2.3.7 Predicted dose-response for other PFCAs

Our findings in the previous Section suggests that Graham and Fuller's Law cannot accurately predict the sampling rate of a compound based on the sampling rate of another compound with different physical and methodological properties. Nonetheless, when used within the same methodology and chemical class, they should prove to be useful for estimating the diffusion of chemicals with very similar properties. Here, we expect this to be the case for other PFCAs diffusing in the PAS compared to TFA, as these are all within the same chemical family consisting of a hydrophobic tail and hydrophilic carboxylate head group where they are expected to behave in the same manner when subject to the same bias. At this time, these two predictive laws are some of the best ways to predict the dose-responses of the other PFCAs without the need to perform further chamber calibrations or orthogonal measurements in the field. This approach also opens the door to estimating atmospheric levels of other volatile acidic PFAS and haloacetic acids (HAAs) that have similar structural features to TFA and no established gas phase calibration methodology (e.g. perfluorosulfonic acids (PFSAs), Gen-X, HAAs). Using E2.1, E2.2, and the measured TFA dose-response in the chamber, the predicted dose-responses of other PFCAs were determined (Table 2.2).

Table 2.2: Dose-response of individual PFCAs and HNO_3. The measured dose-responses were obtained from Carmichael (2022) and this study (Section 2.3.5). The predicted dose-responses were determined using Graham's and Fuller's law based of the dose-response for TFA measured by calibration experiments conducted in this work.

Measured Compounds	PFCA carbon number	Measured Dose-response		
HNO_3	n/a	136 ± 51		
TFA	2	113 ± 12		
Predicted Compounds	**PFCA carbon number**	**Dose-response by Graham's Law**	**Dose-response by Fuller's Law**	**% Difference**
PFPrA	3	136 ± 14	139 ± 15	2%
PFBA	4	155 ± 16	161 ± 17	4%
PFPeA	5	172 ± 18	180 ± 19	4%
PFHxA	6	188 ± 20	197 ± 21	5%
PFHpA	7	202 ± 21	213 ± 23	5%
PFOA	8	215 ± 23	229 ± 24	6%
PFNA	9	228 ± 24	243 ± 26	6%
PFDA	10	240 ± 25	257 ± 27	7%
PFUnDA	11	251 ± 27	270 ± 29	7%
PFDoDA	12	262 ± 28	282 ± 30	7%
PFTrDA	13	273 ± 29	294 ± 31	7%
PFTeDA	14	283 ± 30	306 ± 32	8%

Both laws yield similar predicted values for the ultra-short chain PFCAs (C2-C4) meanwhile the longer chained PFCAs yield higher dose-response slopes with Fuller's in contrast to Graham's Law. This difference is attributed to Fuller's Law use of diffusion corrected volumes, where this correction becomes more divergent for larger molecules, most notably seen by PFTeDA in Table 2.2 where Fuller's obtained a predicted dose-response 8% larger than what was predicted by Graham's Law. Previous studies have shown evidence that Fuller's Law is better at predicting diffusion rates of organic molecules (Boys, 2022; Gu et al., 2018; Tang et al., 2015). Gu et al. (2018) in particular have demonstrated Fuller's Law to predict diffusivities of organic halogenated gasses very well in comparison with measured values. Some of the molecules tested for included fluorinated compounds such as CH_2F_2, hexafluorobezene and 1-

fluorohexane, where the difference between the predicted and measured values were ≤ 9 %. Since PFCAs are organic halogenated molecules, Fuller's Law is likely better suited for predicting the diffusion rates of gas-phase PFCAs. These predicted dose-response values can be used to determine atmospheric mixing ratios of these PFCA homologues using our nylon-based PAS. While the uncertainties in these measurements will stem from the variability in the underlying data used to derive these dose-response values, the systematic errors have been minimized as much as possible through the chamber experiments and recovery work with TFA. The end result will be mixing ratios which should be representative within an order of magnitude or better for these other PFCA homologues, stemming from their very similar physical properties, yielding the first ever quantitative passive sampling method selective for PFCAs.

2.4 Conclusion

Our nylon-based PAS were successfully calibrated for TFA. This was achieved using a simulated atmospheric chamber coupled to a zero-air generator and a permeation oven. These results present the first ever PAS calibrated for $TFA_{(g)}$ with the ability to sample ultra-trace levels as low as 1.33 ppt_v for one week of sampling. Rigorous QA/QC was performed to ensure a robust calibration and therefore quantitation of $TFA_{(g)}$ by PAS and annular denuders within each experiment. The QA/QC performed included positive and negative controls, optimisation of a direct-injection IC-CD separation, and cleanup of the atmospheric chamber. This PAS design also replaced the expensive PTFE overlying filter with a cheaper PP filter with no significant changes seen in the sampling rate and precision. The dose-response for our custom-built PAS was determined to be $113 \pm 12 \frac{\mathrm{TFA}_{(g)}(\mathrm{ng \cdot m^{-3}}) \cdot \mathrm{t(h)}}{\mathrm{PFCA}_{(\mathrm{filter})}(\mathrm{ng})}$, which was found to be different from the theoretical calculated dose-response of $182 \pm 68 \frac{\mathrm{TFA}_{(g)}(\mathrm{ng \cdot m^{-3}}) \cdot \mathrm{t(h)}}{\mathrm{PFCA}_{(\mathrm{filter})}(\mathrm{ng})}$ using Fuller's law based on a HNO_3 calibration and ambient atmosphere method validation for these samplers from Carmichael (2022). A key difference was the previous study did not adjust for extraction efficiency. This does not appear to be the sole reason for this discrepancy and the differences in physical properties of TFA and HNO_3 leading different surface uptake rates likely play a part. The dose-response for the other PFCA homologues were predicted using Graham's and Fuller's law based on TFA's chamber calibration which should be accurate considering their very similar physical properties and the expectation that they are recovered from the PAS with the same success. Out of these two laws, Fuller's law was found to be best suited for predicting the dose-response of organic halogenated compound, as

demonstrated in a previous study (Gu et al., 2018) and will be used for measuring the mixing ratios of those homologues in the next Chapter. This novel PAS represents the first PAS specifically calibrated for $TFA_{(g)}$ and the only PAS selective for $PFCAs_{(g)}$. The calibration of our nylon-based PAS for $TFA_{(g)}$ pave the way for measuring similar difficult to measure compounds while addressing limitations of previous methods, such as selectivity, dynamic range including ultra-trace detection limits, sampling site selection, and labour intensity, while also minimizing cost.

2.5 References

Ahrens, L., Shoeib, M., Harner, T., Lane, D. A., Guo, R., & Reiner, E. J. (2011a). Comparison of annular diffusion denuder and high-volume air samplers for measuring per- and polyfluoroalkyl substances in the atmosphere. *Analytical Chemistry*, *83*(24), 9622–9628. https://doi.org/10.1021/ac202414w

Ahrens, L., Shoeib, M., Harner, T., Lee, S. C., Guo, R., & Reiner, E. J. (2011b). Wastewater treatment plant and landfills as sources of polyfluoroalkyl compounds to the atmosphere. *Environmental Science & Technology*, *45*(19), 8098–8105. https://doi.org/10.1021/es1036173

Barron, L., Nesterenko, P. N., & Paull, B. (2005). Use of temperature programming to improve resolution of inorganic anions, haloacetic acids and oxyhalides in drinking water by suppressed ion chromatography. *Journal of Chromatography A*, *1072*(2), 207–215. https://doi.org/10.1016/j.chroma.2005.03.028

Boys, B. (2022). "Global Trends in Satellite-Derived Fine Particulate Matter & Developments to Reactive Nitrogen in a Global Chemical Transport Model" (Master's thesis). Dalhousie University. Retrieved from https://dalspace.library.dal.ca//handle/10222/11163

Bytnerowicz, A., Padgett, P. E., Arbaugh, M. J., Parker, D. R., & Jones, D. P. (2001). Passive Sampler for Measurements of Atmospheric Nitric Acid Vapor (HNO_3) Concentrations. *The Scientific World Journal*, *1*, 815–822. https://doi.org/10.1100/tsw.2001.323

Bytnerowicz, A., Sanz, M. J., Arbaugh, M. J., Padgett, P. E., Jones, D. P., & Davila, A. (2005). Passive sampler for monitoring ambient nitric acid (HNO) and nitrous acid (HNO) concentrations. *Atmospheric Environment*, *39*(14), 2655–2660. https://doi.org/10.1016/j.atmosenv.2005.01.018

Carmichael, L. (2022). "Determining the Sampling Rates for a New Nylon Passive Sampler to Estimate the Atmospheric Concentrations of Nitric Acid and Perfluoroalkyl Acids Pollutants" (Master's thesis). York University. Retrieved from https://hdl.handle.net/10315/26310

Chung, S. W. C., & Lam, C. H. (2014). Development of an ultraperformance liquid Chromatography–Tandem mass spectrometry method for the analysis of perfluorinated compounds in fish and fatty food. *Journal of Agricultural and Food Chemistry*, *62*(25), 5805–5811. https://doi.org/10.1021/jf502326h

Crilley, L. R., Lao, M., Salehpoor, L., & VandenBoer, T. C. (2023). Emerging investigator series: an instrument to measure and speciate the total reactive nitrogen budget indoors: description and field measurements. *Environmental Science: Processes & Impacts*, *25*(3), 389–404. https://doi.org/10.1039/d2em00446a

Cytiva (Formerly Pall Lab). (n.d.). Teflo Air Sampling Membranes, PTFE. Retrieved from https://ca.vwr.com/store/product/en/4831748/teflo-air-sampling-membranes-ptfe-cytiva-formerly-pall-lab (accessed 2023-05-11).

Ellis, D. A., Martin, J. W., De Silva, A. O., Mabury, S. A., Hurley, M. D., Sulbaek Andersen, M. P., & Wallington, T. J. (2004). Degradation of Fluorotelomer Alcohols: a Likely Atmospheric Source of Perfluorinated Carboxylic Acids. *Environmental Science & Technology*, 38(12), 3316–3321.

Fuller, E. N., Schettler, P. D., & Giddings, J. Calvin. (1966). New Method for Prediction of Binary Gas-Phase Diffusion Coefficients. *Industrial & Engineering Chemistry, 58*(5), 18–27. DOI:10.1021/ie50677a007.

Furlani, T. (2021). "Development, Validation, and Application of Methods for High Time-Response Measurement of Gaseous Atmospheric Chlorinated Species" (Doctoral dissertation). York University. Retrieved from https://hdl.handle.net/10315/26310

Górecki, T., & Namieśnik, J. (2002). Passive sampling. *TrAC Trends in Analytical Chemistry*, *21*(4), 276–291. https://doi.org/10.1016/s0165-9936(02)00407-7

Gu, W., Cheng, P., & Tang, M. (2018). Compilation and evaluation of gas phase diffusion coefficients of halogenated organic compounds. *Royal Society Open Science*, *5*(7), 171936. https://doi.org/10.1098/rsos.171936

Haddad, P. (1988). Studies on Sample Preconcentration in Ion Chromatography VIII. Preconcentration of Carboxylic Acids Prior to Ion-Exclusion Separation. *Journal of Chromatography A*, 447(3), 155–163. DOI:10.1016/s0021-9673(01)91464-5.

Harris, D. C., & Lucy, C. (2015). *Quantitative Chemical analysis*. Macmillan Higher Education.

Javed, M. I., & Brewer, M. (2007). Diazo Preparation via Dehydrogenation of Hydrazones with "Activated" DMSO. *Organic Letters*, *9*(9), 1789–1792. https://doi.org/10.1021/ol070515w

Joudan, S., De Silva, A. O., & Young, C. J. (2021a). Insufficient evidence for the existence of natural trifluoroacetic acid. *Environmental Science: Processes & Impacts*, *23*(11), 1641–1649. https://doi.org/10.1039/d1em00306b

Joudan, S., Gauthier, J. R., Mabury, S. A., & Young, C. J. (2024). Aqueous Leaching of Ultrashort-Chain PFAS from (Fluoro)polymers: Targeted and Nontargeted Analysis. *Environmental Science & Technology Letters*. https://doi.org/10.1021/acs.estlett.3c00797

Joudan, S., Orlando, J. J., Tyndall, G. S., Furlani, T. C., Young, C. J., & Mabury, S. A. (2021b). Atmospheric Fate of a New Polyfluoroalkyl Building Block, $C_3F_7OCHFCF_2SCH_2CH_2OH$. *Environmental Science & Technology*, *56*(10), 6027–6035. https://doi.org/10.1021/acs.est.0c07584

Karásková, P., Codling, G., Melymuk, L., & Klánová, J. (2018). A critical assessment of passive air samplers for per- and polyfluoroalkyl substances. *Atmospheric Environment*, *185*, 186–195. https://doi.org/10.1016/j.atmosenv.2018.05.030

Kawashima, H., Ogata, R., & Gunji, T. (2021). Laboratory-based validation of a passive sampler for determination of the nitrogen stable isotope ratio of ammonia

gas. *Atmospheric Environment*, *245*, 118009. https://doi.org/10.1016/j.atmosenv.2020.118009

Krechmer, J. E., Day, D. A., & Jimenez, J. L. (2020). Always lost but never forgotten: Gas-Phase wall losses are important in all teflon environmental chambers. *Environmental Science & Technology*, *54*(20), 12890–12897. https://doi.org/10.1021/acs.est.0c03381

Lao, M., Crilley, L. R., Salehpoor, L., Furlani, T. C., Bourgeois, I., Neuman, J. A., Rollins, A. W., Veres, P. R., Washenfelder, R. A., Womack, C. C., Young, C. J., & VandenBoer, T. C. (2020). A portable, robust, stable, and tunable calibration source for gas-phase nitrous acid (HONO). *Atmospheric Measurement Techniques*, *13*(11), 5873–5890. https://doi.org/10.5194/amt-13-5873-2020

Matsunaga, A., & Ziemann, P. J. (2010). Gas-wall partitioning of organic compounds in a Teflon film chamber and potential effects on reaction product and aerosol yield measurements. *Aerosol Science and Technology*, *44*(10), 881-892. https://doi.org/10.1080/02786826.2010.501044Górecki, T., & Namieśnik, J. (2002). Passive sampling. TrAC Trends in Analytical Chemistry, 21(4), 276–291. https://doi.org/10.1016/s0165-9936(02)00407-7

Melymuk, L., Robson, M., Helm, P. A., & Diamond, M. L. (2011). Evaluation of passive air sampler calibrations: Selection of sampling rates and implications for the measurement of persistent organic pollutants in air. *Atmospheric Environment*, *45*(10), 1867–1875. https://doi.org/10.1016/j.atmosenv.2011.01.011

Padgett, P. E., Bytnerowicz, A., Dawson, P., Riechers, G. H., & Fitz, D. R. (2004). Design, evaluation and application of a continuously stirred tank reactor system for use in nitric acid air pollutant studies. *Water Air and Soil Pollution*, *151*(1–4), 35–51. https://doi.org/10.1023/b:wate.0000009890.74470.fa

Padgett, P. E. (2010). The effect of ambient ozone and humidity on the performance of nylon and Teflon filters used in ambient air monitoring filter-pack systems. *Atmospheric Pollution Research*, *1*(1), 23-29. https://doi.org/10.5094/APR.2010.004

Perrino, C., De Santis, F., & Febo, A. (1988). Uptake of nitrous acid and nitrogen oxides by nylon surfaces: Implications for nitric acid measurement. *Atmospheric Environment (1967)*, *22*(9), 1925–1930. https://doi.org/10.1016/0004-6981(88)90081-9

Place, B. K., Young, C. J., Ziegler, S. E., Edwards, K. A., Salehpoor, L., & VandenBoer, T. C. (2018). Passive sampling capabilities for ultra-trace quantitation of atmospheric nitric acid (HNO3) in remote environments. *Atmospheric Environment*, *191*, 360–369. https://doi.org/10.1016/j.atmosenv.2018.08.030

Prevedouros, K., Cousins, I. T., Buck, R. C., & Korzeniowski, S. H. (2006). Sources, Fate and Transport of Perfluorocarboxylates. *ChemInform*, 37(11).

Roadman, M. J., Scudlark, J. R., Meisinger, J. J., & Ullman, W. J. (2003). Validation of Ogawa passive samplers for the determination of gaseous ammonia concentrations in agricultural settings. *Atmospheric Environment*, *37*(17), 2317–2325. https://doi.org/10.1016/s1352-2310(03)00163-8

Saber, A. N., Zhang, H., & Yang, M. (2019). Optimization and validation of headspace solid-phase microextraction method coupled with gas chromatography–triple quadrupole tandem mass spectrometry for simultaneous determination of volatile and semi-volatile organic compounds in coking wastewater treatment plant. *Environmental Monitoring and Assessment*, *191*(7). https://doi.org/10.1007/s10661-019-7554-5

Tisch Scientific. (n.d.). Polypropylene Membrane Filters, 2.0 UM, 47mm, Nonsterile, 200 per Pack, SF14908. Retrieved from https://scientificfilters.com/membrane-filters/polypropylene-membrane-filters-sf14908 (accessed 2023-05-11).

Scott, B., Spencer, C., Mabury, S. A., & Muir, D. C. (2006). Poly and perfluorinated carboxylates in North American precipitation. *Environmental Science & Technology*, *40*(23), 7167–7174. https://doi.org/10.1021/es061403n

Shoeib, M., Harner, T., Lee, S. C., Lane, D. A., & Zhu, J. (2008). Sorbent-Impregnated polyurethane foam disk for passive air sampling of volatile fluorinated chemicals. *Analytical Chemistry*, *80*(3), 675–682. https://doi.org/10.1021/ac701830s

Sturges, W. T., & Harrison, R. M. (1989). The use of nylon filters to collect hcl: efficiencies, interferences and ambient concentrations. *Atmospheric Environment*, *23*(9), 1987–1996. https://doi.org/10.1016/0004-6981(89)90525-8

Taylor, R. B., & Sapozhnikova, Y. (2022). Comparison and validation of the QuEChERSER mega-method for determination of per- and polyfluoroalkyl substances in foods by liquid chromatography with high-resolution and triple quadrupole mass spectrometry. *Analytica Chimica Acta*, *1230*, 340400. https://doi.org/10.1016/j.aca.2022.340400

Tang, M., Shiraiwa, M., Pöschl, U., Cox, R. A., & Kalberer, M. (2015). Compilation and evaluation of gas phase diffusion coefficients of reactive trace gases in the atmosphere: Volume 2. Diffusivities of organic compounds, pressure-normalised mean free paths, and average Knudsen numbers for gas uptake calculations. *Atmospheric Chemistry and Physics*, *15*(10), 5585–5598. https://doi.org/10.5194/acp-15-5585-2015

Tao, Y., VandenBoer, T. C., Ye, R., & Young, C. J. (2023). Exploring controls on perfluorocarboxylic acid (PFCA) gas–particle partitioning using a model with observational constraints. *Environmental Science: Processes & Impacts*, *25*(2), 264–276. https://doi.org/10.1039/d2em00261b

Thermo Fisher Scientific. (2022). *Thermo Scientific concentrator and trap columns*. Retrieved from https://www.thermofisher.com/document-connect/document-connect.html?url=https://assets.thermofisher.com/TFS-Assets%2FCMD%2FSpecification-Sheets%2Fps-70526-concentrator-column-ps70526-en.pdf

Tromp, P., Beeltje, H., Okeme, J. O., Vermeulen, R., Pronk, A., & Diamond, M. L. (2019). Calibration of polydimethylsiloxane and polyurethane foam passive air samplers for measuring semi volatile organic compounds using a novel exposure chamber design. *Chemosphere*, *227*, 435–443. https://doi.org/10.1016/j.chemosphere.2019.04.043

Tsai, C. J., Huang, C. H., & Lu, H. H. (2005). Adsorption Capacity of a Nylon Filter of Filter Pack System for HCl and HNO3 gases. *Separation Science and Technology*, 39(3), 629–643.

U.S. Environmental Protection Agency [EPA]. (2018). SW-846 Test Methods: Method 8260D: Volatile organic compounds by gas chromatography/mass spectrometry (GC/MS). Retrieved from https://www.epa.gov/hw-sw846/sw-846-test-method-8260d-volatile-organic-compounds-gas-chromatographymass-spectrometry

U.S. Environmental Protection Agency [EPA]. (2019). Method TO-15A: Determination of volatile organic compounds (VOCs) in air collected in specially prepared canisters and analyzed by gas chromatography/mass spectrometry (GC/MS). Retrieved from https://cfpub.epa.gov/si/si_public_record_report.cfm?dirEntryId=348850

Winberry, W., Ellestad, T., & Stevens, B. (1999, June). *Compendium Method IO-4.2: Determination of reactive acidic and basic gases and strong acidity of atmospheric fine particles (< 2.5 μ)*. United States Environmental Protection Agency. https://www.epa.gov/sites/default/files/2019-11/documents/mthd-4-2.pdf

Wong, F., Shoeib, M., Katsoyiannis, A., Eckhardt, S., Stohl, A., Bohlin-Nizzetto, P., Li, H., Fellin, P., Su, Y., & Hung, H. (2018). Assessing temporal trends and source regions of per- and polyfluoroalkyl substances (PFASs) in air under the Arctic Monitoring and Assessment Programme (AMAP). *Atmospheric Environment*, *172*, 65–73. https://doi.org/10.1016/j.atmosenv.2017.10.028

Wu, J., Martin, J. W., Zhai, Z., Lu, K., Li, L., Fang, X., Jin, H., Hu, J., & Zhang, J. (2014). Airborne Trifluoroacetic Acid and Its Fraction from the Degradation of HFC-134a in Beijing, China. *Environmental Science & Technology*, *48*(7), 3675–3681. https://doi.org/10.1021/es4050264

Ye, R., Di Lorenzo, R. A., Clouthier, J. T., Young, C. J., & VandenBoer, T. C. (2023). A Rapid Derivatization for Quantitation of Perfluorinated Carboxylic Acids from Aqueous Matrices by Gas Chromatography–Mass Spectrometry. Analytical Chemistry. https://doi.org/10.1021/acs.analchem.3c00593

Yu, L., Li, J., & Xu, H. (2017). Graphene/polyaniline electrodeposited needle trap device for the determination of volatile organic compounds in human exhaled breath vapor and A549 cell. *RSC Advances*, *7*(20), 11959–11968. https://doi.org/10.1039/c6ra25453e

Zhang, X., Cappa, C. D., Jathar, S. H., McVay, R. C., Ensberg, J. J., Kleeman, M. J., & Seinfeld, J. H. (2014). Influence of vapor wall loss in laboratory chambers on yields of secondary organic aerosol. *Proceedings of the National Academy of Sciences of the United States of America*, *111*(16), 5802–5807. https://doi.org/10.1073/pnas.1404727111

Chapter Three: Application of gas-phase PFCAs nylon-based passive air samplers in various environments.

E. Vanhauwaert[1], J.T. Clouthier[1], C.J. Young[1], and T.C. VandenBoer[1]

[1]Department of Chemistry, York University, Toronto, ON, Canada.

Author Contributions:

EV prepared with CJY and TCV editing the chapter/manuscript.

CJY and TCV conceptualized the work and acquired the funding. CJY and TCV provided the resources to support this work.

JTC performed all the measurements and data analysis of the AIM-IC-MS data.

EV performed all other experiments, sample collection, and analysis under the guidance of CJY and TCV.

This chapter is formatted in preparation for publication

3.1 Introduction

3.1.1 Sources and formation of PFCAs in the atmosphere

Perfluoroalkyl carboxylic acids (PFCAs), a sub-class and terminal degradation product of per- and polyfluoroalkyl substances (PFAS), are pollutants in the environment that are known to be persistent due to their strong C-F bonds (Martin et al., 2003a; Prevedouros et al., 2005; Siegemund et al., 2000). PFAS unique properties, such as their hydrophobicity, lipophobicity, thermal stability, and resistance to various chemical agents, has prompted them to be produced for several commercial products (Manojkumar et al., 2023). Consequently, PFCAs have been emitted into the environment from their use as processing aids and from degradation reactions of precursor PFAS compounds from commercial products (Wang et al., 2014; Young & Mabury, 2010). Wastewater treatment plants (WWTP) and landfills have been shown to be atmospheric point sources of PFCA as a result from the usage and subsequent disposal of PFAS commercial products (Ahrens et al., 2011, Vierke et al., 2011). The transport of PFCAs in the atmosphere occurs on a much faster timescale compared to other Earth's spheres, enhancing their global distribution (Young & Mabury, 2010). In the atmosphere, PFCAs can be directly emitted or be produced indirectly from precursors that have been emitted into the atmosphere. Direct emissions can stem from PFCA usage, where they can volatise into the air as a gas (Wang et al., 2014) or are emitted into the atmosphere as particles via sea spray aerosols after being ionized in water bodies (e.g. oceans, rivers, etc.), which has been shown to be a contributor to atmospheric PFCAs (Sha et al., 2024). They can also be produced in the atmosphere indirectly from PFAS precursor intermediates via photolysis (R3.1), hydrolysis (R3.2) and reactions with hydroperoxyl radicals (R3.3) (Young & Mabury, 2010).

$$CF_3(CF_2)_nC(O)X + h\nu \rightarrow CF_3(CF_2)_nC(O)OH + C(O)F_2 + HF + HX \quad \textbf{(R3.1)}$$

$$CF_3(CF_2)_nC(O)X + H_2O \rightarrow CF_3(CF_2)_nC(O)OH + HX \quad \textbf{(R3.2)}$$

$$CF_3(CF_2)_nC(O)OO\bullet + HO_2 \rightarrow CF_3(CF_2)_nC(O)OH + O_3 \quad \textbf{(R3.3)}$$

These intermediates are formed via the transformation of various PFAS commercial products that have been emitted into the atmosphere from point sources (e.g. chemical and material production facilities, WWTP, landfill), many of which react photochemically or with photochemically produced compounds, including unstable radicals (Young & Mabury, 2010). Depending on the type of PFCA precursor, different PFCAs can be produced (Table 3.1).

Table 3.1: Terminal degradation PFCA products produced from volatile PFAS compounds, modified from Young and Mabury (2010).

Commercial Compounds	PFCAs							
	C2	C3	C4	C5	C6	C7	C8	C9
	TFA	PFPrA	PFBA	PFPeA	PFHxA	PFHpA	PFOA	PFNA
Halothane	√							
Isofluorane	√							
HCFC-124	√							
HCFC-123	√							
HCFC-225a		√						
HFC-134a	√							
HFC-125	√							
HFC-329	√	√	√					
HFC-227	√							
$CF_3CF=CH_2$	√							
$CF_3CF=CHF$	√							
$CF_3CF=CF_2$	√							
$CF_3CF_2CF=CF_2$		√						
$CF_3CF=CFCF_3$	√							
Fluorotelomers 4:2	√	√	√	√				
Fluorotelomers 6:2	√	√	√	√	√	√		
Fluorotelomers 8:2	√	√	√	√	√	√	√	√
Fluorotelomers 10:2	√	√	√	√	√	√	√	√
Fluorotelomers 12:2	√	√	√	√	√	√	√	√
Fluorotelomers 14:2	√	√	√	√	√	√	√	√
NEtFBSA	√	√	√					
NEtFOSA	√	√	√	√	√	√	√	
NMeFBSE	√	√	√					
NMeFOSE	√	√	√	√	√	√	√	

Short-chain PFCAs (C2-C4), more notably trifluoroacetic acid (TFA), are produced from many more PFAS compounds compared to longer chained PFCAs (Table 3.1). Atmospheric lifetimes of these PFCA precursor commercial compounds are found to be highly variable. For instance, isofluorane and $CF_3CF=CF_2$, both precursors to TFA, have atmospheric lifetimes of 3.1 years and 6-9 days, respectively (Young & Mabury, 2010). This variability in precursor lifetimes is also seen for longer-chain PFCAs. For example, fluorotelomer aldehydes break down much faster (4 days) compared to odd-chain fluorotelomer alcohols (124 days) (Young & Mabury, 2010). Therefore, the specific PFCA precursors that are used commercially and subsequently released will determine the range and spatial distribution of PFCAs in the atmosphere.

3.1.2 Need for atmospheric PFCA measurements

There has been a need to measure perfluoroalkyl carboxylic acid (PFCAs) in the atmosphere due to their persistence, high atmospheric mobility, and potential negative implications to the environment worldwide (Elis et al., 2004; Prevedouros et al., 2005; Wong et al., 2018). Even so, few atmospheric measurements PFCAs exist globally. Measurements

have been made by either indirect sampling via the analysis of deposition samples or direct gas and/or particle sampling of PFCAs.

Indirect sampling via total deposition, a combination of both dry and wet deposition, has been reported by a few studies (Dryer et al., 2010; Kim & Kanna, 2007; Kwok et al., 2010; Lui et al., 2009; Pike et al., 2021; Scott et al., 2006). Pike et al. (2021) and Scott et al. (2006) are the only works to have included measurements of TFA in addition to the longer chained PFCAs, up to 9 carbons. Scott et al. (2006) had also included perfluoropropionic acid (PFPrA) in those measurements. In every instance, TFA deposition levels were found to be the highest PFCA by concentration, regularly an order of magnitude higher compared to other PFCAs (Pike et al., 2021; Scott et al., 2006). Deposition levels of PFPrA are often second highest (Scott et al., 2006). While total deposition has provided important insight such as relative abundance of atmospheric PFCAs, it is unable to provide gas phase and particle phase concentrations. This is due to dry and wet deposition removing both gaseous and particulate matter from the atmosphere (EPA, 2024), where the distribution of PFCAs in both phases is not possible to discern, unlike current direct measurement (Wu et al., 2014).

Most direct measurements for gas and particle phase PFCAs have been performed for PFCAs with a carbon chain length of 4 or higher (≥C4), due to reverse phase liquid-chromatography (LC-MS) analysis limitations, described in Section 1.1.6. Recent work by Vierke et al. (2011) used high-volume samplers and PUF-XAD passive air samplers to obtain extensive measurements of gas and particle phase ≥C4 PFCAs at a WWTP in Ontario, Canada. In that study, ≥C4 PFCA levels spanned the range of 0.009-150 pg/m^3 where the particle phase reached an upper limit of 150 pg/m^3 while the gas-phase reached as high as 50 pg/m^3. Higher particle as opposed to gas phase loadings, suggests a partitioning preference for the particle phase for ≥C4 PFCAs. However, like many other studies, this work unable to measure TFA or PFPrA, despite their generally greater atmospheric abundances compared to their ≥C4 PFCA counterparts (Scott et al., 2006; Ye et al., 2023). Studies that have measured gas and particle phase TFA have classified it as a haloacetic acid rather than a PFCA (Martin et al., 2003b). As a result, measurements of TFA have typically been made separate from other PFCAs with 3 carbons or more (≥C3). Wu et al. (2014) is one of the few recent studies measuring gas and particle phase TFA using an annular denuder and a quartz filter pack, where particle levels were found to reach as high as 500 pg/m^3 and gas-phase up to 3500 pg/m^3. These TFA trends suggest a partitioning preference for the gas phase under the environmental conditions of this prior work. Ye et al. (2023) is the only study to have measured gas-phase PFPrA, with the single

measurement reported to be 14.9 pg/m^3. To our knowledge, no particle-phase PFPrA has been reported to date.

While direct measurements have been performed for PFCAs, they are fairly scarce, especially for TFA and PFPrA. Many of those measurements were performed with high-volume samplers, annular denuders and/or PUF-XAD passive air samplers, where several limitations exist such as artifacts for high-volume samplers (Tao et al., 2023), high maintenance and cost for annular denuders and extensive sample preparation for PUF-XAD passive air samplers (Ahrens et al., 2011), as described in detail Sections 1.1.4 and 2.1.1. All of these studies have used either LC-MS or GC-MS analysis methods, where more limitations exist such as typical reverse phase LC having an inability to retain, and therefore reliably quantify, TFA and PFPrA (Janda et al., 2008) and GC requiring extensive sample work-up (Ye et al., 2023). These issues are described in detail in Section 1.1.6. Overall, there is a need for a better direct measurement method for atmospheric PFCAs that overcomes many limitations of current sampling techniques that will allow temporally resolved measurements at large spatial scale, while also inclusive of TFA and PFPrA atmospheric measurements.

3.1.3 Objectives

The goal of this work is to deploy our custom-built nylon PAS for $PFCAs_{(g)}$ described in Chapter 2 for sampling in multiple locations across Canada over the course of a year. Sampling locations include urban areas, remote areas in endangered whale habitats, a wastewater treatment plant and an indoor lab. Concentrations from passive air samples will be quantified predominantly via IC-MS analysis to determine mixing ratio of $PFCAs_{(g)}$ at those locations. Trends including potential sources will be discussed.

3.2 Methods

3.2.1 Materials and chemicals

Sodium carbonate (Na_2CO_3) (>99.5%), Glycerol (>99%), dichloromethane (DCM; ACS reagent Grade) and NaOH stock solution (49-51% in DIW) were obtained from Sigma Aldrich (ON, Canada). Methanol (MeOH) of both HPLC and Optima® LC-MS grades were obtained from Fisher Chemical (ON, Canada). The purchase of TFA (HPLC grade) was made from EMD Millipore (MA, US); PFPrA, PFBA and PFPeA (>97%) from Sigma Aldrich (MO, US); and PFHxA (>97%) from Synquest, (FL, US). Stock solutions of native PFCAs for GC-MS were prepared in ethyl acetate (EtAc; HPLC Grade; Anachemia VWR, PA, US) at 500 µg/mL, which were diluted to working stock concentrations. Mass-labeled $^{13}C_2$-TFA (>97%)

was purchased from Toronto Research Chemicals (ON, Canada); $^{13}C_3$-PFBA, $^{13}C_2$-PFOA, and $^{13}C_2$-PFDA for GC-MS analysis were purchased as a mixture in MeOH (2 µg/mL; MPFAC-C-IS) from Wellington Laboratories (ON, Canada). These compounds were combined into one HPLC MeOH solution and used as internal standards (IS) for GC-MS analysis. Diphenyl diazomethane (DDM; >90%) was synthesized in-house using established methods (Javed & Brewer, 2007) or was purchased from Toronto Research Chemicals (ON, Canada), but at a lower purity for use as the derivatization agent for GC-MS analysis (Ye et al., 2023). Sodium salts of TFA (>98%) and PFPrA (>99%) were obtained from Sigma Aldrich (ON, Canada). The sodium salts of PFBA (>98%), PFPeA (purity not reported) and PFHxA (>98%) were obtained from Synquest (FL, US). Stock solutions of sodium salts of PFCAs for IC-MS analysis were prepared in ultrapure Milli-Q water (18.2 MΩ·cm at 25 °C, Direct 8; EMD Millipore) at 1000 µg/mL, which were diluted to working stock concentrations. Mass-labeled $^{13}C_1$-TFA (T786038) was purchased from Toronto Research Chemicals (ON, Canada) and dissolved in MeOH to reach a concentration of 50 mg/ml. Mass-labeled $^{13}C_4$-PFBA, $^{13}C_3$-PFPeA, and $^{13}C_2$-PFHxA were individually obtained from Wellington Laboratories (ON, Canada) and dissolved in MeOH (50 µg/mL; MPFBA, M3PFPeA & MPFHxA). These mass-labeled compounds were combined into one Milli-Q water solution for use as an internal standard in IC-MS analysis.

3.2.2 Nylon-based passive air samplers' components, sample preparation and extraction

The nylon-based passive air samplers were prepared and extracted as described in Section 2.2.4. Briefly, they are composed of a nylon filter and polypropylene (PP) overlying filter, where chemisorption of acids occurs on the nylon filters via diffusion through the PP overlying filters. The sampler filters are cleaned with a Na_2CO_3 solution and DIW, dried, then assembled and stored in Ziploc bags made out of low-density polyethylene. They were removed from the Ziploc bags and mounted inside a weather shield to start sampling. At the end of a sampling period, they were detached from the weather shield and placed back into the Ziploc bags. Sample filters were extracted in 3 mM NaOH in Milli-Q water for IC-MS analysis or extracted in 0.1 M NaOH in MeOH, reconstituted, and derivatized for GC-MS analysis.

3.2.3 Sampling locations

The PAS were deployed in three areas in Canada (Figure 3.1) to explore the importance of $PFCAs_{(g)}$ in rural/remote at-risk whale habitat, in urban areas, and in indoor locations.

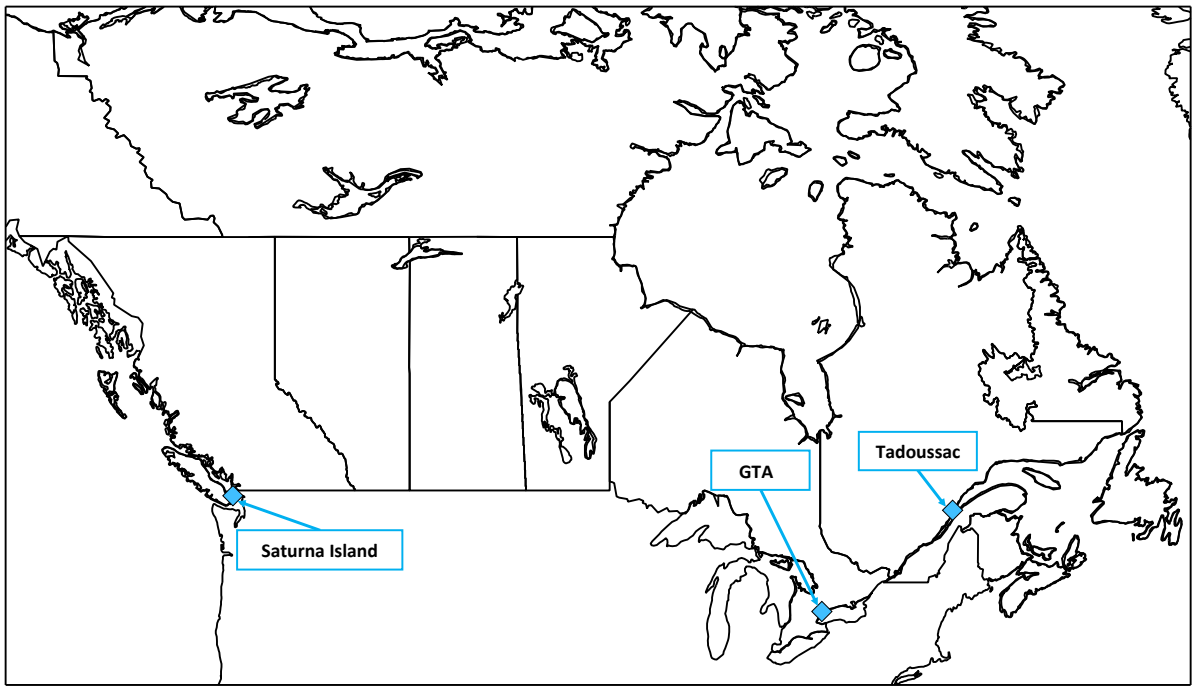

Figure 3.1: PAS sampling locations in Canada

Each PAS was deployed at least 40 cm off the ground or higher to ensure minimal bias associated with close proximity to surfaces. Field blanks were brought to the site and exposed for 10 seconds before being sealed again within Ziploc bags. Sampling periods were usually 2-3 months at each location (with some exceptions, see Table 3.1) to ensure most PFCAs were found above method detection limits. Samples were collected in six locations that can be classed into four general location types: ambient urban, ambient rural/remote, indoor, and near point source. Details of each sampling location are as follows and in Table 3.2:

Ambient urban:

Petrie Science and Engineering Building rooftop: Samplers were hung on the south railing of the Air Quality Research Station on top of the Petrie Science and Engineering Building at York University in Toronto. They were positioned 4 m to the inlet of the ambient ion monitoring ion chromatography with mass spectrometry instrument (AIM-IC-MS), for orthogonal measurement intercomparisons. This sampling site is an urban environment in a large university campus located near many commercial buildings, residential homes and busy roads, with many possible sources of PFCAs and its corresponding precursors.

Moccasin Trail Park: Samplers were hung on a wooden structure on top of the ravine slope of Moccasin Trail Park in the Don River Valley in Toronto. This sampling site is located in an urban environment near many parks, commercial buildings, residential homes and busy roads, with many possible sources of PFCAs and its corresponding precursors.

Ambient rural/remote:

Tadoussac: Sampling occurred on a remote farm located approximately 750 m from the St. Lawrence River. Samplers were hung on a metal pole stabilised by guy wires. This sampling occurred alongside annular denuder samplers and total and wet deposition samplers, for future orthogonal and complimentary intercomparisons. Tadoussac is located in the St. Lawrence Estuary, which is the habitat of the endangered Beluga Whales (Government of Canada, n.d.). Considering PFCAs have been detected in their tissue and are suspected to have negative effects the reproductive success of these mammals (Barrett et al., 2021), this location is well suited for assessing the importance of PFCAs in the atmosphere.

Saturna Island: Sampling occurred on a remote Government of Canada National Air Pollution Surveillance (NAPS) station approximately 1 km from the Salish Sea. Samplers were hung on one of the railings of the NAPS station sampling tower. This sampling occurred alongside annular denuder samplers and total and wet deposition samplers, for future orthogonal and complimentary intercomparisons. Saturna Island is located in the Salish Sea, which is the habitat of the endangered Orca whales (Government of Canada, n.d.), also suspected to be negatively affected by pollutants such as PFCAs. Measuring PFCAs in the atmosphere is important for determining the amount of PFCAs being transported to this location in the atmosphere.

Indoor:

Petrie Science and Engineering Building indoor laboratory: Samplers were hung on a retort stand in the middle of a large laboratory. PFCA compounds are regularly used for research in the laboratory. The laboratory has good ventilation and the use of PFCAs is often handled in a well vented fume hood.

Near point source:

Wastewater Treatment Plant: Samplers were deployed for a month at a large wastewater treatment plant in the greater Toronto area (GTA) where past measurements have demonstrated it to be a source of PFAS compounds, including some PFCAs (≥C4) (Ahrens et al., 2011). These wastewater treatment plants are composed of several stages of cleaning process, including: a primary clarification tank for gravity-based solids removal, an aeration tank with air pumped through the liquid to promote microbial biodegradation of pollutants, and a secondary clarification tank for quiescent settling of the microorganism-laden biomass for final effluent polishing. These stages of treatment can be (and often are) performed in wastewater

tanks that have direct contact with the atmosphere. Passive air samplers were deployed at 4 spots within the treatment plant: at a reference site, at a primary clarifier, at an aeration tank and at a secondary clarifier (Figure 3.2).

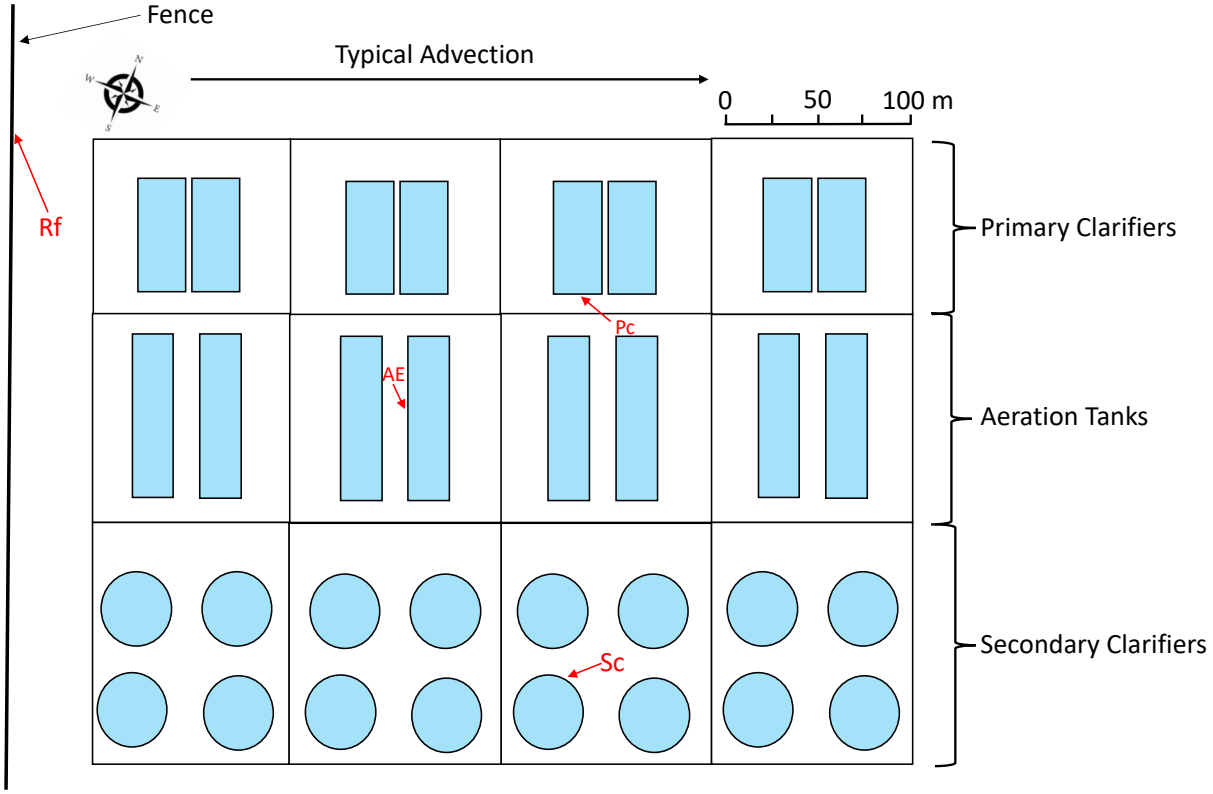

Figure 3.2: WWTP aerial view of the different PAS sampling locations shown in red, which includes the fence line reference location (Rf), the Primary clarifier (Pc), the Aeration Tank (AE) and the Secondary Clarifier (Sc).

For the reference site, samplers were hung on the perimeter fence of the treatment plant located upwind of typical wind directions in the region. For the primary clarifier, samplers were hung on a fence near turbulent water outflow of a primary clarifier pool. For the aeration tank, samplers were hung on a fence right beside the aeration tank pool. For the secondary clarifier, samplers were hung on a fence right on top of the turbulent water outflow of a secondary clarifier pool. Since TFA and PFPrA have never been quantified before at a wastewater treatment plant, this presents an opportunity for determining a new point source for these compounds.

Details on the number of samples deployed, sampling periods, number of replicates, analysis method used, and exact sampling location can be found in Table 3.2. Note, the exact location of the wastewater treatment plant cannot be disclosed.

Table 3.2: Sampling locations, dates, replicates, and analysis method details for PAS.

Locations	Sub-locations	Latitude and Longitude	Sampling Start Date	Sampling End Date	Number of Replicates	Analysis Method
Petrie Science Building Rooftop, York University, Toronto, ON	n/a	43.7735, -79.5070	2022-05-16	2022-07-07	3	GC-MS
			2022-07-07	2022-08-04	3	IC-MS
			2022-07-07	2022-09-14	3	IC-MS
			2022-09-14	2022-11-23	3	IC-MS
			2022-11-23	2022-12-05	3	IC-MS
			2022-11-23	2023-03-09	3	IC-MS
			2023-04-27	2023-06-26	3	IC-MS
Moccassin Trail Park, Toronto, ON	n/a	43.7319, -79.3359	2022-04-16	2022-07-04	3	GC-MS
			2022-07-04	2022-09-29	3	IC-MS
			2022-09-29	2022-12-06	3	IC-MS
			2022-12-06	2023-03-18	3	IC-MS
			2023-04-27	2023-06-28	3	IC-MS
Tadoussac, QC	n/a	48.1421, -69.6917	2022-01-14	2022-04-18	1	IC-MS
			2022-04-18	2022-06-09	2	IC-MS
			2022-06-09	2022-10-12	3	IC-MS
Saturna Island, BC	n/a	48.7752, -123.1283	2021-12-14	2022-12-04	2	IC-MS
Petrie Science Building Indoor Laboratory, York University, Toronto, ON	n/a	43.7735, -79.5070	2022-04-16	2022-05-19	3	GC-MS
			2022-05-19	2022-06-27	3	GC-MS
Waste-Water Treatment Plant, ON	Reference Location	n/a	2023-05-25	2023-06-01	3	IC-MS
			2023-05-25	2023-06-23	3	IC-MS
			2023-06-01	2023-06-16	3	IC-MS
			2023-06-16	2023-06-23	3	IC-MS
	Primary Clarifier		2023-05-25	2023-06-01	3	IC-MS
			2023-06-01	2023-06-16	3	IC-MS
			2023-06-16	2023-06-23	3	IC-MS
	Aeration tank		2023-05-25	2023-06-01	3	IC-MS
			2023-06-01	2023-06-16	3	IC-MS
			2023-06-16	2023-06-23	3	IC-MS
	Secondary Clarifier		2023-05-25	2023-06-01	3	IC-MS
			2023-06-01	2023-06-16	3	IC-MS
			2023-06-16	2023-06-23	3	IC-MS

3.2.4 Ion chromatography with mass spectrometry (IC-MS)

The ion chromatography system is composed of a Thermo Scientific™ Dionex™ ICS-6000 system outfitted with dual pump (DP) and dual column and detector (DC) compartments. The autosampler uses a 5 mL syringe to inject 750 µL of the sample on a Thermo Scientific™ Dionex™ IonPac™ TAC-ULP1 anion-selective concentrator column (5×23mm, 18 µm dp, 6% DVB). A Thermo Scientific™ Dionex™ IonPac™ AG24 guard (2×50mm, 11 µm dp) and AS24 analytical column combination (2×250mm, 7 µm dp, 55% DVB, alkanol quaternary ammonium exchanger) were used for the separation. A 2mm Thermo Scientific™ Dionex™ ADRS 600 Dynamically Regenerated Suppressor was operated in external water mode to remove Na^+ and OH^- from the eluent before reaching the conductivity detector and mass spectrometer. The external water supplied was Milli-Q and set for delivery at a flow of 1

mL/min. The suppressed eluent then flows through a conductivity detector thermostated at 30 °C and operated with a data acquisition rate of 5 Hz before combining with 0.2 mL/min Optima methanol and entering the Thermo Scientific™ ISQ™ EC single quadrupole mass spectrometer. The single quadruple mass spectrometer was operated in negative electrospray ionisation mode (ESI^-) at 450 °C, performed in selective ion monitoring (SIM) with an ion transfer tube at 250 °C.

Two different gradients and temperature control programs were used for the analysis of samples because the AS24 column was replaced part way through analysis. The analyte retention one the new column was found to have shifted compared to the older column. The older AS24 column used the following gradient: 0.35 mL/min, 25 mM of NaOH in DIW for 7 min, increased to 52 mM of NaOH in 4.9 min, kept at 52 mM of NaOH for 10 min, brought back to 25 mM of NaOH in 0.1 min and kept at 25 mM of NaOH for 3 min. The column temperature was set to 24 °C and the current for the suppressor was set to 50 mA for the run. The brand-new AS24 column used the following gradient: 0.35 mL/min, 25 mM of NaOH in DIW for 7 min, increased to 52 mM of NaOH in 4.9 min, kept at 52 mM of NaOH for 3.1 min, brought to 60 mM of NaOH in 0.5 min and kept at 60 mM of NaOH for 12.4 min, then brought back to 25 mM of NaOH in 0.1 min and kept at 25 mM of NaOH for 3 min. The column temperature was set to 28 °C and the current for the suppressor was set to 57 mA for the run.

Ten-point calibrations were performed with C2-C6 PFCA standards in DIW, ranging from 10-10000 ng/L. Samples, blanks and standards vials were spiked with mass-labelled C2, C4-C6 PFCA internal standards before analysis. Each PFCA was corrected for matrix effects and instrument fluctuations with its corresponding mass-labelled internal standard, except PFPrA which used the $^{13}C_4$-PFBA mass-labelled internal standard (IS). This internal standard has a different retention time from PFPrA and may not properly account for any experienced ion suppression that can occur for PFPrA in each sample. It is expected that the quantification for PFPrA will be less robust then the other PFCAs in this method, especially when the samples experience large matrix effects at those retention times due to ion suppression for both PFPrA and the IS of PFBA.

3.2.5 Gas chromatography with mass spectrometry (GC-MS)

Details on the gas-chromatography with mass-spectrometry (GC-MS) analysis method can be found in Section 2.2.7. Briefly, the system uses a 5% phenyl-based column with hydrogen (H_2) as a carrier gas to separate diphenyl diazomethane-derivatized PFCAs. A single

quadruple mass spectrometer is then used as a detector in ECNI mode with selective-ion monitoring (SIM) for diagnostic PFCA fragments.

3.3 Results and discussion

3.3.1 Ion chromatography with mass spectrometer method

Ion-chromatography with mass spectrometry was used as the primary analysis method since derivatization and other sample preparation steps were not required, reducing the time and potential for sample contamination which can improve the throughput and method detection limits (MDL). Separation of PFCAs from major anions is important to limit the potential impact of ion suppression during electrospray ionisation, which can lead to large increases on the MDL. Figure 3.3 demonstrates the separation of PFCAs on the conductivity of PAS samples for the old column and new column methods.

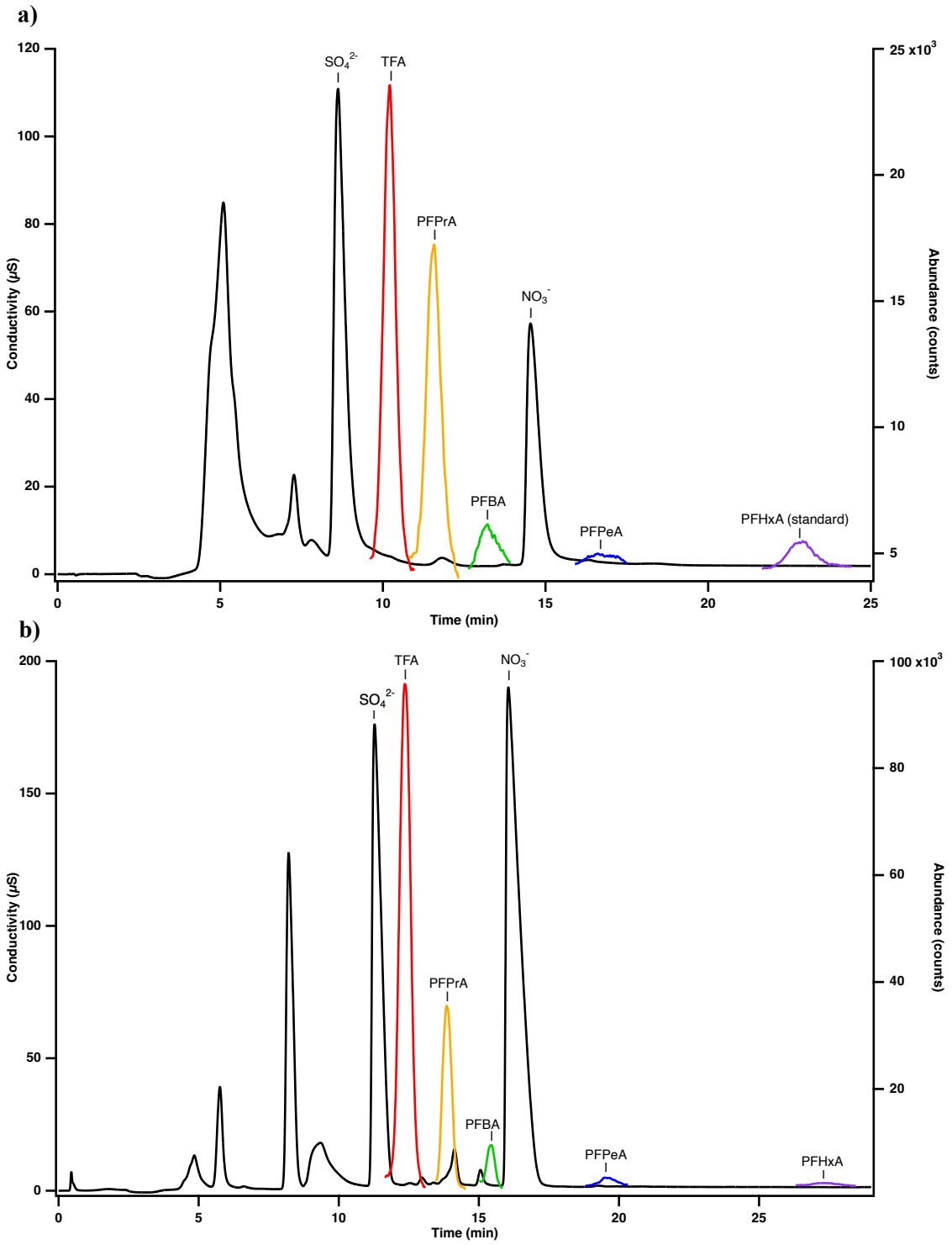

Figure 3.3: Chromatograms representing the separation of PFCAs in PAS samples, where the black trace is conductivity from the conductivity detector (CD) and the coloured traces are the mass abundances from the mass spectrometer (MS). The time delay between both detectors was corrected for. (A) represents the separation with the 24 °C method from a Petrie rooftop sample (Sep-Nov 22 in Figure 3.5) meanwhile (B) represents the separation with the 28 °C method from a Petrie rooftop sample (Apr-Jun 23 in Figure 3.5). Note: PFHxA was not detected in the (A) sample and so PFHxA from the closest run standard was overlaid instead.

Good separation can be seen for PFCAs to that of major anion signal in PAS samples, specifically from the atmospherically abundant sulphate and nitrate precursors, minimising the impact of these matrix components on ion suppression. The samples used in the chromatograms above are one of the most concentrated PAS samples in terms of abundance in conductivity detection. As such, the nitrate and sulphate peaks are smaller in most other samples where the ion suppression impact from the minor overlap between TFA and sulphate was minimal. Also, the smaller unknown peaks in the conductivity detector found between nitrate and sulphate that may cause ion suppression for TFA, PFPrA and PFBA were not observed in most PAS samples. Figure 3.3b demonstrates improved peak shape compared to Figure 3.3a due to use of the new AS24 column, where improvements can be seen from the previous tailing of nitrate and sulphate peaks in Figure 3.3a. The tailing peaks worsened to peak splitting, leading to the need of a new AS24 column and changes to the previous method due to a non-uniform increase in retention for different analyte types. Overall, the new 28°C method with the new column obtained comparable MDL to the previous method (Section S3.1 in Appendix B).

3.3.2 Orthogonal PAS and AIM-IC-MS intercomparison

Orthogonal $TFA_{(g)}$ measurements between our nylon-based PAS and an ambient ion monitoring ion chromatography mass spectrometer instrument (AIM-IC-MS) were performed in the field in order to further validate the calibration of these samplers performed in Chapter 2 using a simulated atmospheric chamber. These measurements were performed at the end of the fall in 2022 where the inlet of the AIM-IC-MS was 4 m from the placement of the PAS on the railing. A comparison between $TFA_{(g)}$ measurements made by PAS and average hourly measurement of the AIM-IC-MS is shown in Figure 3.4.

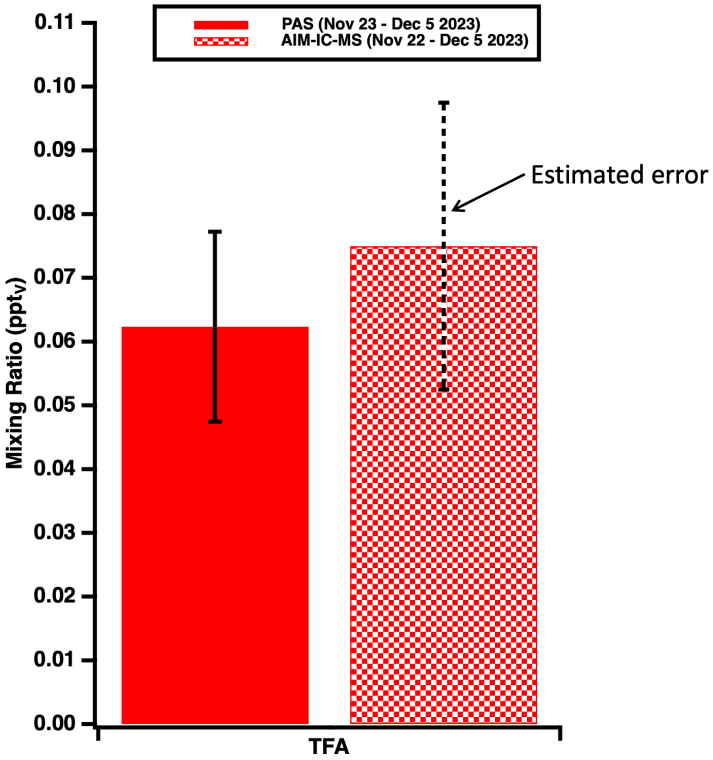

Figure 3.4: Measurements of gas-phase TFA from PAS versus an AIM-IC-MS instrument. The measurement from the AIM-IC-MS represents an average of the hourly measurements during this time period. This average includes half of the AIM-IC-MS MDL (being as low as 0.0219 ppt_v for $TFA_{(g)}$) for hourly measurements that fell below its MDL. Its highest hourly measurement was found to be 2.047 ppt_v. The error bars for the PAS measurement represents one standard deviation of the replicates (n=3). The dashed error bar for the AIM-IC-MS represents a conservative error estimate (VandenBoer et al., 2012).

A 17% difference is found between both measurements, where a Welch two tailed t-test at a 95% confidence interval indicates no significant statistical different between both measurements ($t_{calculated} = 0.55 < t_{table} = 4.31$). It is also important to consider that the average temperature during this sampling period was 1 °C meanwhile the chamber experiment's average temperature was 27 °C. Place et al. (2018) had determined that a ±10% discrepancy can exist from temperatures that range from 10 to 35 °C when sampling with nylon-based PAS. Thus, some of the difference in both values is likely due to an underestimation from our PAS measurements caused by winter-like temperatures. Had this temperature effect been properly corrected for in this measurement, the difference between both values would have been found be smaller. This demonstrates good agreement between both measurements and further validates the nylon-based PAS method for sampling $TFA_{(g)}$. The use of PAS in this context has

shown to be an important tool for orthogonal measurements of $TFA_{(g)}$, especially when $TFA_{(g)}$ from samplers that perform hourly measurements are predominately found below the MDL.

3.3.3 Toronto outdoor passive air samples

Measurements of $PFCAs_{(g)}$ were performed at two different locations in the GTA over the course of a year using our custom-built PAS. These sampling locations are located 14.5 km from each other and are both ambient urban locations not known to be close to any point sources. The PAS used the calibrated dose-response of $TFA_{(g)}$ from Section 2.3.5 and Fuller's law predicted dose-responses for the remaining PFCAs (see Section 2.3.7). The replicates, which takes into account the inter-sample variability and the analytical uncertainty, were deployed for approximately two-to-three-month increments, with some exceptions (Table 3.2). Understanding the relative gas-phase mixing ratios of PFCAs can help understand the source signatures, the preferred degradation products from those precursors and the gas-particle partitioning preference which can impact their atmospheric transport. Figure 3.5 demonstrates

$PFCA_{(g)}$ measurements made at Air Quality Research Station on top of the Petrie Science and Engineering Building.

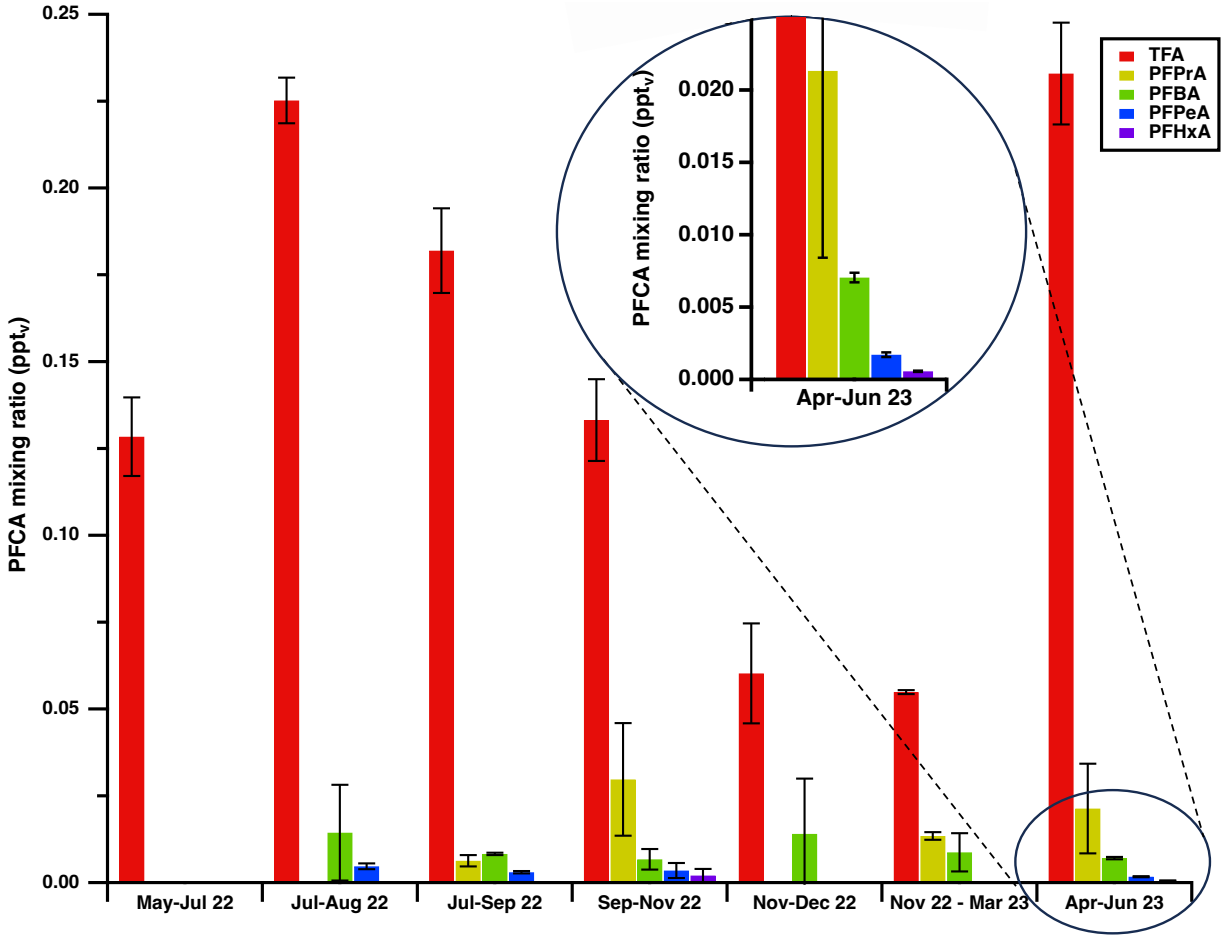

Figure 3.5: Measurements of gas-phase PFCAs at the Petrie science building rooftop using PAS. The error bars represent one standard deviation of the replicates (n=3).

The relative mixing ratios of $PFCAs_{(g)}$ decrease with increasing chain-length. The shortest PFCA, TFA, is consistently found with the highest mixing ratio. This chain-length relationship can be more effectively seen in inset of Figure 3.5, where $PFHxA_{(g)}$ is found above the method's detection limit with the lowest mixing ratio. This trend is consistent with relative levels reported for atmospheric deposition and air measurements in other studies (MacInnis et al., 2017; Pickard et al., 2020; Scott et al., 2006). In contrast to these prior studies that focused on mass-based measurements, this study utilizes mixing ratios (ppt_v), a quantity independent of the molecular mass of each PFCA. This relative abundance of PFCA trend is consistent with known sources as ultra-short-chain PFCAs, especially TFA, which can be formed from many more PFAS compounds than their longer chained counterparts (Young & Mabury, 2010). Between samples, a seasonal dependence can be seen for $TFA_{(g)}$, where mixing ratios are higher in the summer and lower during the winter (Figure 3.5). Martin et al. (2003b) observed the

same trend for gas and particle phase TFA measurements in the atmosphere performed in Toronto and Guelph in the early 2000s. This seasonal trend is not clearly present for $PFCAs_{(g)}$ with higher chain lengths. Ahrens et al. (2013) also did not observe a seasonal trend for gas- and particle-phase PFBA and PFPeA measured in Toronto. This may indicate important differences between $TFA_{(g)}$ and ≥C3 $PFCAs_{(g)}$ in terms of sources and sinks and driven by their physical properties. While the degradation of both TFA and ≥C3 PFCAs precursors are mostly photochemically dependent, their production is also highly dependent on the availability of their corresponding precursors in the atmosphere. The seasonal variations in atmospheric composition could also affect their yields. Thus, the production of TFA being seasonally dependant, in contrast to ≥C3 PFCAs, is likely due to these previous considerations. One of new types of refrigerants that have been implemented in the recent years, 2,3,3,3-tetrafluoropropene (HFO-1234yf), is expected to react with •OH and •Cl in the atmosphere to produce a much higher yield of TFA compared to the previously used refrigerants (Burkholder et al., 2015; Luecken et al., 2009; Ye et al., 2021). Considering HFO-1234yf is used as a heat transfer fluid, its emissions, which can occur from leaks from usage in cooling systems, are seasonally dependent where their use is dramatically higher in the summer compared to the other three seasons (Wang et al., 2018). This may be one of the important contributions to the seasonal dependence of TFA seen in Figure 3.5.

Global emissions of shorter-chained PFCAs and their precursors are expected to continue to rise for the foreseeable future, as described in Section 1.1.4. $TFA_{(g)}$ levels are seen to be almost two times higher during the spring of 2023 compared to the spring 2022 (Figure 3.5), which may be in part linked to the increased use of these new refrigerants. An important increase was also seen when comparing PFCA levels, including TFA, from PAS measurement in the fall of 2022 to annular denuder measurements made by Ye et al. (2023) in the fall of 2021 at the same location (Figure 3.6).

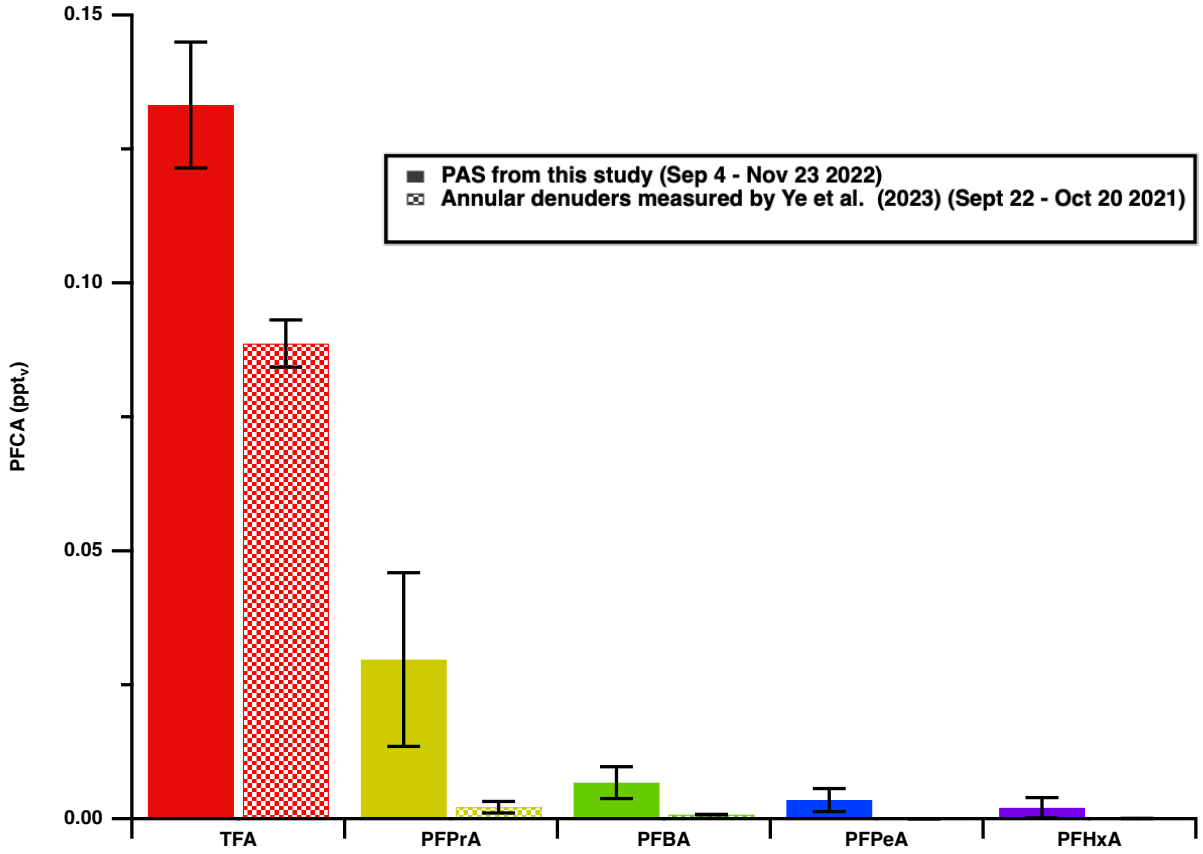

Figure 3.6: Measurements of gas-phase PFCAs at the Petrie science building rooftop using PAS and annular denuders from Ye et al. (2023). The error bars represent one standard deviation of the PAS and annular denuder replicates (n=3).

This may indicate an ongoing annual increase of $TFA_{(g)}$ mixing ratios in the urban air of Toronto, reflecting increasing emissions in the region, stemming from the production and use of many commercial product, such as refrigerants, packaging materials, semiconductors and many more, where many of these products are emitted at wastewater treatment plants, waste management sites (e.g. landfills) and many more (Ahrens et al., 2011; Wang et al., 2014). This trend has only been observed for three consecutive years, where two were strongly impacted by SARS-CoV-2 impacts on societal behaviour, which could impact use and release of TFA-precursors. More annual measurements are needed to confirm this trend and better track its drivers and variability.

Measurements with a similar duration and time frame were performed at another location in Toronto at Moccasin Trail Park, situated on the Don Valley (Figure 3.7).

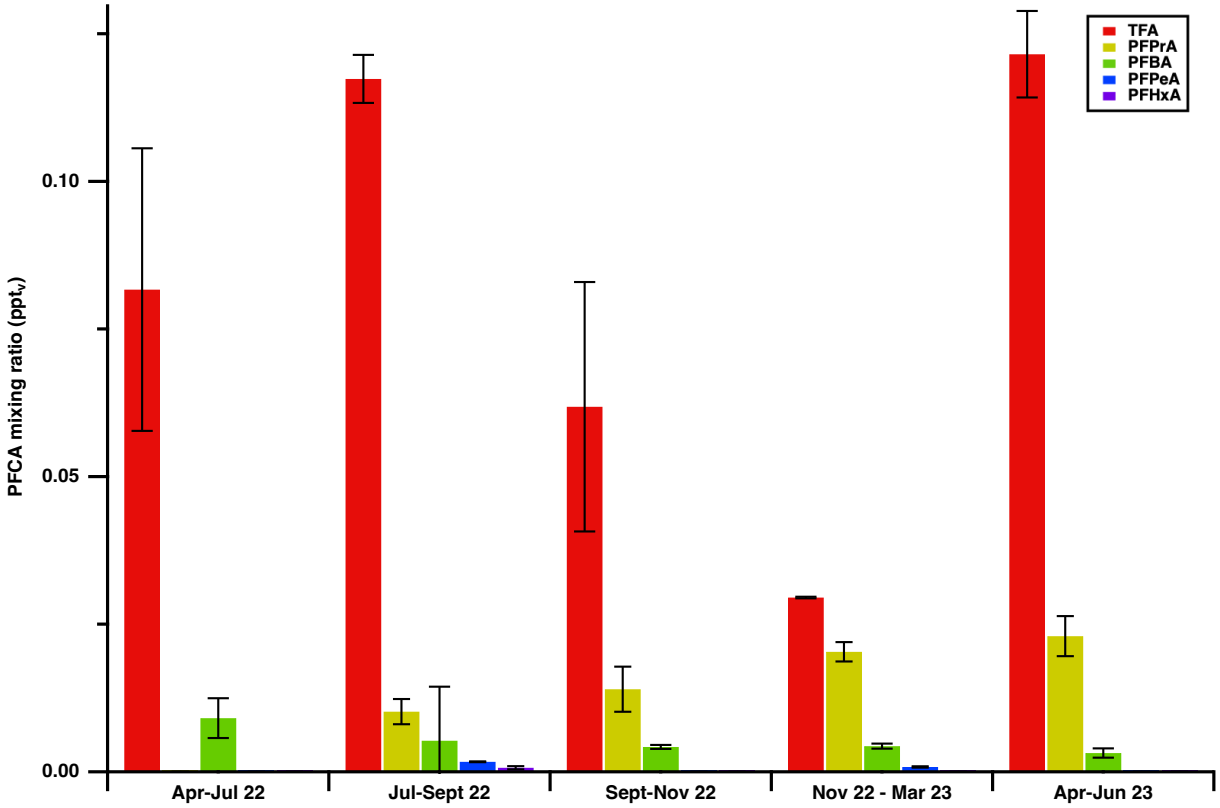

Figure 3.7: Measurements of gas-phase PFCAs at Moccasin Trail Park using PAS. The error bars represent one standard deviation of the replicates (n=3).

Here, the same chain-length-associated atmospheric mixing ratio trend was observed, with the relative mixing ratios of $PFCAs_{(g)}$ decreasing with increasing chain-length and $TFA_{(g)}$ consistently present with the highest mixing ratio. The same seasonal dependence was also seen for $TFA_{(g)}$, being higher in the summer and lower during the winter meanwhile the same seasonal independence for the other PFCAs was observed. Unique to this location, there appears to be a small gradual increase in $PFPrA_{(g)}$ mixing ratios over time of 1.5 ppq_v/month on average (assuming 1 month = 30 days). Meanwhile, the opposite is seen for $PFBA_{(g)}$, where a small decrease over time can be seen of 5.1 ppq_v/month on average. This distinction between both locations is likely related to differences in minor emissions from short lived PFPrA and PFBA precursors (e.g. fluorotelomers used in textiles, food packaging, etc.) or direct emissions. Differing from this, the $TFA_{(g)}$ levels are consistently 1.5 to two times as high at the YorkU Air Quality Research Station compared to the Moccasin Trail Park sampling location. As for the other $PFCAs_{(g)}$, levels are typically found to be comparable at both locations. This may indicate that the TFA-specific precursors in the region are primarily short-lived in the atmosphere and/or there is important direct TFA emissions meanwhile the precursors for the ≥C3 PFCAs in the region are predominantly longer lived, allowing for ≥C3 PFCAs to be more well mixed within

the region. This may also indicate that the YorkU Air Quality Research Station resides close to larger emissions of short lived TFA-specific precursors or direct TFA emissions compared to the Moccasin Trail Park location. Such larger emissions may stem from the many commercial facilities nearby as well as the campus itself. While there's a fume hood exhaust near the YorkU Air Quality Research Station, it likely didn't affect our $TFA_{(g)}$ measurements. Acetone measurements, a marker for fume hood exhaust, were taken using a Vocus PTR instrument during a summer research campaign in 2023 at the same location, where these measurements showed no influence from the exhaust on our data.

3.3.4 Remote passive air sampling at endangered whale habitats

Measurements of gas-phase PFCAs were performed at two different remote locations; at Tadoussac located in the St. Lawrence Estuary and at Saturna Island located in the Salish Sea (Figure 3.8).

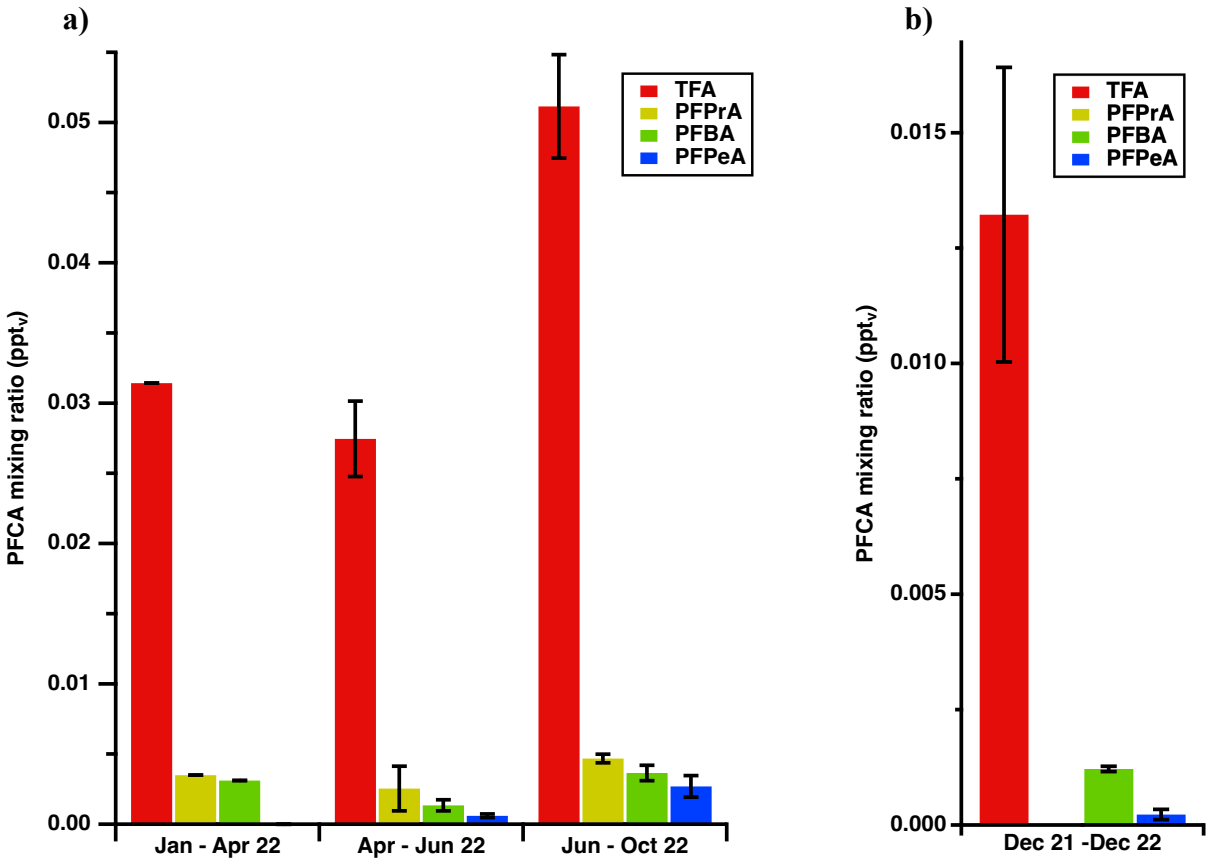

Figure 3.8: Measurements of gas-phase PFCAs at Tadoussac (A) and at Saturna Island (B) using PAS. The error bars represent one standard deviation of the replicates (n=1 to 3).

Both are located in the habitat of endangered whales, where PFCAs have been detected in their tissue and suspected to have negative effects to the reproductive success of these mammals

(Barrett et al., 2021). Due to the remoteness of the locations, our PAS were deployed for longer periods of time compared to the Toronto samplers to ensure detectable levels of the PFCAs were collected (Table 3.2). At both locations, we see the same decrease in mixing ratio with increasing PFCA chain length trend, where $TFA_{(g)}$ is consistently the highest. Figure 3.8a demonstrates the same seasonal TFA mixing ratio trend as was observed in Toronto, where $TFA_{(g)}$ levels are found to be the highest during the summer months. Gas-phase $PFCA_{(g)}$ levels at these remote locations are generally found to be lower than those in Toronto. For example, $TFA_{(g)}$ mixing ratios at Tadoussac and Saturna island were found to be 31-51 ppq_v and 13 ppq_v respectively and $PFBA_{(g)}$ mixing ratios were found to be 1.4-3.7 ppq_v and 1.2 ppq_v respectively. In every instance, $PFCAs_{(g)}$ levels were found to be lower at Saturna island compared to Tadoussac. This is likely due to wind patterns, other meteorological conditions and/or a difference in regional emission sources making Tadoussac more suspectable to long-range transport of $PFCAs_{(g)}$ and its corresponding precursors. This is in agreement with modeling studies that estimate larger deposition of PFCAs (<C8) from some precursors in the region around Tadoussac versus the region around Saturna island (Thackray et al., 2020; Wang et al., 2018). Both remote locations have lower $PFCAs_{(g)}$ mixing ratios then Toronto. It is understandable that urban centres like Toronto have many more local point sources of short lived PFCA precursors as well as also being influenced from long lived PFCA precursors stemming from Canada, outside of the GTA, and from the United States of America. This observation also follows model estimates where the GTA is expected to receive larger deposition of PFCAs (<C8) from some precursors versus the remote regions of Tadoussac and Saturna island (Thackray et al., 2020; Wang et al., 2018). While $PFCAs_{(g)}$ levels are low in these remote regions, it is important to note that these compounds have short atmospheric lifetimes due to their chemical and physical properties and as a result, readily deposit and accumulate into the nearby environment (Rayne et al., 2009). Therefore, despite their low concentrations, the atmospheric transport of these compounds and their precursors is still significant for impacting the $PFCA_{(g)}$ levels in these remote regions, especially considering that they do not degrade.

3.3.5 Indoor laboratory PFCA measurements

Indoor measurements using PAS were performed in a laboratory at York University where PFCAs are used for research purposes, such as preparation of analytical standards and physical property experiments. The results reflect the exposure mixing ratios in an atypical

workplace environment where fluorinated chemicals are in use. Figure 3.9 demonstrates two measurements made of $PFCAs_{(g)}$ in an indoor lab, each during a monthly period.

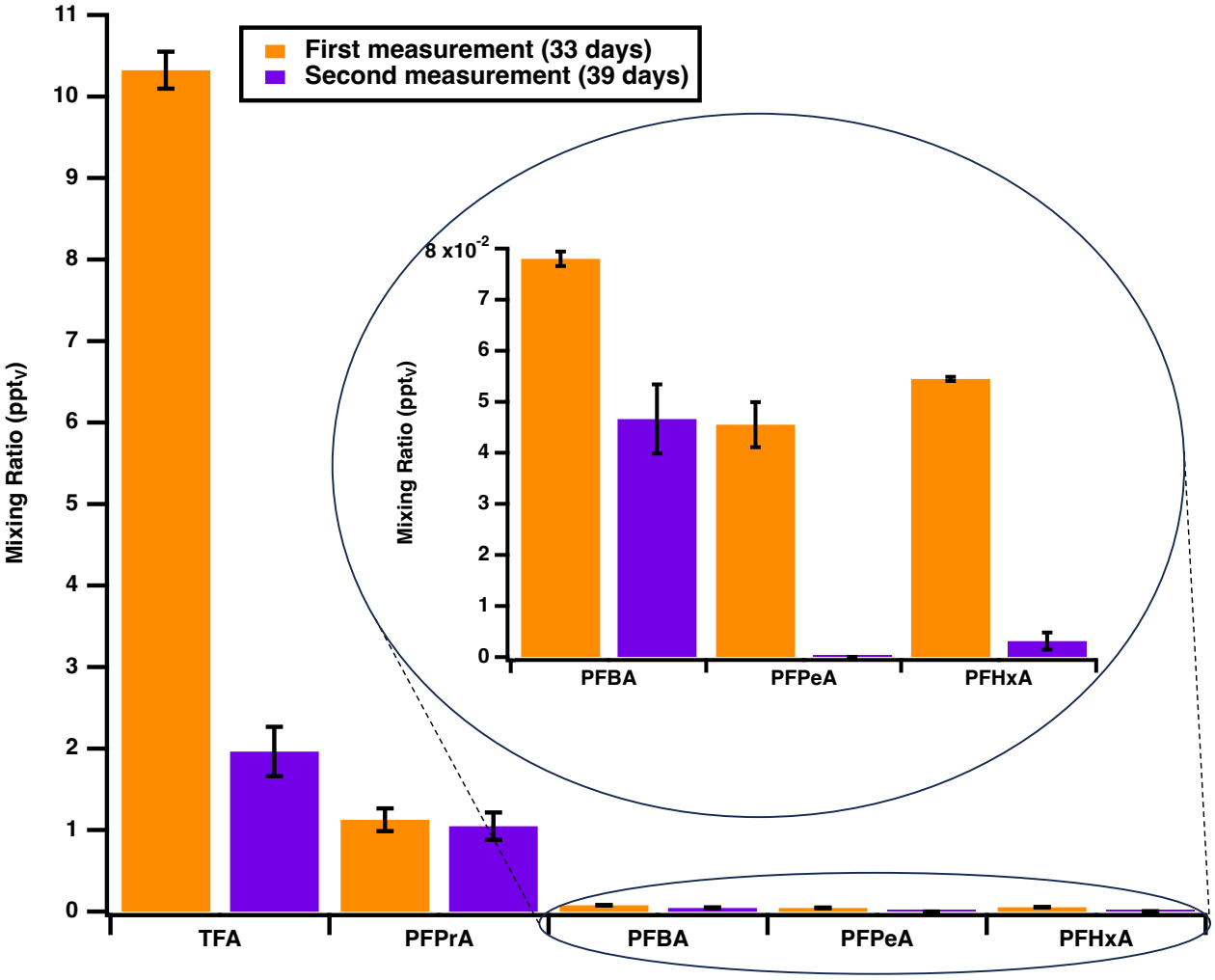

Figure 3.9: Measurements of gas-phase PFCAs in an indoor laboratory at the Petrie Science building. The error bars represent one standard deviation of the replicates (n=3).

The first month was a period of active usage of the lab space, with many research projects handling PFCA compounds, such as the use of PFCA standards or PFCA permeation tubes. The second month desmonstrates a period with minimal usage in the lab space due to ongoing research evaluations for researchers in the lab. The first month clearly has higher mixing ratios and therefore emissions of $PFCAs_{(g)}$ within the lab, despite care taken by all lab members according to the MSDS use of these compounds with further restriction to the handling of high purity materials to take place only in the fumehood. In particular, $TFA_{(g)}$ was found to be aproximetly 46 times higher then the highest measured ambient outdoor levels discussed above. During the low activity period of the second month, $PFCA_{(g)}$ levels were found to have decreased by a factor of five to 19, with the exception of $PFPrA_{(g)}$. For $TFA_{(g)}$ in particular, the

levels were approximately five times lower then the previous month, but still approximetly 9 times higher compared to the measurements made outside on the rooftop of the same building. The observed decrease in emissions is consistent with expectations, as minimal emissions of PFCAs were anticipated with sufficient ventilation still being present (e.g., 0.72 air changes per hour measured in another lab in the same building; Furlani et al., 2023). However, levels of certain PFCAs, particularly the most volatile homologues like TFA and PFPrA, remained high compared to outdoor air mixing ratios. This indicates that one or more emission sources were present despite ventilation acting as a strong sink. It is possible that some research activities involving PFCAs might have happened and contributed to these emissions. This could also be due to these compounds being re-emitted from surfaces they had previously adsorpted onto as shown from a study for gas-phase acids (Wang et al., 2020). Results from our previous chapter indicate that PFCAs have strong adsorption properties demonstrated by $TFA_{(g)}$ from its significant wall losses from chamber experiments (Appendix A, Section S2.5), where delayed re-emission is possible. While atypical from most work environments, this demonstrates the importance of using low cost PAS to measure these compounds in indoor workplace environments. These samplers offer a convenient and cost-effective way to not only monitor exposure to $PFCAs_{(g)}$ but also to assess associated risks and the efficacy of mitigation methods implemented. This allows us to create a more comprehensive picture of the situation and take targeted action if deemed necessary, while remainning low cost and non-intrusive. As there are currently no exposure guidelines for airborne PFCAs, these samplers serve as a critical first step in their development.

3.3.6 Wastewater treatment plant measurements of PFCAs

Measurements at a wastewater treatment plant (WWTP) using PUF-XAD embedded resin PAS have been used to measure gas-phase polyfluoroalkyl substances, including $PFCAs_{(g)}$, in a previous study (Ahrens et al., 2011). The study found that $PFBA_{(g)}$, $PFPeA_{(g)}$ and $PFHxA_{(g)}$ levels in the atmosphere to be higher at the WWTP compared to a nearby upwind reference site, demonstrating that it was a source atmospheric PFCAs. However, the study did not obtain measurements for gas-phase TFA and PFPrA due to their method's limitations. Measurements of gas-phase PFCAs were performed with our custom-built nylon PAS at this same WWTP (Figure 3.10). Out of the four measurement locations within the WWTP, one of them is a reference site typically found upwind from the WWTP for comparison to the emissions stemming the WWTP water bodies (Figure 3.2).

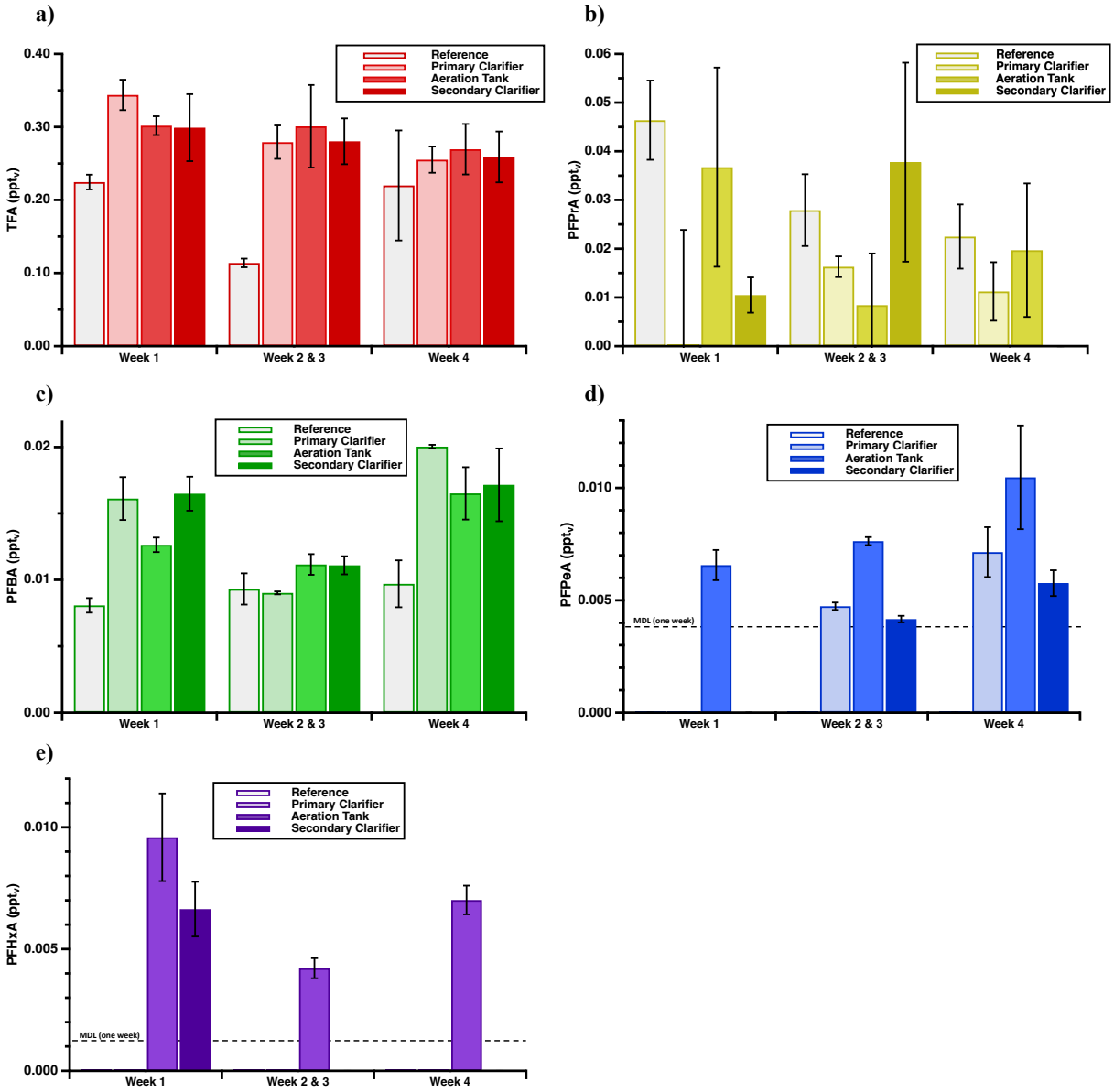

Figure 3.10: Measurements of gas-phase TFA (A), PFPrA (B), PFBA (C), PFPeA (D) and PFHxA (E) at a WWTP using PAS. The error bars represent one standard deviation of the replicates (n=3). The black trace represents the method's detection limits (MDL) for one week of sampling.

In most cases, levels of gas-phase TFA, PFBA, PFPeA and PFHxA at the primary clarifier, aeration tank and secondary clarifier are higher in comparison to the reference site. This strongly suggests the WWTP remains an emission source for $PFCAs_{(g)}$. For $TFA_{(g)}$ in particular, levels were found to be up to 3 times higher compared to the reference location, which strongly suggests the WWTP as an emission source of $TFA_{(g)}$. To our knowledge, this is the first study to identify a non-industrial atmospheric point source of TFA. $PFPeA_{(g)}$ and $PFHxA_{(g)}$ levels were found to be higher at the aeration tank in comparison to the primary and secondary

clarifiers. This may highlight the aeration process of wastewater as an important mechanism for the transfer of neutral PFCA precursors from the wastewater into the atmosphere, before being transformed to $PFCAs_{(g)}$ by photochemical reactions. We speculate that $PFCAs_{(g)}$ may also be emitted from particulate matter that is generated by WWTP water bodies through a process similar to sea-spray or lake-spray aerosols (Olson et al., 2019; Sha et al., 2024). Sha et al. (2024) estimate that sea-spray aerosols can contribute to significant amounts of particulate PFCAs in the atmosphere, equal or greater than other known global sources of PFCAs to the atmosphere from manufacturing emissions followed by precursor degradation. Dasgupta et al. (2007) have shown that $HCl_{(g)}$ can be produced from sea-spray aerosols. Considering WWTP's water bodies are turbulent and rich in suspended particles, a similar mechanism is plausible for the introduction of $PFCAs_{(g)}$ into atmosphere. However, it is important to know that evidence is lacking for this mechanism, and this should be considered speculation at best, demonstrating the need for more atmospheric PFCA measurements.

Evidence of $PFPrA_{(g)}$ emissions from the WWTP was not found because the propagated analytical error levels for PFPrA, the inter-sample variability and analytical uncertainty, were higher than the other PFCA homologues. This is, in part, due to it being the only PFCA without its own mass-labelled internal standard and using $^{13}C_4$-PFBA as an internal standard instead. It is possible that the internal standard that was used for the quantitative determinations of PFPrA was not entirely suitable. For example, $^{13}C_4$-PFBA has a different retention time from PFPrA, so will not properly account for any experienced ion suppression that can occur for PFPrA in a given sample. While we did have a $^{13}C_1$-PFPrA internal standard, it was found to be highly contaminated with TFA and thus unsuitable for use as an internal standard applied to quantitative analysis. In the future, it is recommended that a suitable internal standard for PFPrA is found and used for a more robust quantification of the compound.

Measurements from the fourth week of this study were compared to measurements by Ahrens et al., (2011) performed at the same WWTP in 2009 with PUF XAD-4 embedded passive air samplers. Sites 1, 5, 9 and 10 from Ahrens et al., (2011) were selected for comparison as the closest sampling sites to this study. The fourth week from our study was chosen for this comparison as it has more measurements found above the MDLs and the levels are found furthest from the MDLs compared to other weeks, leading to a more comprehensive evaluation. Unlike our study where measurements were performed weekly/biweekly, the PUF XAD-4 PAS were left to sample at the site for approximately 63 days (Ahrens et al., 2011). Figure 3.11 demonstrates this comparison for $PFBA_{(g)}$, $PFPeA_{(g)}$ and $PFHxA_{(g)}$.

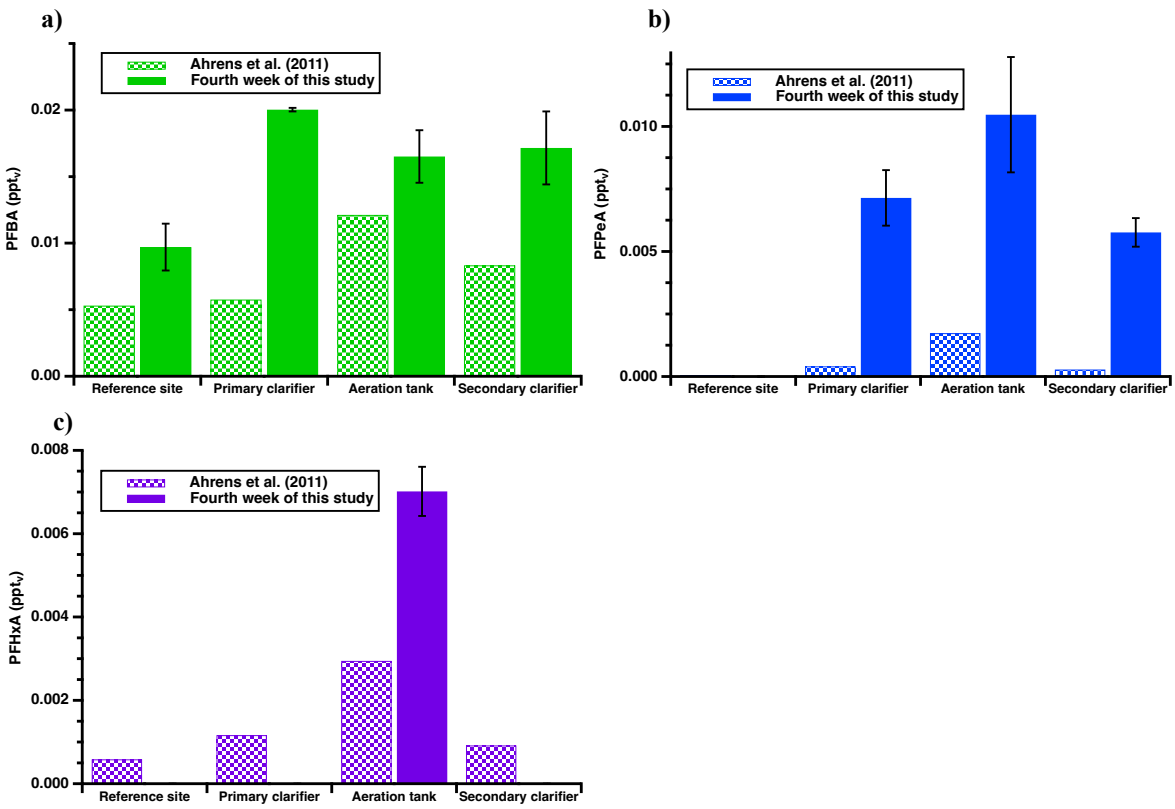

Figure 3.11: Measurements of gas-phase PFBA (A), PFPeA (B) and PFHxA (C) at a WWTP in 2023 with Nylon-based PAS versus in 2009 with PUF XAD-4 imbedded PAS. The error bars represent one standard deviation of the replicates (n=3).

Agreement is seen by both studies where $PFCAs_{(g)}$ levels are higher near the WWTP water bodies compared to an upwind reference site, more notably shown at the aeration tank due to the turbulence from the aeration process. In all cases, levels were found to be higher in this study. The observed difference in atmospheric mixing ratios from both studies might be explained by the timing of sample collection. Ahrens et al. (2011) collected samples across a few months (July to September 2009) when temperatures are generally highest in the summer meanwhile the measurements made from the fourth week of this study was during the month of June. Considering levels are found to be higher in our study and both studies were conducted in the summer, it is unlikely temperature played a role in the difference in mixing ratios from both studies. A difference may also be due to these measurements being made more than a decade apart. The available amounts of PFAS compounds in the wastewater may have been higher in our study compared to Ahrens et al. (2011) leading to higher emissions of PFCAs. While plausible, the evidence backing up this claim is lacking in the context of PFAS in wastewater. It is also likely $PFCAs_{(g)}$ are generally higher now in the atmosphere than over decade ago, contributing to some of the differences in our measurements compared to Ahrens

et al. (2011). This is more evidently seen when comparing the reference site measurements in Figure 3.10a, where $PFBA_{(g)}$ levels are almost twice as high. Measurements made by Ahrens et al. (2013) in 2010, about 3 km away from Petrie science and engineering building rooftop, demonstrate that $PFBA_{(g)}$ and $PFPeA_{(g)}$ levels were indeed lower over a decade ago compared to current levels (Figure 3.5).

3.4 Conclusion

In conclusion, measurements of $PFCAs_{(g)}$ were conducted across multiple locations in Canada using nylon-based passive air samplers, including at ambient urban, ambient rural/remote, indoor, and near point source locations. These measurements have provided valuable insights into the distribution and sources of these compounds while achieving detection limits as low as 0.003 ppt_v for one week of $TFA_{(g)}$ when analyzed using IC-MS. These low detection limits were achieved by optimizing the IC-MS method to ensure minimal ion suppression through good separation of PFCAs from the major anions. Measurements in these studies revealed that $TFA_{(g)}$ consistently exhibited the highest mixing ratio among the PFCAs analyzed, with levels peaking in the summer and decreasing in the winter, likely due to increased use of heat transfer fluids, such as HFO-1234yf, and increase levels of OH radicals in the summer seasons. In contrast, no distinct seasonal trend was observed for other PFCAs. Sampling at two different locations in Toronto demonstrate $TFA_{(g)}$ spatial variability, where levels are found to be 1.5 to two times higher at one location compared to the other. Conversely, no major differences is seen for ≥C3 $PFCAs_{(g)}$ at both locations. These differences suggest that $TFA_{(g)}$ in the region is predominantly influenced by short-lived precursors and/or direct emissions meanwhile ≥C3 $PFCAs_{(g)}$ in the region are predominantly influenced by long-lived precursors. Annual increases of $TFA_{(g)}$ in the same region were also found for three consecutive years, potentially suggesting yearly increases in usage of TFA and/or corresponding precursors. Levels at two remote endangered whale habitats demonstrate that $PFCAs_{(g)}$ are lower compared to measurements made in Toronto, especially at Saturna island which obtained the lowest $PFCAs_{(g)}$ levels. This data further indicated that urban areas, exemplified by Toronto, serve as regions of emission for global PFCAs transport and contamination. Further, the application of passive air samplers to monitor indoor $PFCAs_{(g)}$ in a research lab setting demonstrated their effectiveness in tracking the decrease of gas-phase PFCA contamination, likely due to reduced lab use of PFCAs and continuous ventilation. Equally important, measurements at wastewater treatment plants (WWTP) identified C2-C6 $PFCAs_{(g)}$ as being emitted relative to upwind measurements, except for $PFPrA_{(g)}$. This presents the first study to identify a non-industrial

atmospheric point source of $TFA_{(g)}$. The WWTP as an emission source of $PFPrA_{(g)}$ was not seen due to elevated error compared to the other PFCA homologues, likely due to the use of $^{13}C_4$-PFBA as an internal standard. Following this, the calibration of our nylon-based PAS for TFA was tested in the field by orthogonal measurements to an AIM-IC-MS instrument, where no significant difference is seen between both samplers when accounting for temperature effects. Overall, these studies are the first PAS to conduct $PFPrA_{(g)}$ measurements and the most extensive studies to date to measure $TFA_{(g)}$ with PAS. This advancement expands our understanding of the presence and behavior of these specific PFCAs in the environment. Moreover, this work obtained one of the most extensive data regarding the distribution, sources, and seasonal variations of gas-phase PFCAs in multiple locations across Canada at an ultra-trace level, all while keeping sampling cost low and reducing field logistics due to their passive sampling nature.

3.5 References

Ahrens, L., Harner, T., Shoeib, M., Kobližková, M., & Reiner, E. J. (2013). Characterization of two passive air samplers for per- and polyfluoroalkyl substances. *Environmental Science & Technology*, *47*(24), 14024–14033. https://doi.org/10.1021/es4048945

Ahrens, L., Shoeib, M., Harner, T., Lee, S. C., Guo, R., & Reiner, E. J. (2011). Wastewater treatment plant and landfills as sources of polyfluoroalkyl compounds to the atmosphere. *Environmental Science & Technology*, *45*(19), 8098–8105. https://doi.org/10.1021/es1036173

Barrett, H., Du, X., Houde, M., Lair, S., Verreault, J., & Peng, H. (2021). Suspect and nontarget screening revealed Class-Specific temporal trends (2000–2017) of poly- and perfluoroalkyl substances in St. Lawrence Beluga whales. *Environmental Science & Technology*, *55*(3), 1659–1671. https://doi.org/10.1021/acs.est.0c05957

Burkholder, J. B., Cox, R. A., & Ravishankara, A. R. (2015). Atmospheric degradation of ozone depleting substances, their substitutes, and related species. *Chemical Reviews*, *115*(10), 3704–3759. https://doi.org/10.1021/cr5006759

Dasgupta, P. K., Campbell, S. W., Al-Horr, R., Ullah, S. M. R., Li, J., Amalfitano, C., & Poor, N. (2007). Conversion of sea salt aerosol to NaNO3 and the production of HCl: Analysis of temporal behavior of aerosol chloride/nitrate and gaseous HCl/HNO3 concentrations with AIM. *Atmospheric Environment*, *41*(20), 4242–4257. https://doi.org/10.1016/j.atmosenv.2006.09.054

Dreyer, A., Matthias, V., Weinberg, I., & Ebinghaus, R. (2010). Wet deposition of poly- and perfluorinated compounds in Northern Germany. *Environmental Pollution*, *158*(5), 1221–1227. https://doi.org/10.1016/j.envpol.2010.01.030

Ellis, D. A., Martin, J. W., De Silva, A. O., Mabury, S. A., Hurley, M. D., Sulbaek Andersen, M. P., & Wallington, T. J. (2004). Degradation of Fluorotelomer Alcohols: a Likely Atmospheric Source of Perfluorinated Carboxylic Acids. *Environmental Science & Technology*, 38(12), 3316–3321.

Furlani, T. C., Ye, R., Stewart, J., Crilley, L. R., Edwards, P. M., Kahan, T. F., & Young, C. J. (2023). Development and validation of a new in situ technique to measure total gaseous chlorine in air. *Atmospheric Measurement Techniques*, *16*(1), 181–193. https://doi.org/10.5194/amt-16-181-2023

Janda, J., Nödler, K., Brauch, H., Zwiener, C., & Lange, F. T. (2018). Robust trace analysis of polar (C2-C8) perfluorinated carboxylic acids by liquid chromatography-tandem mass spectrometry: method development and application to surface water, groundwater and drinking water. *Environmental Science and Pollution Research*, *26*(8), 7326–7336. https://doi.org/10.1007/s11356-018-1731-x

Kim, S., & Kannan, K. (2007). Perfluorinated acids in air, rain, snow, surface runoff, and lakes: relative importance of pathways to contamination of urban lakes. *Environmental Science & Technology*, *41*(24), 8328–8334. https://doi.org/10.1021/es072107t

Kwok, K., Taniyasu, S., Yeung, L. W. Y., Murphy, M. B., Lam, P. K., Horii, Y., Kannan, K., Petrick, G., Sinha, R. K., & Yamashita, N. (2010). Flux of Perfluorinated Chemicals through Wet Deposition in Japan, the United States, And Several Other Countries. *Environmental Science & Technology*, *44*(18), 7043–7049. https://doi.org/10.1021/es101170c

Liu, W., Jin, Y., Quan, X., Sasaki, K., Saito, N., Nakayama, T., Sato, I., & Tsuda, S. (2009). Perfluorosulfonates and perfluorocarboxylates in snow and rain in Dalian, China. *Environment International*, *35*(4), 737–742. https://doi.org/10.1016/j.envint.2009.01.016

Luecken, D., Waterland, R. L., Papasavva, S., Taddonio, K. N., Hutzell, W. T., Rugh, J., & Andersen, S. O. (2009). Ozone and TFA Impacts in North America from Degradation of 2,3,3,3-Tetrafluoropropene (HFO-1234yf), A Potential Greenhouse Gas Replacement. *Environmental Science & Technology*, *44*(1), 343–348. https://doi.org/10.1021/es902481f

MacInnis, J. J., French, K., Muir, D. C. G., Spencer, C., Criscitiello, A. S., De Silva, A. O., & Young, C. J. (2017). Emerging investigator series: a 14-year depositional ice record of perfluoroalkyl substances in the High Arctic. *Environmental Science: Processes & Impacts*, *19*(1), 22–30. https://doi.org/10.1039/c6em00593d

Manojkumar, Y., Pilli, S., Rao, P. V., & Tyagi, R. D. (2023). Sources, occurrence and toxic effects of emerging per- and polyfluoroalkyl substances (PFAS). *Neurotoxicology and Teratology*, *97*, 107174. https://doi.org/10.1016/j.ntt.2023.107174

Martin, J. W., Mabury, S. A., Solomon, K. R., & Muir, D. C. G. (2003a). Bioconcentration and tissue distribution of perfluorinated acids in rainbow trout (*Oncorhynchus mykiss*). *Environmental Toxicology and Chemistry*, *22*(1), 196–204. https://doi.org/10.1002/etc.5620220126

Martin, J. W., Mabury, S. A., Wong, C. S., Noventa, F., Solomon, K. R., Alaee, M., & Muir, D. C. G. (2003b). Airborne haloacetic acids. *Environmental Science & Technology*, *37*(13), 2889–2897. https://doi.org/10.1021/es026345u

Olson, N. E., May, N. W., Kirpes, R. M., Watson, A., Hajny, K. D., Slade, J., Shepson, P. B., Stirm, B. H., Pratt, K. A., & Ault, A. P. (2019). Lake Spray Aerosol Incorporated into Great Lakes Clouds. *ACS Earth and Space Chemistry*, *3*(12), 2765–2774. https://doi.org/10.1021/acsearthspacechem.9b00258

Pickard, H. M., Criscitiello, A. S., Persaud, D., Spencer, C., Muir, D. C. G., Lehnherr, I., Sharp, M., De Silva, A. O., & Young, C. J. (2020). ICE Core Record of Persistent Short-Chain fluorinated Alkyl Acids: Evidence of the impact from global environmental Regulations. *Geophysical Research Letters*, *47*(10). https://doi.org/10.1029/2020gl087535

Place, B. K., Young, C. J., Ziegler, S. E., Edwards, K. A., Salehpoor, L., & VandenBoer, T. C. (2018). Passive sampling capabilities for ultra-trace quantitation of atmospheric nitric acid (HNO3) in remote environments. *Atmospheric Environment*, *191*, 360–369. https://doi.org/10.1016/j.atmosenv.2018.08.030

Prevedouros, K., Cousins, I. T., Buck, R. C., & Korzeniowski, S. H. (2005). Sources, Fate and transport of perfluorocarboxylates. *Environmental Science & Technology*, *40*(1), 32–44. https://doi.org/10.1021/es0512475

Rayne, S., Forest, K., & Friesen, K. J. (2009). Estimated congener specific gas-phase atmospheric behavior and fractionation of perfluoroalkyl compounds: Rates of reaction with atmospheric oxidants, air-water partitioning, and wet/dry deposition lifetimes. *Journal of Environmental Science and Health. Part a, Toxic/Hazardous Substances & Environmental Engineering*, *44*(10), 936–954. https://doi.org/10.1080/10934520902996815

Government of Canada. *Research to support the protection of whales in Canadian waters*. (n.d.). November 14, 2021, from https://www.dfo-mpo.gc.ca/campaign-campagne/protectingwhales-protegerbaleines/research-recherche-eng.html

Scott, B., Spencer, C., Mabury, S. A., & Muir, D. C. (2006). Poly and perfluorinated carboxylates in North American precipitation. *Environmental Science & Technology*, *40*(23), 7167–7174. https://doi.org/10.1021/es061403n

Sha, B., Johansson, J., Salter, M., Blichner, S. M., & Cousins, I. T. (2024). Constraining global transport of perfluoroalkyl acids on sea spray aerosol using field measurements. *Science Advances*, *10*(14). https://doi.org/10.1126/sciadv.adl1026

Siegemund, G., Schwertfeger, W., Feiring, A. E., Smart, B. E., Behr, F. E., Vogel, H. A., & McKusick, B. C. (2000). Fluorine Compounds, organic. *Ullmann's Encyclopedia of Industrial Chemistry*. https://doi.org/10.1002/14356007.a11_349

Tao, Y., VandenBoer, T. C., Ye, R., & Young, C. J. (2023). Exploring controls on perfluorocarboxylic acid (PFCA) gas–particle partitioning using a model with observational constraints. *Environmental Science: Processes & Impacts*, *25*(2), 264–276. https://doi.org/10.1039/d2em00261b

Thackray, C. P., Selin, N. E., & Young, C. J. (2020). A global atmospheric chemistry model for the fate and transport of PFCAs and their precursors. *Environmental Science. Processes & Impacts*, *22*(2), 285–293. https://doi.org/10.1039/c9em00326f

US Environmental Protection Agency [EPA]. (2024, January 16). *Air-surface exchange process overview*. https://www3.epa.gov/airquality/

VandenBoer, T., Markovic, M., Petroff, A., Czar, M., Borduas, N., & Murphy, J. (2012). Ion chromatographic separation and quantitation of alkyl methylamines and ethylamines in atmospheric gas and particulate matter using preconcentration and suppressed conductivity detection. *Journal of Chromatography A*, *1252*, 74–83. https://doi.org/10.1016/j.chroma.2012.06.062

Vierke, L., Ahrens, L., Shoeib, M., Reiner, E. J., Guo, R., Palm, W., Ebinghaus, R., & Harner, T. (2011). Air concentrations and particle–gas partitioning of polyfluoroalkyl compounds at a wastewater treatment plant. *Environmental Chemistry*, *8*(4), 363. https://doi.org/10.1071/en10133

Wang, C., Collins, D. B., Arata, C., Goldstein, A. H., Mattila, J. M., Farmer, D. K., Ampollini, L., DeCarlo, P. F., Novoselac, A., Vance, M. E., Nazaroff, W. W., & Abbatt, J. P. D. (2020). Surface reservoirs dominate dynamic gas-surface partitioning of many indoor air constituents. *Science Advances*, *6*(8). https://doi.org/10.1126/sciadv.aay8973

Wang, Z., Cousins, I. T., Scheringer, M., Buck, R. C., & Hungerbühler, K. (2014). Global emission inventories for C4–C14 perfluoroalkyl carboxylic acid (PFCA) homologues from 1951 to 2030, Part I: production and emissions from quantifiable sources. *Environment International*, *70*, 62–75. https://doi.org/10.1016/j.envint.2014.04.013

Wang, Z., Wang, Y., Li, J., Henne, S., Zhang, B., Hu, J., & Zhang, J. (2018). Impacts of the Degradation of 2,3,3,3-Tetrafluoropropene into Trifluoroacetic Acid from Its Application in Automobile Air Conditioners in China, the United States, and Europe. *Environmental Science & Technology*, *52*(5), 2819–2826. https://doi.org/10.1021/acs.est.7b05960

Wong, F., Shoeib, M., Katsoyiannis, A., Eckhardt, S., Stohl, A., Bohlin-Nizzetto, P., Li, H., Fellin, P., Su, Y., & Hung, H. (2018). Assessing temporal trends and source regions of per- and polyfluoroalkyl substances (PFASs) in air under the Arctic Monitoring and Assessment Programme (AMAP). *Atmospheric Environment*, *172*, 65–73. https://doi.org/10.1016/j.atmosenv.2017.10.028

Wu, J., Martin, J. W., Zhai, Z., Lu, K., Li, L., Fang, X., Jin, H., Hu, J., & Zhang, J. (2014). Airborne Trifluoroacetic Acid and Its Fraction from the Degradation of HFC-134a in Beijing, China. *Environmental Science & Technology*, *48*(7), 3675–3681. https://doi.org/10.1021/es4050264

Ye, G., Fang, Y., Zhang, G., Ni, H., Youxiang, Z., Han, X., & Chen, G. (2021). Experimental Investigation of Vapor–Liquid Equilibrium for 2,3,3,3-Tetrafluoropropene (HFO-1234yf) + *trans*-1,3,3,3-Tetrafluoropropene (HFO-1234ze(E)) at Temperatures from 284 to 334 K. *Journal of Chemical & Engineering Data*, *66*(4), 1741–1753. https://doi.org/10.1021/acs.jced.0c01033

Ye, R., Di Lorenzo, R. A., Clouthier, J. T., Young, C. J., & VandenBoer, T. C. (2023). A Rapid Derivatization for Quantitation of Perfluorinated Carboxylic Acids from Aqueous Matrices by Gas Chromatography–Mass Spectrometry. *Analytical Chemistry*. DOI:10.1021/acs.analchem.3c00593.

Young, C. J., & Mabury, S. A. (2010). Atmospheric perfluorinated Acid Precursors: Chemistry, occurrence, and impacts. In *Reviews of Environmental Contamination and Toxicology* (pp. 1–109). https://doi.org/10.1007/978-1-4419-6880-7_1

Chapter Four: Conclusion and future directions.

E. Vanhauwaert[1], C.J. Young[1], and T.C. VanderBoer[1]

[1]Department of Chemistry, York University, Toronto, ON, Canada. Author Contributions: CJY and TCV conceptualized the work and acquired the funding. CJY and TCV provided the resources to support this work.

EV prepared and CJY including TCV edited the manuscript.

4.1 Conclusion and future directions for Chapter 2

In conclusion, the calibration of the nylon-based passive air sampler (PAS) for gas-phase trifluoroacetic acid (TFA) was successful and represents a significant advancement in atmospheric monitoring. This achievement was obtained thanks to use of a simulated atmospheric chamber paired to a zero-air generator and a permeation oven. These results demonstrate the first-ever PAS calibrated for $TFA_{(g)}$, with the capability to sample ultra-trace levels as low as 1.33 ppt_v over a one-week sampling period. Comprehensive quality assurance and quality control (QA/QC) measures were implemented to ensure a robust calibration and accurate quantification of $TFA_{(g)}$ by PAS and annular denuders within each experiment. The QA/QC procedures included positive and negative controls, optimization of a direct-injection ion chromatography with conductivity detection (IC-CD) separation method, and thorough cleaning of the atmospheric chamber. Additionally, this PAS design replaced the expensive polytetrafluoroethylene (PTFE) overlying filter with a more cost-effective polypropylene (PP) filter, without observing any significant changes in the sampling rate and precision. The determined gas-phase TFA dose-response of 113 ± 12 ($\frac{TFA_{(g)}(ng \cdot m^{-3}) \cdot t(h)}{TFA_{(filter)}(ng)}$) from chamber experiments deviates notably from the theoretically calculated value of 182 ± 68 ($\frac{TFA_{(g)}(ng \cdot m^{-3}) \cdot t(h)}{TFA_{(filter)}(ng)}$) using Fuller's law based on a gas-phase nitric acid ($HNO_{3\,(g)}$) calibration from ambient atmosphere method validation for these samplers from Carmichael (2022). Unlike prior studies, our calibration considered extraction efficiency, revealing its importance but not exclusively explaining the observed discrepancy. The differences in the physical properties of TFA and $HNO_{3\,(g)}$ likely contribute to their varying surface uptake rates, which may also play a role in the observed differences The dose-response rates for the other perfluorinated carboxylic acid (PFCAs) homologues were predicted using Graham's and Fuller's laws, based on the chamber calibration for $TFA_{(g)}$. This approach should provide accurate predictions, considering the very similar physical properties of the PFCA homologues and the expectation that they are recovered from the PAS with comparable success. Of the two laws used, Fuller's law was found to be the most suitable for predicting the dose-response of organic halogenated compounds, as demonstrated in a previous study (Gu et al., 2018). This novel PAS represents the first PAS specifically calibrated for $TFA_{(g)}$ and the only PAS selective for $PFCAs_{(g)}$. The calibration of our nylon-based PAS for $TFA_{(g)}$ paves the way for measuring similar challenging compounds, while addressing limitations of previous methods, such as

selectivity, dynamic range including ultra-trace detection limits, sampling site selection, and labor intensity, all while minimizing costs.

Building on this milestone, additional work is imperative to evaluate different factors influencing the sampling rate of nylon-based PAS. Notably, the PAS were calibrated at a specific temperature, relative humidity (RH) and minimal level of particulate matter (PM). While Section 2.3.6 shows that the impact of these factors is not significant in most conditions, conducting chamber calibrations at a wide range of temperatures, RH and PM levels can be effective to quantify the exact magnitude of their influence on the sampling rate of these samplers, especially in extreme conditions which can sometimes occur. Furthermore, chamber calibrations for other perfluorinated carboxylic acids (PFCAs) should be undertaken to thoroughly evaluate the predictive capabilities of both Graham's and Fuller's laws. Additionally, the saturation levels of the current nylon-based PAS setup have yet to be determined. Establishing these saturation levels is crucial to prevent bias in the sampling rate for long term sampling, ensuring that the PAS is not overly exposed and optimizing the duration for which PAS units are deployed. As well, it will be beneficial to expand this sampling approach to other volatile acidic per- and polyfluoroalkyl substances (PFAS) and haloacetic acids (HAAs) that share structural similarities with trifluoroacetic acid (TFA) to help address the current lack of measurements for these species. In summary, while our findings present a robust and the only calibrated PAS method for measuring gas-phase TFA, we recognize the need for more work to enhance the robustness of the sampling method even further.

4.2 Conclusion and future directions for Chapter 3

In summary, the investigation into gas-phase PFCAs in Canada, utilizing nylon-based passive air samplers at various locations, including at ambient urban, ambient rural/remote, indoor, and near point source locations, has yielded valuable insights into the distribution and sources of these compounds. These insights were obtained as a result of detection limits as low as 0.003ppt$_v$ for one week of TFA$_{(g)}$ when analyzed using ion chromatography with mass spectrometry (IC-MS). Optimizations were performed to this IC-MS method to achieve these low detections limits by ensuring minimal ion suppression with good separation from major atmospheric anions and PFCAs. Ambient measurements using PAS indicate that TFA$_{(g)}$ consistently displayed the highest concentration among the analyzed PFCAs, peaking in summer and decreasing in winter, likely a result to increased use of heat transfer fluids (e.g. HFO-1234yf) in the summer. Notably, no distinct seasonal trend was observed for other

PFCAs. Measurements taken at two different sites in Toronto show spatial variability in the levels of total $TFA_{(g)}$, where they were found to be 1.5 to two times higher at one location compared to the other. In contrast, no significant difference in levels of ≥C3 $PFCAs_{(g)}$ was observed between the two locations. These findings suggest $TFA_{(g)}$ was predominantly influenced by short-lives precursors and/or direct emissions meanwhile ≥C3 $PFCAs_{(g)}$ in the same region are predominantly influenced by long-lived precursors. This study also found annual increases in the levels of $TFA_{(g)}$ within the same geographic region over three consecutive years which may potentially indicate yearly increases in the usage of TFA and/or its corresponding precursor compounds in the region. Measurements taken at two remote endangered whale habitats show that the levels of $PFCAs_{(g)}$ are lower compared to the levels observed in Toronto. The site on Saturna Island, in particular, recorded the lowest $PFCAs_{(g)}$ concentrations among all the locations examined. These findings demonstrate that urban areas, as demonstrated by Toronto, serve as important regions of emissions for global $PFCA_{(g)}$ distributions. The use of PAS also demonstrated their efficacy in indoor lab settings, tracking the reduction of gas-phase PFCA contamination over time from reduced use of these compounds in the laboratory and with continuous ventilation. Furthermore, measurements at wastewater treatment plants (WWTP) identified C2-C6 $PFCAs_{(g)}$ as emission sources relative to upwind measurements, with the exception of $PFPrA_{(g)}$. The WWTP did not appear to be an emission source of $PFPrA_{(g)}$ due to elevated error compared to the other PFCAs homologues, likely a result of using $^{13}C_4$-PFBA as the internal standard. Additionally, the calibration of the nylon-based PAS for $TFA_{(g)}$ was field-tested through orthogonal measurements against an ambient ion monitoring ion chromatography mass spectrometer (AIM-IC-MS) instrument where no significant difference was observed when accounting for temperature effects. Taking everything into account, this is first instance of outdoor measurements of $PFPrA_{(g)}$ using passive air samplers and represents the most extensive investigation measuring $TFA_{(g)}$ with this method, with Carmichael et al. (2022) being the sole other study to have conducted a few TFA measurements performed with passive air samplers. These advancements significantly enhance our understanding of the presence and behavior of these specific PFCAs in the environment by providing one of the most comprehensive $PFCAs_{(g)}$ data sets on the distribution, sources, and seasonal variations across multiple locations in Canada at an ultra-trace level, all while maintaining cost-effectiveness and reduced field logistic sampling.

Looking ahead, this sampling technique aims to enhance our comprehension of PFCAs. Continuous expansion of a PAS network monitoring in Toronto and other regions is essential

for validating suspected yearly increases of $TFA_{(g)}$ and as well as other important trends. It would also be important to incorporate mass-labelled PFPrA in the analysis to yield more accurate results for gas-phase PFPrA analysis. Furthermore, deploying passive air samplers to measure $PFCAs_{(g)}$ in indoor settings offers the opportunity to assess $PFCAs_{(g)}$, where measurements are lacking, to determine whether they reach significant levels and to provide insights on indoor sources and associated risks. Additionally, expanding measurements to other suspected emission sources beyond wastewater treatment plants is crucial in order to understanding major sources contributing to PFCA contamination. Such knowledge would allow for the ability to address and reduce major source points that are not currently well established. Pursuing these future directions will undoubtedly contribute to advancing our knowledge of PFCAs, their sources and their behavior.

4.3 Reference

Gu, W., Cheng, P., & Tang, M. (2018). Compilation and evaluation of gas phase diffusion coefficients of halogenated organic compounds. *Royal Society Open Science*, *5*(7), 171936. https://doi.org/10.1098/rsos.171936

Appendices

Appendix A: Supporting Material for Chapter Two: Method development and validation of gas-phase PFCAs nylon-based passive air samplers using an atmospheric chamber for calibration.

S2.1 Atmospheric chamber operating procedure

Start-up: Weatherproof caps are inserted into the chamber by opening the chamber and hung on the retort stands, as depicted in Figure 2.1. Due to their size and difficulty of inserting them in the chamber, they are never removed between different chamber experiments. The chamber access sleeve is then sealed gas-tight with a PFA pinch rod/clamp. The mass-flow controllers (MFC) are set to the desired flow rates as follows: MFC 1 at 8.8 L/min, MFC 2 at 2.5 L/min, MFC 3 at 1 L/min, MFC 4 at 7.5 L/min without yet turning on the pumps. In order to correct for any lost calibration in the MFCs setpoints, their flows are measured independently where the lines are disconnected from the chamber and the necessary pumps are turned on from the experimental setup. The flow rates of each MFC are measured using a calibrated flow meter (MesaLabs, Definer 220, S/N 132596) and adjusted as necessary to reach the desired values mentioned above by changing the setpoint values on the control box (CCR, Model 400). The total flow into the chamber is 10 L/min while the outflow is 9.7-9.8 L/min. It is important to obtain these conditions to prevent any damage to the chamber, the pumps, or other parts of the system from over-filling (causing the chamber to potentially burst), or due to high- or low-pressure issues. The small imbalance is easily monitored over time and the rate of inflation is so small that the added volume is removed when sample PAS are removed. Once the desired flows in and out are obtained, the tubing was reconnected to the chamber.

Chamber cleanup: The permeation oven is disconnected from the gas handling lines for this procedure. The chamber is then flushed with zero air at approximately 0% RH until the contamination is found to be at a minimum and no longer change. A proxy for cleanliness is used through the detectable ionic analytes in the extract of a denuder installed on the outflow line. Typically, dry flushing the chamber for a period of a two days was found to be acceptable. If the contamination is found to be large, the chamber can be flushed with ozone in dry air and/or flushed with water vapour by bubbling pre-extracted 18.2 MΩ·cm deionised water in the inflow impinger and shining UV-light (Light sources, INC. U.S.A, FS40T12-UVB-BP, S227) to create OH radicals. For such intensive oxidation cleaning, a chemical scrubber composed of Purakol® is connected to the outflow of the chamber to remove these oxidants

from the gas flow in order to protect the MFC and pump materials. This oxidation procedure is effective at degrading precursor sources for acids from the chamber, but not acids themselves as they do not degrade with either of these oxidants. Acids, including TFA, can only be removed from the chamber by physical removal during dry flushing where they repartition from chamber surfaces into the gas flow.

Chamber equilibration: This step introduces gas-phase TFA to the chamber to prepare it for a calibration experiment. The N_2 gas required to carry the TFA from the permeation oven is turned on and the oven is heated to 60 °C. The outflow of the permeation oven is bubbled into DIW while the chamber is still being cleaned to ensure the TFA permeation device remains emitting at a constant rate and that the emitted gas is scrubbed out of the diverted airflow and not released into the room air. To add TFA to the chamber, the outflow of the permeation oven is connected to the gas handling lines. Once the chamber has been sufficiently flushed, the inflow impinger and the permeation oven is reconnected to obtain the flow path denoted in Figure 2.1. The chamber is then left for two to three days of continuous flow-through to allow the walls and tubing throughout to reach equilibrium at the experimental humidity and mixing ratio of $TFA_{(g)}$ for a planned calibration experiment. Since TFA is a strong acid, it is expected to interact with the chamber walls, so an equilibration period is required to stabilize the mixing ratio present in the experimental system.

Inserting passive air samplers in the chamber and initiating a dose-response calibration experiment: The Pimoroni Enviro+ sensor is turned on outside the chamber for recording temperature and relative humidity and the outflow of the chamber is capped so that an overflow of the setup toward the access sleeve can be obtained, preventing room air from entering the chamber to the greatest extent possible and retaining the equilibrated chamber conditions. The flow rates of MFCs 1 and 3 are measured. The access sleeve of the chamber is then quickly opened, and the twelve PAS are inserted and attached to the weatherproof caps on retort stands that have also equilibrated inside the chamber. The PAS field blank is exposed momentarily to the atmosphere inside of the chamber for a few seconds. The Pimoroni Enviro+ sensor is inserted into the chamber and it is then quickly sealed with its clip. The opening and closing of the access sleeve to insert the PAS and to collect the blank takes approximately 1 min or less to perform. The outflow denuder is then exchanged with a newly coated denuder and the outflow impinger is rinsed and filled with clean 18.2 MΩ·cm deionised water, which takes approximately 10-20 s to perform. The times of all these activities and changes are recorded.

The outflow tubing of the chamber is then quickly reconnected so that the desired flow balance is reobtained for the experiment.

Removing passive air samplers and finishing a dose-response calibration experiment: After two or three days of PAS exposure to the controlled atmosphere, the first three passive samplers need to be collected from the chamber. At this time, the outflow denuder is also removed and capped. The outflow tubing of the chamber is disconnected and capped. The access sleeve is opened by removing the clip and the PAS are removed from the chamber. The PAS sampling media are capped to form covered petri dish caps, with the covers secured using lab tape, and sealed in a Ziploc bag. The access sleeve is closed shut again with a clip. The opening and closing of the access sleeve to remove the PAS takes approximately 10 s to perform. A newly coated annular denuder is then connected to the outflow of the chamber and the tubing is reconnected, which takes approximately 5-10 s, so that the mixing ratio that the remaining PAS were exposed to can be quantitatively determined on an ongoing basis at each collection timepoint. This procedure is repeated for the subsequent triplicates of PAS collected and an associated denuder on the third, fourth and fifth days of a typical calibration experiment. Once the last set of PAS and denuder are removed, the chamber is once again dry flushed for a few days to prepare it for the next run.

S2.2 Supporting Figures for the materials and methods

This section contains supporting Figures for field deployment steps for our nylon-based PAS (Figure S2.1) and the derivatization for PFCAs with DDM for the GC-MS method (Figure S2.2).

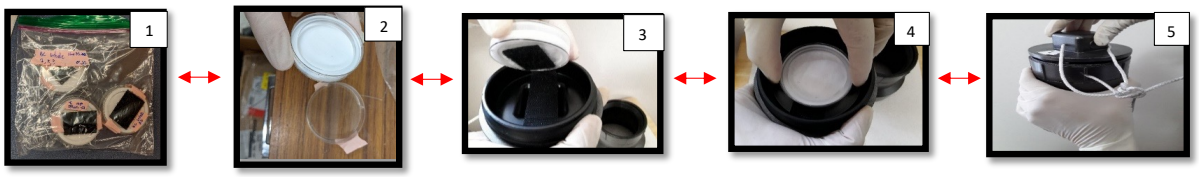

Figure S2.1: Steps for field deployment assembling of our custom-built nylon passive samplers (Carmichael, 2022).

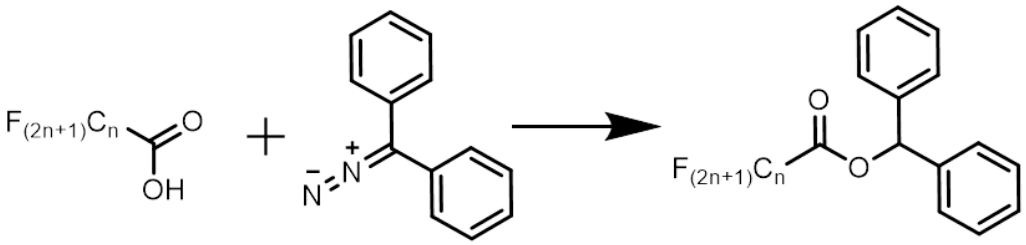

Figure S2.2: Derivatization of PFCAs with DDM

S2.3 Supporting Figures for the results and discussion

This section contains the supporting Figure for the separation of TFA and PFPrA in both 15°C and 33 °C IC methods (Figure S2.3). Poor separation is seen between TFA and PFPrA (R_{min} < 1.5) in the 15 °C method whereas good separation is seen between TFA and PFPrA (R_{min} > 1.5) using the 33 °C IC method. These findings show that improved IC selectivity between PFCAs homologues is achieved at higher temperatures.

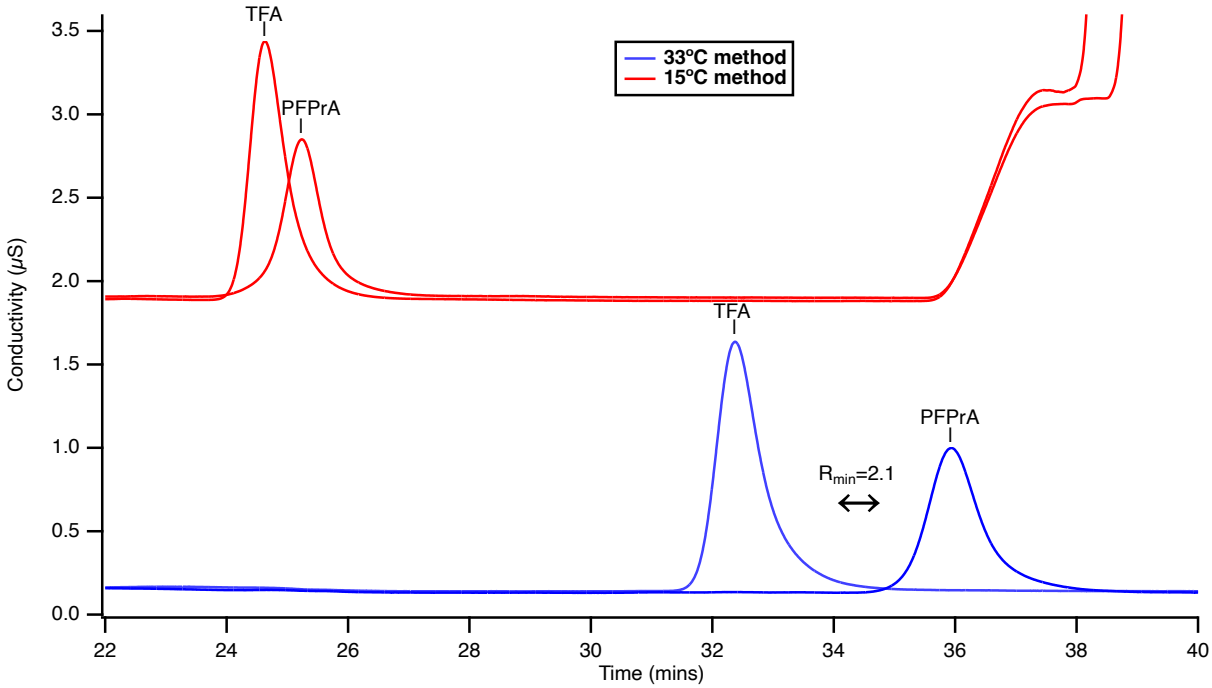

Figure S2.3: Separation of TFA and PFPrA with the 15 °C and 33 °C ion chromatography methods. Note that the 15 °C method has an applied conductivity offset of +1.8 µS to clearly depict the performance of both methods.

S2.4 T-test

This section details the t-test calculations to determine if a statistically significant difference exists between experimental and/or theoretical values of the dose-response rates.

When a statistically significant difference is identified in this context, it allows knowledge of whether identification of causes creating this major difference, such as biases, variations in physical properties, or limitations in predictive capabilities need to be thought about and enumerated. A Welch two sample unequal variances t-test was used in this chapter, where the $t_{calculated}$ was obtained using Equation S3.1, where $\bar{x}$ is the mean, s is the variance of the mean and n is the sample size of the mean.

$$\mathbf{t_{calculated}} = \frac{\bar{x}_1 - \bar{x}_2}{\sqrt{\frac{s^2_1}{n_1} + \frac{s^2_2}{n_2}}} \qquad \textbf{(E S3.1)}$$

The t_{table} values were obtained from Excel. Table S1 represents the results of the Welch t-test for the uptake of PFCA on nylon-based PAS with PTFE overlying filters versus PP overlying filters. In this comparison, the t_{table} is found to be larger than $t_{calculated}$, which indicates no statistical differences between both values.

Table S1: A Welch t-test for the uptake of PFCA on nylon-based PAS with PTFE overlying filters versus PP overlying filters. This statistical analysis was performed at a 95% confidence level. The t_{table} was obtained from Excel.

PFCA	$t_{calculated}$	t_{table}
TFA	2.21	2.78
PFPrA	0.34	
PFBA	2.23	
PFPeA	1.15	
PFHxA	1.95	

S2.5 Chamber wall losses

The chamber is composed of PFA that acts as a surface-interaction deactivating material due to the presence of fluorinated carbon chains that exhibit minimal intermolecular interactions. However, this material is not fully inert. Gas-phase acids, such as TFA, may partially adsorb to the chamber walls. The same adsorption can occur for water vapour, which is found in much higher concentration than TFA in the calibration experiments. In the presence of surface water, TFA can dissolve and irreversibly ionize if sufficient water is present at the interface. While a minor consideration, a small amount of $TFA_{(g)}$ may also escape the chamber during the several seconds when chamber is opened to insert and remove PAS. To obtain an

approximation of the TFA losses from these processes, we measured the TFA in the chamber and compared it to the measured permeation rate for TFA from our oven. The losses were found to range between 44 to 74 % depending on the experiment duration (Figure S2.4). A decrease in losses is generally seen with an increased number of experiments indicating that TFA started occupying more adsorption sites within the chamber at a constant mixing ratio, leading to less loss over time. The results in Figure S2.4 demonstrate that it would be erroneous to use the constant emission rate from the permeation oven to state the mixing ratio of TFA present in the chamber during the dose-response calibration experiments. Instead, best practice would be to follow our methodology of measuring the TFA mixing ratio in the outflow of the chamber, as this accounts for these expected strong wall interactions, including losses to the sampler weather shields, that can reduce the TFA mixing ratio in the chamber.

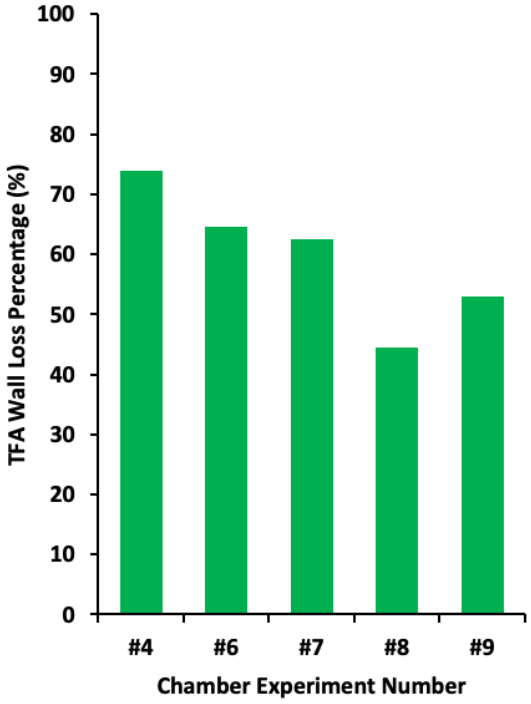

Figure S2.4: TFA wall losses from chamber experiments.

S2.6 PAS method detection limits

The method detection limits were determined as the mean plus three times the standard deviation of the PAS method blanks. If no signal is detected in the method blanks, the limit of detection was determined as three times the signal to noise ratio, using calibration standards and method blanks. These method detection limits can be found in Table S2.2 and are expressed in mixing ratios (ppt_v) to account for variations between methods, such as differences in flow or diffusion rates, extraction volumes, dilutions and concentration factors. This allows for a

more accurate comparison between methods. These detection limits are also time dependant, where longer exposure of these samplers leads to improved detection limits. Additionally, some variability in the detection limits exists due to fluctuations in blank signals and instrument noise levels on different days of analysis.

Table S2.2: Method detection limits (MDL) in mixing ratios for a time period equivalent to one week of ambient atmospheric sampling. Note, these demonstrate the lowest detection limits obtained for the data presented in this Chapter, but they can be extended much lower when deployed for months in the field.

PFCAs	IC-CD		GC-MS
	PAS (ppt_v)	Annular denuders (ppt_v)	PAS (ppt_v)
TFA	3.72	1.62	1.33
PFPrA	-	-	0.36
PFBA	-	-	0.09
PFPeA	-	-	0.06
PFHxA	-	-	0.96

Appendix B: Supporting Material for Chapter 3. Application of gas-phase PFCAs nylon-based passive air samplers in various environments.

S3.1 PAS method detection limits

The method's detection limits were determined as the mean plus three times the standard deviation of the PAS method blanks. If no signal is detected in the method blanks, the limit of detection was determined as three times the signal to noise ratio, using calibration standards and method blanks. These method detection limits can be found in Table S3.1 and are expressed in mixing ratios (ppq_v) to account for variations between methods, such as differences in diffusion rates, extraction volumes, dilutions, and concentration factors. This allows for a more accurate comparison between methods. These detection limits are also time dependant, where longer exposure of these samplers leads to improved detection limits. Additionally, some variability in detection limits exists due to fluctuations in blank signals and instrument noise levels on different days of analysis.

Table S3.1: Method detection limits (MDL) in mixing ratios for a time period equivalent to one week of ambient atmospheric sampling. Note, these demonstrate the lowest detection limits obtained for the data presented in this Chapter, but they can be extended much lower when deployed for months in the field.

PFCAs	GC-MS (ppq_v)	IC-MS 24 °C (ppq_v)	IC-MS 28 °C (ppq_v)
TFA	158	7	3
PFPrA	188	5	15
PFBA	91	13	5
PFPeA	66	2	4
PFHxA	33	5	1